University of Southern Queensland

Faculty of Engineering and Surveying

CHEMICAL RESISTANCE OF GEOPOLYMER CONCRETE AGAINST H_2SO_4 & NaOH

A dissertation submitted by

Brock William Tomkins

in fulfilment of the requirements of

Courses ENG4111 and 4112 Research Project

towards the degree of

Bachelor of Engineering/Business

(Civil/Supply Chain Management)

Submitted: October, 2011

Abstract

The purpose of this project is to develop innovative environmental green concretes and study their performance, particularly the chemical resistance. The concretes under investigation include fly-ash based geopolymer concrete (FAGC) and red-mud based geopolymer concrete (RMGC). The chemical resistance tests involve sodium hydroxide and sulphuric acid at 20^{O}C and 90^{O}C. To understand the relative significance of these results, they are contrast alongside the performance of ordinary Portland cement concrete (OPC) in the same conditions.

Geopolymer concrete is the name given to concrete where the binder is entirely replaced by an inorganic polymer formed between a strong alkaline solution and an aluminosilicate source. The ratio and quantity of alkaline solution used can affect – amongst other factors – the concrete strength and curing time. Aluminosilicate sources include but are not limited to red-mud, fly-ash, blast furnace slag and kaolin. The variability of geopolymer binders and activators increase the difficulty of manufacturing a homogenous and universal geopolymer concrete standard. Currently, geopolymer concrete exhibits as good as, and in some areas superior engineering properties to normal concrete.

Carbon emissions can be significantly reduced by using aluminosilicate geopolymer binders instead of Portland cement (which releases 1 t of CO_2 per tonne of production). Compared to Portland cement, fly-ash based geopolymer concrete can reduce carbon emissions by 80% which has the potential to reduce global emissions by approximately 2.1 billion tonnes a year. This is equivalent to taking two thirds of global traffic off the roads each year.

In this project OPC, FAGC and RMGC samples were cast in 200x100mm cylindrical moulds. After these samples cured for a minimum of 14 days, chemical testing began. The samples were submerged for 7, 14, 28 and 56 days, sulphur capped and compression tested. Results comprised the analysis of testing data, macro analysis and microscopy.

Results indicated OPC experienced some strength deterioration in both an acid environment (-24.9 to -25.6%) and an alkaline environment (-2.2 to -13.3%). FAGC was found to have better acid resistance (+3.8 to -17.6%) and even experienced strength enhancement in sodium hydroxide (+29.1 to +55.7%). Interestingly, RMGC exhibited a strength increase of 52.4% in sulphuric acid while also displaying strength enhancement of +50.5% in sodium hydroxide. This performance suggests that FAGC and RMGC are both suitable replacements for the existing bunding slab at QAL.

University of Southern Queensland

Faculty of Engineering and Surveying

ENG4111 and ENG4112 *Research Project*

Limitations of Use

The Council of the University of Southern Queensland, its Faculty of Engineering and Surveying, and the staff of the University of Southern Queensland, do not accept any responsibility for the truth, accuracy or completeness of material contained within or associated with this dissertation.

Persons using all or any part of this material do so at their own risk, and not at the risk of the Council of the University of Southern Queensland, its Faculty of Engineering and Surveying or the staff of the University of Southern Queensland.

This dissertation reports an educational exercise and has no purpose or validity beyond this exercise. The sole purpose of the course pair entitled "Research Project" is to contribute to the overall education within the student's chosen degree program. This document, the associated hardware, software, drawings, and other material set out in the associated appendices should not be used for any other purpose: if they are so used, it is entirely at the risk of the user.

Professor Frank Bullen
Dean
Faculty of Engineering and Surveying

Certification

I certify that the ideas, designs and experimental work, results, analyses and conclusions set out in this dissertation are entirely my own effort, except where otherwise indicated and acknowledged.

I further certify that the work is original and has not been previously submitted for assessment in any other course or institution, except where specifically stated.

Brock William Tomkins

Student Number: w0050056560

B Tomkins.

Signature

27-10-11

Date

Acknowledgements

The large number of samples that I had to test meant that each activity needed to be done many times. The following people had great patience and helped me tremendously with my project. I would like to thank GHD for the flexible hours they allowed me to work. I would also like to thank my family for the support they have provided throughout the year.

Mr Daniel EISING	Thankyou Daniel for assisting me with casting, sulphur capping and saw cutting of the concrete samples
Mr Tom GLASBY	A big thanks to Tom for agreeing to be my industrial supervisor and supporting me thoughout the year.
Dr Mark LYNCH	Thanks to Mark (Chemistry Lecturer) who provided me with crucial advice on material selection
Mr Atul SAKHIYA	Thankyou to Atul for assisting with compression testing and saw cutting of samples for microscopy analysis
Mr Mohan TRADA	Another big thankyou goes to Mohan for helping me access Z108 for a seemingly endless number of compression tests
Dr Hao WANG	Thanks to Hao for supervising me and providing continuous support throughout the year
Mr Zuhua ZHANG	A big thankyou goes to Zuhua for his many hours of assistance in P2, by helping me to prepare tests, gain access to equipment and perform testing

Contents

List of Figures

List of Tables

Nomenclature

The following abbreviations are used throughout this dissertation

ASR	=	Alkali Silica Reaction
Al-Si	=	Aluminosilicate
ASTM	=	American Society for Testing and Materials
B.F.S.	=	Ground granulated blast furnace slag
EFC	=	Earth friendly concrete (EFC is a type of FAGC)
F.A.	=	Fly-ash
FAGC	=	Fly-ash based Geopolymer Concrete
OPC	=	Ordinary Portland cement
QAL	=	Queensland Alumina Limited (Alumina refinery in Gladstone)
R.M.	=	Red-mud
RMGC	=	Red-mud based Geopolymer Concrete

CHAPTER 1 Introduction

This project aims to develop innovative environmental green geopolymer concretes and study the performance, particularly the chemical resistance of these concretes. The scope of this report will comprise preparation, testing and analysis of fly-ash based geopolymer concrete (FAGC) and red-mud based geopolymer concrete (RMGC). Commercially known as Earth Friendly Concrete (EFC), the mix design of this concrete is part of the intellectual property owned by Wagners and is not made publicly available. The mix design of this concrete is part of the intellectual property owned by Wagners and is not made publicly available. The RMGC samples were made with an emphasis on the use of red-mud (a waste component of alumina production) but also comprised fly-ash and blast furnace slag. A batch of ordinary Portland cement (OPC) concrete prepared by Wagners will also be tested in order to provide a relative comparison to the FAGC and RMGC test results. For a more holistic comparison, the chemical resistance of other OPC concretes will be investigated.

The samples used for this project consisted of 22 OPC, 22 FAGC and 11 RMGC samples. As measured by a calibrated pH tester, testing will assess the resistance of these samples to pH1.5 H_2SO_4 and pH12 NaOH. The chemical solutions will be monitored once a week to retain a 1M concentration (5% by wt.), with the temperatures assessing chemical resistance at 90^{o}C and ambient 20±2^{o}C temperatures. Chemical testing will be performed over a period of 8 weeks at which time the samples will be comparatively analysed for changes.

Research papers thus far indicate there are many properties of geopolymer concrete that compare favourably to ordinary concretes. By replacing Portland cement (which releases 1 t of CO_2 per tonne of production) with geopolymer technology, carbon emissions can be reduced by 80% (Wagners 2011). Worldwide application of geopolymer concretes therefore has the potential to reduce CO_2 emissions by 2.1 billion tonnes which is equivalent to taking to two thirds of the worlds' traffic off the roads (CDIAC 2010; BPN 2011). The ultimate aim of this project is to encourage a greater use of geopolymer concrete technology in the building and construction industry.

1.1 Background

1.1.1 History of Geopolymer

Geopolymers were first discovered by Professor V.D. Glukhovsky of the former Soviet Union during the 1950s and was given the name 'soil cements'. A French man by the name of Davidovits began similar work in the 1970s naming these materials 'geopolymers', which refers to an amorphous inorganic polymer formed through the ionic bonding reaction between an aluminosilicate (Al-Si) material and a strong alkaline solution (Tavor et al. 2007). Geopolymers are able to be synthesised from a variety of aluminosilicate sources such as polysilicates, zeolites, kaolinite, metakaolin, calcium, rocks, silica, fly-ash, blast furnace slag, phosphate and organic minerals.

The first industrial efforts into this material were recorded in Saint-Quentin, France in 1972. During this year it was discovered that water-resistant ceramic tiles could be created at temperatures below 450^{O}C and that one component of clay (kaolinite) reacted with caustic soda at 150^{O}C. This application began in the ceramic industry by Neils Olgen in 1934 and later in Russia in 1963.

It was in 1978 when Davidovits proposed that an Al-Si compound could polymerise with an alkaline solution. This led to the idea of cement replacement and the subsequent creation of 'Geopolymer Concrete'. Hundreds of papers have since been published, with interest in geopolymer concrete growing exponentially. Since its inception, there have been four internationally hosted geopolymer seminars with the first two in France in 1988 and 1999, the third in Melbourne in 2002 and the fourth held concurrently in Perth and Saint-Quentin in 2005 (Davidovits 2008).

1.1.2 Significance

Geopolymer concrete has many documented advantages over traditional concretes and its chemical composition can explain most of these advantages. Some geopolymer concrete properties with superior performance to ordinary concrete include compressive strength, chemical resistance, thermal resistance, less shrinkage and expansion (Wagners 2011). The ensuing literature review (see Section 2.1) discusses the properties and various applications that geopolymers have, which are specified in Table 1.

Table 1: Geopolymer Applications (Davidovits 2008)

Geopolymer Applications	
Cements and Concretes	Host matrix in waste encapsulation
Composites for automobiles and aircraft	Industrial applications
Decorative applications	Infrastructure repair and strengthening
Fire & heat resistant material	Low cost ceramic processing
Foamed Geopolymer	Low tech and low CO_2 building material
Foundry applications	Refractory items
High tech resin systems	Thermal insulation

1.1.3 Classification of Silicates

In classifying silicates, W.L. Bragg published a classification method in 1937 which employs the theory of distinct silicate or aluminate anions as the basic unit of constitution. This fundamental unit is a tetrahedral complex consisting of a small cation (such as Si or Al) that lies in tetrahedral coordination with 4 oxygen anions to produce SiO_4 or AlO_4. This can be understood by Pauling's first rule of a polysialate relationship as illustrated in Figure 1.

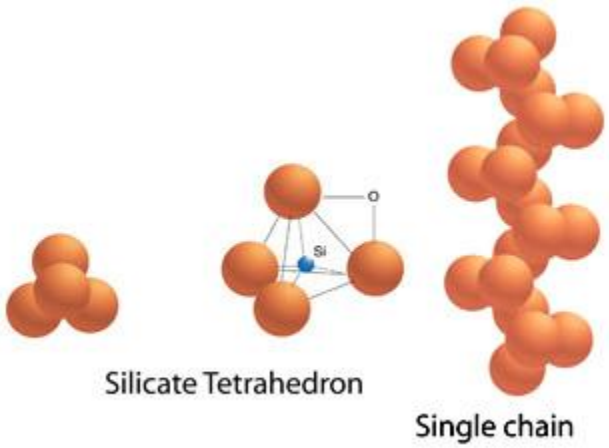

Figure 1: Tetrahedral Complex (Christiansen & Hamblin 2007)

The silicon-oxygen bond should never be ionic; it should be polar and covalent. This is because individual silicon and oxygen atoms can't move freely within the crystalline structure. Covalent bonding is more general and holds for silicates, Al-Si (such as zeolites), alumino-phosphates and geopolymers. Aluminosilicate based geopolymers such as polysialate consist of SiO_4 and AlO_4 tetrahedra which are linked alternatively by sharing all the oxygen atoms (Davidovits 1976).

Table 2: Chemical Structure of Polymers (Davidovits 2008)

Polymer	Chemical Structure
Methane (equivalent to polysilane)	C-H-C-H
Poly(silane)	Si-H-Si-H
Poly(siloxonate)	Si-O-Si-O
Poly(sialate)	Si-O-Al-O
Poly(sialate-disiloxo)	Si-O-Al-O-Si-O-Si-O

1.2 Objectives

Upon completion of this project (ENG4111, ENG4112) it is expected that I will:

1. **Understand** what a geopolymer is through publicly and privately accessible literature. The history of geopolymers, where they were first used, who pioneered their use in concrete, their significance and the comparative advantage of geopolymer concretes to ordinary concretes.
2. **Investigate Chemical Resistance** properties of OPC, FAGC & RMGC.
   Cast 22 OPC, 22 FAGC and 11 off RMGC concrete samples. Each type of concrete will be tested at 7, 14, 28 and 56 days in the following conditions:
   - H_2SO_4 solution: 20^OC and 90^OC
   - NaOH solution: 20^OC and 90^OC

   In each condition, 4 to 5 samples will be tested.
3. **Compare** properties of Chemical Resistance.
   Through chemical testing, compression testing and microscopy analysis, a comparison and conclusion will be made.

1.3 Scope

The scope of this project involves a study of the performance of OPC, FAGC and RMGC with a focus on chemical resistance. FAGC and RMGC will be investigated and compared to OPC. The red-mud binder in RMGC was obtained from Queensland Alumina Limited (QAL) in Gladstone which – like most alumina refineries – uses the Bayer Process to extract aluminium oxide from bauxite. This extraction involves mixing the bauxite with high temperature Sodium Hydroxide (NaOH), of which the residue spills onto a bunding slab at 90 to 105^OC. QAL has expressed interest in the potential of geopolymer concrete as an alternative to their current refinery's bunding slab. In addition to QAL's request to assess the replaceability of their existing bunding slab with a geopolymer concrete, the red-mud waste from the Bayer Process will be used to cast a hybrid geopolymer concrete in an effort to find an alternative use for this red-mud. The potential for this red-mud waste as a cementitious material in geopolymer concrete includes:

- Reduced storage and environmental costs incurred by alumina refineries
- Increased recycling within the alumina industry &
- When looking at the resource to waste ratio, the relative reduction in waste-related costs compared to fly-ash and blast furnace slag would be much larger.

1.4 Limitations

Limitations experienced throughout this project are now discussed. It was originally planned to test the samples under these conditions at 112 and 168 days but due to time and material constraints this was not possible. To reduce the frequency of practical testing, as many samples as possible were placed in solution at the same time. Consequently the individual curing time between each of the concretes, were not consistent at commencement of the chemical testing. Velocity of flow in an alumina refinery was not emulated due to equipment constraints. The bunding slab engineer from QAL also stated he believed flows were not

mechanically abrasive. To encourage chemical attack samples were processed in a Wagners grinding machine, however the RMGC samples were not processed in this machine. Before compression testing, samples will also be sulphur capped. The disadvantage with sulphur capping is that it influences the force and displacement readings.

1.5 Risk Assessment and Safety

There was risk involved in arranging the delivery of equipment and preparing materials for the chemical resistance tests, but safety concerns were minimal to none. The practical components of this project involved slight to severe risk. The size of this project requires significant information and data entry which will involve use of a computer. It is therefore important to maintain a healthy life balance and have regular breaks to prevent repetitive strain injuries.

1. Casting

Risk:	Skin coming in contact with high pH concrete mix.
Hazard:	High pH concrete slurry
Likelihood:	Possible
Exposure:	Frequent
Consequences:	**Insignificant** • Irritation to contact area of skin (i.e. Eczema)
Control Measures:	• Wear chemically resistant gloves • Wear steel caps

2. Sample Grinding

Risk:	Incorrect placement of samples could cause debris to fly unpredictably across the room
Hazard:	• Circular grinding blade
Likelihood:	Unlikely
Exposure:	Infrequent
Consequences:	**Moderate** • Eye damage • Cuts and abrasions
Control Measures:	• Wear steel caps • Wear safety glasses

3. Chemical Resistance Testing

Risk:	Direct skin contact with high temperature chemical solutions.
Hazard:	• Diluting acids and alkalis for chemical testing • Handling these chemicals at ambient and high temperatures
Likelihood:	Possible
Exposure:	Frequent
Consequences:	**Moderate** • Severe chemical burns • Possible blindness
Control Measures:	• Wear steel caps • Wear chemically resistant gloves • Wear safety glasses

4. Sulphur Capping

Risk:	Contact of skin with liquid sulphur and inhalation of gas fumes.
Hazard:	• Heating receptacle • High temperature sulphur and • Associated fumes
Likelihood:	Possible
Exposure:	Infrequent
Consequences:	**Minor** • Irritation • Sulphur burns • Inhalation and dizziness • Possible blindness
Control Measures:	• Wear steel caps • Wear safety glasses • Keep vacuum fan on low before and after sulphur is heated

5. Compression Testing

Risk:	Electrical Shock, Pinching and Debris could fly from the sample.
Hazard:	• Turning the Device on • Placing the sample • Loading the device to failure
Likelihood:	Unlikely
Exposure:	Occasionally (<50 instances)
Consequences:	**Minor** • Electrical shock • Cuts and abrasions
Control Measures:	• Wear closed in shoes • Engage safety screen • Wear safety glasses

1.6 Dissertation Outline

The remaining structure of this dissertation is indicated below:

Chapter 2: Literature Review

This section discusses the importance regarding OPC, the advantages and disadvantages of geopolymer concrete, fly-ash geopolymer concrete and red-mud geopolymer concrete. There is also a brief discussion on carbon emissions, encapsulation of wastes and heavy metals, chemical resistance and the alkali-silica reaction.

Chapter 3: Methodology

This chapter summarises the process followed by organising, preparing, testing and analysing the concrete samples.

Chapter 4-6: OPC, FAGC and RMGC

These chapters investigate, analyse and discuss the performance of OPC, FAGC and RMGC in the specified conditions.

Chapter 7: Comparative Discussion

The deterioration of other concretes investigated in the literature review will be investigated and compared to results from Chapters 4 to 6 for a more holistic comparison. Following this investigation, test results from Chapters 4 to 6 are comparatively analysed and discussed.

Chapter 8: Conclusions and Future Work

This chapter will discuss the conclusions and make suggestions for potential future work.

CHAPTER 2 Literature Review

This chapter performs a literature review of topics considered important to the project concerning formation of the FAGC samples, the advantages and disadvantages of geopolymer concrete, fly-ash (F.A.) and its use in concretes, Portland cement concretes, the role of red-mud (R.M.), carbon emissions, waste encapsulation, chemical resistance and the alkali silica reaction (ASR). Use of industrial waste and reduction of carbon emissions are major factors in the appeal that industry has shown towards this construction material.

2.1 Ordinary Portland Cement Concretes

2.1.1 Major and Minor Constituents

A major component and reason for the high strengths of ordinary Portland cement concretes compared to hydrated limes is due to tricalcium silicate (C_3S) which is a compound (formed at 1400^{O}C) that's had the opportunity to combine with the maximum quantity of lime. As indicated by Czernin (1980) these high strengths require a lot of energy, as heating lime and silica (74% and 26% respectively) to any temperature below 1250^{o}C only produces dicalcium silicate (C_2S) and quick lime which is essentially a hydrated lime. Constituents of a typical Portland cement are show in Table 3.

Table 3: Portland Cement Oxide Composition

Oxide	Mass (%)
SiO_2	20.0
Al_2O_3	6.0
Fe_2O_3	3.0
CaO	63.0
MgO	1.5
SO_3	2.0
K_2O	1.0
Na_2O (balance)	1.0
LOI	2.0
Insoluble Residue	0.5
Total	**100.0**

Water and carbon dioxide are expelled during loss on ignition (LOI) which is defined as the percentage weight loss from heating a material or cement sample to 1000^{o}C. The percentage LOI should not exceed 5% or it will have adverse effects on the final cement. The insoluble residue is a fraction of clay-like compounds which are insoluble in hydrochloric acid. Magnesium oxide (MgO) is the component of cement responsible for the green-grey colour of concrete and is found in small quantities in limestone. Some 'dolomitic' limestones contain excessive quantities of MgO which can have a delayed expansion time of several years. Due to this delayed expansion property, dolomitic limestone is not used in cement manufacture (Czernin 1980).

2.1.2 Crack Control

Where a freshly poured concrete surface is allowed to dry, a pattern of cracks will often develop. These cracks can be widespread, are generally less than 25mm in length and do not cause structural damage. However freeze-thaw conditions can exacerbate the effect by causing damage from expansion and eventual spalling around the surface. The best way to avoid these cracks is to keep the concrete surface as wet as possible for at least 3 hours up to one day after pouring. Australian Standards permit the maximum moisture loss of 0.055 g/cm^2 of a surface in a 72 hour period (Orchard 1979). A close pattern of hair cracks known as crazing can also occur within the first year of pouring concrete. These cracks are caused by carbonation or differential shrinkage between the surface and internal body of a concrete specimen. Much like other crack mitigation strategies, keeping the concrete wet is the best way to ensure homogenous drying.

2.1.3 Efflorescence

Efflorescence is a common phenomenon which occurs on concrete brickwork and masonry which manifests as a white powder on the surface of those materials. The solution of sulphates or salts such as sodium, potassium and calcium penetrate the concrete. As water evaporates from the concrete, the salts are redeposited on the concrete surface.

2.2 Advantages and Disadvantages of Geopolymer Concrete

2.2.1 Advantages

Higher mechanical properties are a major reason for the continued investigation of geopolymer concrete. Literature on geopolymers is extensive and diverse and so too are the materials that are able to create geopolymer concrete. Quality of the final specimen is highly dependent on the source locality and quality of:

- The Al-Si source
- The activator
- The aggregate source and its grading
- The water source and
- The mix quantities of each material

Existing literature has looked at a range of different binders, activators and aggregates and the results all list similar advantages. As shown in Section 1.1.1, there is a large range of materials able to synthesise geopolymers and they are abundantly available through quarries or from industry by-products. Utilising industry waste like fly-ash from coal power plants and blast furnace slag from iron production creates a synergy. Storage and disposal costs facing the industry are reduced from the new demand that was previously non-existent.

As suggested by Allen and Brent (2010), CO_2 separation and geosequestration is of major concern in industrialised countries. This is a carbonation process whereby the presence of strong acids and alkaline causes carbonates to dissolve and release carbon dioxide. Basic ores also undergo carbonation after extended periods of exposure to strong chemicals. This

dissertation aims to reinforce existing documentation on the chemical resistance of geopolymer concrete which currently indicates this material is an excellent alternative to OPC under such conditions (Rangan 2008).

Shrinkage is one factor considered an advantage of geopolymer concrete. As confirmed by Glasby (2011, pers. comm., 4 May) the heat release during curing of fly-ash geopolymer concrete is much less when compared to typical concrete. The curing temperature of a 40 MPa OPC concrete peaked at 65-70^{O}C before returning to 25-30^{O}C within 2 days of curing. Taking the same time to return to ambient temperature, a batch of 40 MPa FAGC resulted in the curing temperature only peaking at 40^{O}C.

Table 4: Curing Temperature of OPC and FAGC (^{O}C)

Time (hours)	OPC	FAGC
0	22	21
3	30	30
6	39	39
9	62	40
12	65	39
15	69	38
18	63	36
21	56	34
24	50	32
27	45	31
30	42	29
33	39	27
36	36	26

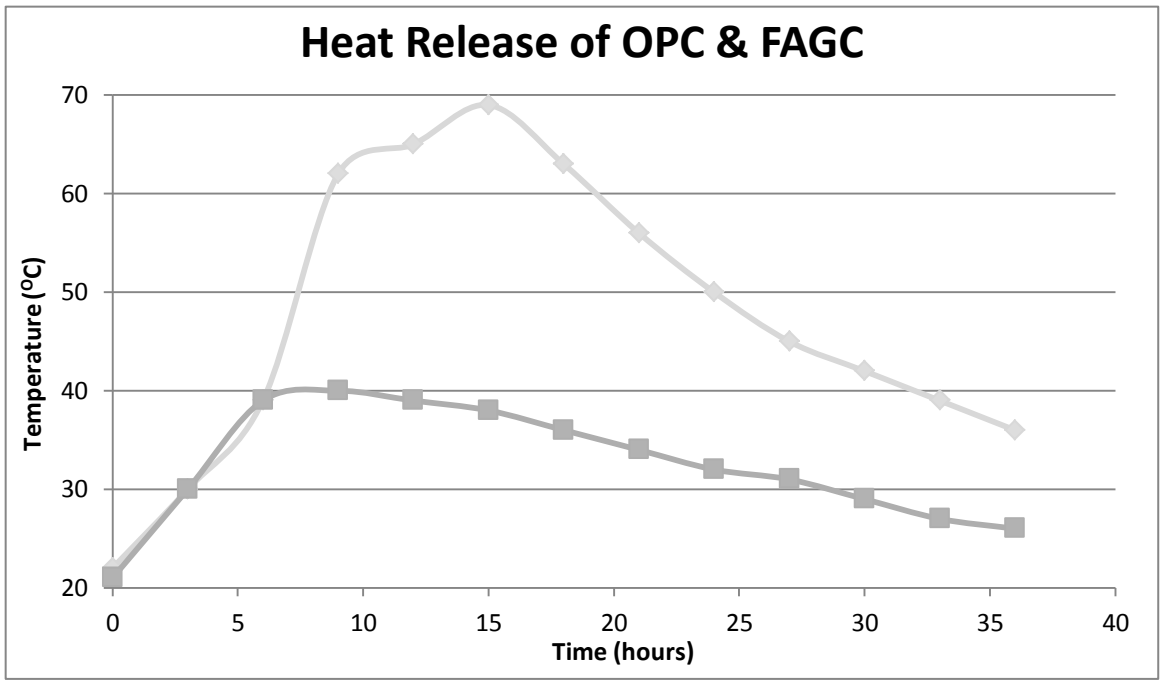

Figure 2: Heat Release of OPC and FAGC Concretes (Glasby 2011)

Heat release for the duration of curing is a major cause of macro and hairline cracking. The magnitude of shrinkage is exacerbated in hydraulic structures such as dams, weirs and tanks where the large surface area of concrete releases enormous quantities of energy. This is another area where geopolymer concrete has an advantage over OPC.

2.2.2 Disadvantages

The main disadvantage surrounding geopolymer concrete is the slow speed at which industry is embracing it. This is the result of at least three individual factors, the first being that information relating to service life and durability of this material is yet to be quantified due to the young relative age of research in this field. The financial and environmental costs of geopolymer are also highly variable. Williams (et al. 2011) indicates that costs can be cheaper or more expensive than Portland cement depending on a) the material source location, b) the energy source and c) modes of transport. Australia's 38 coal fired power plants generate an abundance of fly-ash that can be effectively used to reduce the local cost of building materials. At present, only a small amount of the total F.A. stockpile is used for concrete manufacture. Where the Al-Si source and other components are imported the financial benefits will obviously be reduced. Lastly, guidelines on recommended practice are still under review at this stage (CIA 2011).

2.3 Fly Ash and FAGC

Fly-ash describes any fine material which has been precipitated from the stack gases of furnaces burning solid fuel. Coal power plants create fly-ash in very large quantities as a by product of electricity generation. Fly-ash is an Al-Si material which means it can be used in the creation of geopolymers. It was initially used in concrete to act as a pozzolan, enhancing workability and strength amongst other properties as well as being able to reduce the severity of ASR (Alasali & Malhotra 1991).

2.3.1 Production of Fly Ashes

The first step in the electricity generation process is the combustion of finely ground coal at temperatures between $850^{O}C$-$1800^{O}C$. After being injected at high speed with a stream of hot air into a furnace, the coal is burnt instantaneously. While in suspension, the remaining material melts. All the fine material is then carried out by flue gases on rapid cooling and then solidifies into fine ash particles. After being removed from the boiler, 80% of this ash material is what's known as fly-ash. As per ASTM 618 there are two types of fly-ashes; class F is low in calcium oxide (CaO) with a content of less than 10% and is derived from bituminous coals. Class C is high in CaO with greater than 10% content and is produced from sub-bituminous and lignite coals (Davidovits 2008). ASTM C989 specifies typical class F fly-ash as having 4.3% CaO and typical class C fly-ash as having 27.4% CaO (Grace 2006).

2.3.2 Fly Ash Geopolymer Concrete

Wagners CFT division has recently introduced an innovative new concrete product that has very low carbon emissions. This chemically activated Al-Si binder completely replaces Portland cement with 80-90% blast furnace slag and fly-ash with the activating solution taking up the remaining 10-20%. This construction material has multiple advantages

including improved fire and heat resistance, high early strength, minimal shrinkage and less embodied energy. Compared to Portland cement – the embodied energy of which releases 800-1000 kg of CO_2 per tonne of production – FAGC emits 80% less green house gas.

Concrete is one of the most commonly used construction materials in the world. Production of cement in 2006 was 2.55 billion tonnes with more recent figures showing 2009 production at 3 billion tonnes indicating an increase in production by 18% over 3 years (Cembureau 2009) which will continue to increase with population. This growth highlights the need for sustainable initiatives in all types of infrastructure.

2.3.3 Existing Fly Ash based Research

A technical paper on FAGC by Hardjito (2005) concluded that this material showed excellent resistance to sulphate attack, undergoes low creep and suffers very little drying shrinkage. Another paper titled 'Structural Evolution of Fly Ash Based Geopolymers in Alkaline Environments' by Sindhunata (2008) revealed that immersing geopolymers in diluted pH14 alkaline solutions has little effect in terms of framework leaching of gel, pore network alteration or gel crystallisation. However, it was mentioned that more concentrated caustic solutions caused intense leaching and an eventual collapse of the mesoporous gel structure.

A paper by Phair et al. (2002) titled 'Fly Ash-Based Geopolymeric Binders Activated with Sodium Aluminate', discovered that an aluminate activated geopolymer was mechanically superior to typical hydroxide and silicate activated geopolymers. The major conclusion of this paper was that an aluminate activator also reduced energy costs. Hou et al. (2007) has suggested (2007) that using only sodium hydroxide to activate the geopolymer results in a weak bond between the paste and aggregate. His research indicated sodium hydroxide in combination with sodium silicate (liquid glass) was essential in ensuring a stable bond between the paste and aggregate. A simple way of assessing bond strength is by investigating the ease with which the binding paste flakes off the aggregate. A higher compressive strength typically reflects stronger bonding of the paste and aggregate.

2.4 Red Mud and RMGC

With up to 50% Al_2O_3 content, bauxite is one of the most important existing aluminium ores. The seven alumina refineries in Australia use the Bayer Process to immerse bauxite in dissolved sodium hydroxide (NaOH) at approximately 175^{o}C. The alumina is converted into aluminium hydroxide $Al(OH)_3$ and dissolved in the hydroxide solution, which will be smelted to produce aluminium in the next process. The remaining bauxite is a useless material called red-mud. The grades of bauxite in Australia range from 30-50 wt.% alumina content which results in bauxite residues of 1-2 tonnes per tonne of alumina production. The resource to waste ratio presents a very large disposal issue with substantial environmental implications. The Bayer Process involves a number of important steps which are listed below (AAC Ltd 2010) and illustrated by Figure 3.

- Bauxite grinding Bauxite particles are ground to <1.5mm
- Slurry storage Solution of hot NaOH is added to the Bauxite

- Digestion — Hydrated alumina is removed leaving alumina in solution
- Clarification — Undissolved ore solids are removed
- Precipitation — Hydrate slurry is formed and then classified by size. Fine particles are recycled in the precipitation process.
- Calcination — The coarse particles are transferred here and heated to 1000^{O}C. Chemically combined water is eliminated and Alumina is produced

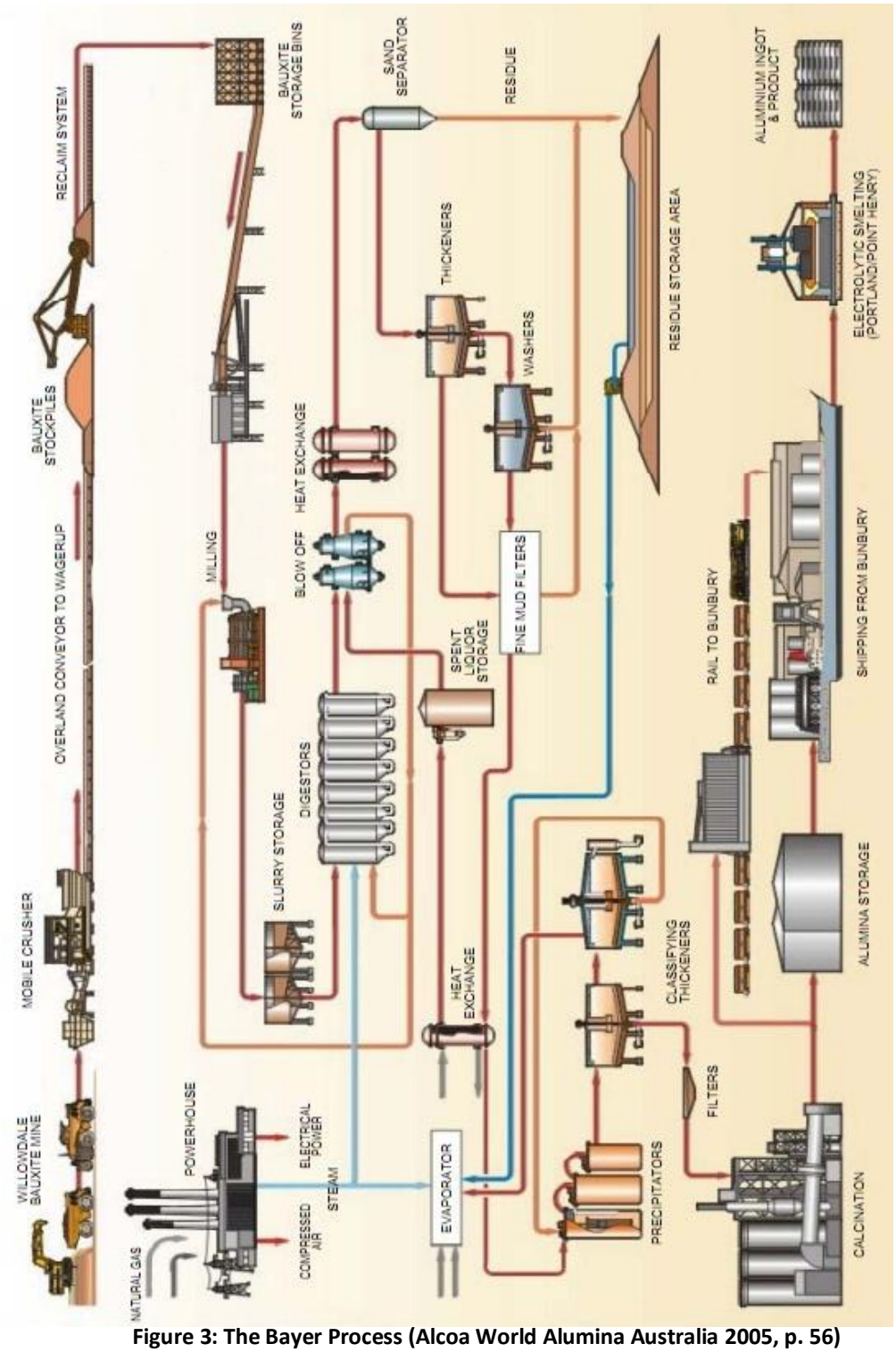

Figure 3: The Bayer Process (Alcoa World Alumina Australia 2005, p. 56)

2.4.1 Red Mud, Production in Australia

Australia is one of the world's largest producers of bauxite and alumina with a total of seven smelter grade alumina refineries.

Table 5: Alumina Refineries in Australia (AAC Ltd 2010)

Location	Operating Company
Gove, NT	Rio Tinto Alcan
Kwinana, WA	Alcoa
Pinjarra, WA	Alcoa
QAL, QLD	Rio Tinto Alcan
Wagerup, WA	Alcoa
Worsley, WA	BHP Billiton
Yarwun, QLD	Rio Tinto Alcan

Lottermoser (2010, p. 182) indicates that Australia currently produces up to 60 Mt of R.M. each year. Banvolgyi and Huan (2010, p. 2) confirm the density of R.M. is in the range of 2.6-3.5 t/m^3. Using these figures and the current Rawlinson construction cost guide (2011), a rate of \$5/m^3 has been interpolated for the storage and treatment of R.M. which equates to an approximate yearly storage cost of \$100M. This figure doesn't include the costs required to design and construct the red-mud dams currently used in dry mud stacking strategies.

2.4.2 Disposal Strategies

Red mud is a bauxite residue product after alumina has been dissolved during the Bayer Process. After the R.M. has spilled onto a bunding slab at 90-105^{O}C, dry mud stacking is one strategy which involves spreading the waste in layers and allowing those layers to dry. In its immediate state the pH level of R.M. is too high and does not permit plant growth. To stack more layers, each previous layer must be allowed to dry. By adding sea water to neutralise the R.M. to an approximate pH of 8.5, plant growth is possible.

In an effort to find an application for this otherwise useless material, an experimental batch of QAL R.M. based geopolymer concrete (RMGC) will be created and compared to the OPC and FAGC samples.

2.5 Carbon Emissions

The typical Portland cement production process involves calcination of limestone and silicate based materials at 1400^{O}C. At this temperature the calcium carbonate present in limestone, clays and shales convert to calcium oxide and carbon dioxide. The fuel required to heat, calcinate ($CaCO_3 \rightarrow CaO + CO_2$) and transport the cement are the primary sources of green house gas emission. Davidovits began to focus on CO_2 mitigation at Pennstate University materials research lab in 1990 by comparatively investigating the CO_2 emissions of fly-ash based geopolymer cement, kaolin based geopolymer cement and ordinary Portland cement. The results showed that 1 t of these materials produced 0.12, 0.18 and 1.08 tonnes of CO_2 respectively.

In 2009 Australia consumed approximately 8 million tonnes of cement with CO_2 emissions in the range of 6.3 million tonnes. As stated earlier (refer Section 2.3.2), the embodied energy required to produce 1 t of Portland cement releases 800-1000 kg of CO_2 into the atmosphere. Second to the burning of fossil fuels, the cement industry is the second largest emitter of carbon dioxide at approximately 6-8% of total global emissions. In contrast, the FAGC being used is an environmentally friendly concrete made by Wagner's whose binding components are comprised of 80-90% Al-Si. With cement binder representing 10-15% of concrete by mass, the reduction in CO_2 emissions from the final product is 60-70% (Wagners 2011). Consequently, this concrete has the potential to reduce CO_2 emissions in Australia by 3.8m-4.4m tonnes per year (CIF 2009). Global cement production as of 2010 was estimated to be 3.3 billion tonnes. Thus if geopolymer concrete were to replace OPC on a global scale it would have the potential to reduce carbon emissions by 2.1 billion tonnes per year (BPN 2011). To put this in perspective, 30.3 billion tonnes of carbon emissions were recorded globally in 2009 and the burning of fossil fuels was responsible for approximately 70% (CDIAC 2010; Datablog 2010). As of 2011, the World Resources Institute indicated that cars were responsible for 3.3bn tonnes of global emissions which equated to approximately 15% of global fossil fuel related emissions. Therefore, replacing OPC concretes with geopolymer concrete would be equivalent to taking two thirds of the world's traffic off the road each year.

2.6 Encapsulation of Waste Materials

2.6.1 Heavy Metal Encapsulation

With a high affinity towards heavy metal ions, geopolymers have the ability to solidify radioactive elements such as mercury, cadmium and cobalt. The polymer chain is typically composed of Al-Si but they can be replaced with toxic heavy metals. This ability stems from the large pore volume and surface area of the geopolymer matrix which can act as a host. One such encapsulation method is the Mercury Intrusion Process (MIP). It was mentioned by Sindhunata (2006) that an increase in curing temperature generally increases the total pore volume and surface area. This allows for a more intensive reaction process which in some cases can increase compressive strength. This encapsulation method tends to be emphasised by industrialised countries and was started by Canada in 1987. Contrary to industrialised countries, developing countries have a tendency to focus on reducing CO_2 emissions (Sindhunata et al. 2006, p. 3565).

2.6.2 Recycling Waste Water

Recycling of Wastewater by Immobilisation in geopolymer concrete (Tavor et al. 2007) is research that has developed from the information mentioned in Section 2.6.1. By using phenol to represent the organic/inorganic compounds in wastewater, conclusions showed diminished compressive strengths within the first 28 days. However, after this time the difference became negligible with strengths approximately returning to the original documented 85 MPa. The only notable variance in these strengths was where a different Al-Si source was used to polymerise the geopolymer (refer Section 1.1).

2.6.3 Other Research

The most significant property and reason for interest in geopolymers has come about due to their ability to, 'transform soft, disaggregated, or sludge like wastes into hard and cohesive solids in remarkably short time frames' (Tavor, Wolfson & Shamaev, 2007, p. 6801). Mine tailings are high in aluminium and silicon content which makes them the ideal candidate for a new construction material. The large volumes, associated storage and maintenance cost of mine tailings that Australia produces, creates a viable waste disposal mechanism for mining companies. Excellent chemical resistance and stability also makes geopolymer concrete an excellent candidate in the backfilling of obsolete mines which may otherwise deteriorate materials not resistant to acid or alkaline attack (Wagners 2011; Zhang L et al. 2011).

2.7 Chemical Resistance

2.7.1 Chemical Bunding

In assessing chemical resistance, it is important to choose a bunding material capable of handling volatile chemicals. Three suitable materials were investigated for this project; polyethylene, nickel alloy and pyrex. Basell Polyolefins (2010, pp. 13-20) and Borealis (1999, pp. 9-14) states that the behaviour of Low Density, Medium Density and High Density Polyethylene at 20^{o}-60^{o} when under the action of hydrochloric acid or sodium hydroxide is 'resistant' at any concentration where resistant is defined as, 'tensile strength at yield and elongation at break unchanged'. However, performance of polyethylene at 90^{O}C was not resistant. Despite research indicating nickel alloys were suitable for testing at both ambient and high temperatures, the material cost of nickel was too high for the available budget. Pyrex was found to be the most suitable material for chemical resistance testing due to its' availability, comparatively low price and high chemical resistance. This was confirmed by USQ Lecturer Dr Lynch (2011, pers. comm., 27 May). Consequently a number of 4.8 litre pyrex dishes were obtained to act as bunding for the chemicals.

2.7.2 Chemical Resistance of Cement

Concrete is bound by an alkaline hydrated cement paste which has a pH of 11±1. It will therefore dissolve in the presence of acids which are usually present in industrial wastes, mine tailings and in some waters. Chemical attack by acids can be particularly severe where the pH<4 and even worse where the acid solution has a velocity able to cause mechanical abrasion (Young et al. 1998). The exact velocities which accelerate chemical attack are variable and difficult to measure. The easiest way to measure the degree of attack would be to test a range of samples and compare the effects from different pH levels and velocities.

Chemical resistance of cement paste is directly related to its permeability, with less permeable pastes being more resistant to chemical attack. Sulphates (i.e. calcium, sodium or potassium) attack the aluminates in the cement and the subsequent reaction (where moisture is present) causes expansion leading to cracking. Severity of these attacks is generally determined by the concentration, temperature and velocity (or stagnation) of the solution (ASIC 2008).

2.7.3 Chemical Resistance of Other Concretes

For a more holistic comparison of the performance of concretes used in this project, the deterioration of other ordinary concretes under similar conditions has been investigated. Elena and Ivan (2003) investigated the chemical resistance of OPC, blast furnace slag (B.F.S.) Portland cement and sulphoaluminate belite (SAB) cement under the action of hydrochloric acid, sodium chloride and sodium sulphate. As recorded by Elena and Ivan, compression testing of these three concretes at 90 and 180 days revealed the performance shown by Table 6 (2003, p. 146).

Table 6: Mortars strength after 90 & 180 days in water, 0.5% HCl, 10% NaCl & 5% Na_2SO_4 solution

Solution	Time (days)	Compressive Strength		
		OPC (% Strength Retention)	**BFSPC** (% Strength Retention)	**SAB** (% Strength Retention)
Water	90	46.0 (100)	34.5 (100)	37.3 (100)
	180	48.4 (100)	37.8 (100)	56.0 (100)
0.5% HCl	90	38.6 (83.9)	28.0 (81.2)	28.6 (76.8)
	180	37.2 (76.9)	27.8 (73.5)	27.3 (48.8)
10% NaCl	90	40.8 (88.7)	28.0 (81.2)	43.8 (117)
	180	43.0 (88.8)	32.8 (86.9)	52.7 (94.1)
5% Na_2SO_4	90	52.2 (111)	40.5 (117)	43.8 (122)
	180	44.7 (92.5)	40.8 (107)	52.6 (94.0)

2.8 Alkali Silica Reaction (ASR)

In certain regions across the world, trouble with pop-outs and close pattern cracking in concrete work has become a common phenomenon. The most typical consequence of this phenomenon is widespread expansion, which sometimes leads to complete disruption and disintegration of the concrete. This expansion is due to the reaction between silica in the aggregate and alkalis in the cement (Orchard 1979). The cement alkalis are able to cause the same effect through a reaction with carbonates in the aggregate. This is known as the alkali silica reaction or alkali aggregate reaction. More specifically Bensted states (2002, p. 265), 'ASR is the reaction between hydroxyl ions in the pore solution of a concrete and certain forms of silica occasionally present in significant quantities in the aggregate'.

The product of ASR is a gelatinous hydrate gel containing the elements of silica, sodium, potassium, calcium and water. The volume of this alkali-silica gel is much greater than the silica consumed and its composition can vary from 0-20% Na_2O, 0.4-19% K_2O, 0.1-60% CaO and 28-68% SiO_2. The most important fact is that the alkali-silica gel can only form in the presence of calcium hydroxide $Ca(OH)_2$ or hydrated lime (Bensted & Barnes 2002, p. 265).

Figure 4: ASR Cracking (Bensted & Barnes 2002, p. 268)

To form $Ca(OH)_2$ calcium oxide must first come into contact with water which is expressed by $CaO + H_2O \rightarrow Ca(OH)_2$. As indicated by Figure 4, the beam that is covered from rainfall has no ASR cracking. Literature on the effects of this phenomenon in regards to geopolymer concrete is limited; however the calcium oxide content is still of interest (Bensted & Barnes 2002). Typical CaO quantities for Al-Si sources have been investigated from various locations. X-ray Fluorescence was also performed by Cement Australia to determine the constituents

of the Al-Si sources used to make RMGC for this project (refer Table 28). A comparison of the calcium oxide composition in these binder materials is shown by Table 7.

Table 7: Calcium Oxide Present in RMGC Binder

Component	Percentage	CaO/Al-Si (wt.%)	CaO in Binder (%)
Bosnian Red Mud	40%	3.96[+]	1.58
Gladstone Fly Ash	30%	3.48[*]	1.04
Typical ASTM C989 Slag	30%	39.20[#]	11.76
TOTAL	100%	N/A	14.38
Gladstone Red Mud	40%	5.20	2.08
Millmerran Fly Ash	30%	6.90	2.07
South East Asian Slag	30%	43.2	12.96
TOTAL	100%	N/A	17.11

(Source: [+]Cablik V. 2007, *Sindhunata et al. 2008 & [#]Grace W.R. 2006)

The only other material in a concrete mix containing calcium is DG20 and DG10 aggregate (approximately 10 wt.%) which is due to the fact that the majority of all aggregates are obtained and graded from basalt (geology.com 2011).

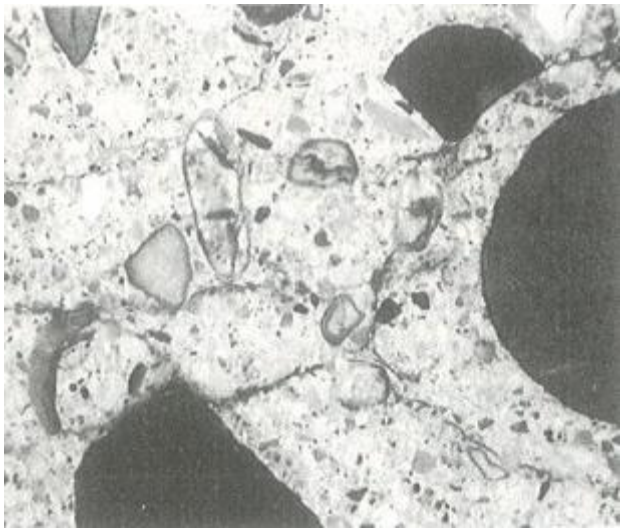

Figure 5: Internal crack pattern induced by ASR (Bensted & Barnes 2002, p. 269)

Nave indicates (2002) calcium is one of the most abundant minerals found in the earth's crust (approximately 3.6 wt.%) which is reflected in the composition of igneous rocks. Since cementitious materials are earth based derivatives, the development of calcium hydroxide is inevitable. Furthermore, calcium oxide is the primary constituent (63 wt.%) in portland cement (Bensted and Barnes 2002). Whilst the quantity of CaO in RMGC and other geopolymer concretes is much lower than OPC, alkali-silica gel has been found with CaO compositions as low as 0.1%. As is common practice, the effects of ASR are best minimised through the addition of fly-ash and other pozzolans in the mix design or by preventing contact with water after the curing process. Waterproof surface coatings can therefore help to prevent the formation of calcium hydroxide. For example, heating sodium silicate to 100^{O}C will precipitate all water out of the solution causing it to harden into a glass. Once

formed, this glass will not melt below temperatures of 650^{O}C (IMPCO 2010). This makes sodium silicate ideal for sealant applications such as the water proofing of concrete surfaces.

The most common type of consequence from ASR is map cracks, particularly in concrete sections which are lightly reinforced or loaded. Where the expansion is restrained by reinforcement or a specific loading, the crack has a tendency to form parallel to the direction of the restraint. Bensted (2002, p.267) indicates that deleterious ASR is rarely associated with spalling or scaling of concrete work. Other indicators of ASR occurrence are for the cracks to be bordered by sizeable zones of light coloured concrete and the appearance of permanent dampness where cracks meet. Crack widths are typically less then 1mm and penetrate the surface from 20-40mm deep. ASR cracking is generally only visible in concrete that has aged from 1-10 years. Load tests and destructive tests have been performed on affected structures and they have led to the conclusion that deleterious ASR can – but rarely does – have an adverse effect on structural performance (Orchard 1979; Bensted & Barnes 2002).

Where there is ingress from external alkali sources, the severity of ASR expansion can be affected. Hence, the R.M. bunding slab at QAL could be experiencing premature deterioration as a result of ASR being accelerated by the high concentration of alkali (225-235 g/L) in the R.M. waste. Whilst limited, research suggests that geopolymer concretes also suffer from ASR. The extent of ASR depends on the type, source location and quantity of binder as well as the activator (Trevor 2007). Referring to Table 7, RMGC contains no more than approximately 10 wt.% of calcium oxide. By comparing CaO quantities, the formation of $Ca(OH)_2$ in this concrete should therefore be much less than that experienced by OPC. Ultimately, there is still much research to be done on the physical and chemical differences of this phenomenon in regards to geopolymer concrete.

CHAPTER 3 Methodology

3.1 Cast & Number Concrete Samples

Table 8: Sample Age & ID

Chemical Testing Age	Sample ID		
H_2SO_4 at 20±2^{O}C			
7	OPC-1	FAGC-1	
14	OPC-2	FAGC-10	
28	OPC-3	FAGC-3	
28	OPC-4	FAGC-4	
56	OPC-5	FAGC-5	
H_2SO_4 at 90^{O}C			
7	OPC-6	FAGC-8	RMGC-7
14	OPC-19	FAGC-17	RMGC-9
28	OPC-7	FAGC-6	RMGC-8
56	OPC-8	FAGC-7	
NaOH at 20±2^{O}C			
7	OPC-9	FAGC-9	
14	OPC-10	FAGC-2	
28	OPC-11	FAGC-11	
28	OPC-12	FAGC-12	
56	OPC-16	FAGC-13	
NaOH at 90^{O}C			
7	OPC-15	FAGC-16	RMGC-4
14	OPC-18	FAGC-18	RMGC-5
28	OPC-13	FAGC-14	RMGC-6
56	OPC-14	FAGC-15	

Testing occurred during the months of August and September and at the commencement of chemical testing the ambient temperature was 18.3^{O}C while the oven temperature was maintained at 90^{O}C. As recorded by the Bureau of Meteorology (2011), the minimum and maximum mean monthly temperature during these months ranged from 18.2 to 21.05^{O}C. This temperature range is implied wherever 20^{O}C has been stated as the testing temperature.

3.2 Pre-testing Requirements

Original research pointed towards medium and high density polyethylene as being the best material to contain NaOH and H_2SO_4. For high temperatures and high concentrations of NaOH, nickel alloys were recommended as highly suitable by a number of sources. After further enquiry and discussion with chemistry professionals, pyrex was advised to be one of the finest NaOH resistant materials available (Lynch 2011, pers. comm., 27 May). Furthermore, pyrex is readily available and significantly cheaper than the alternatives.

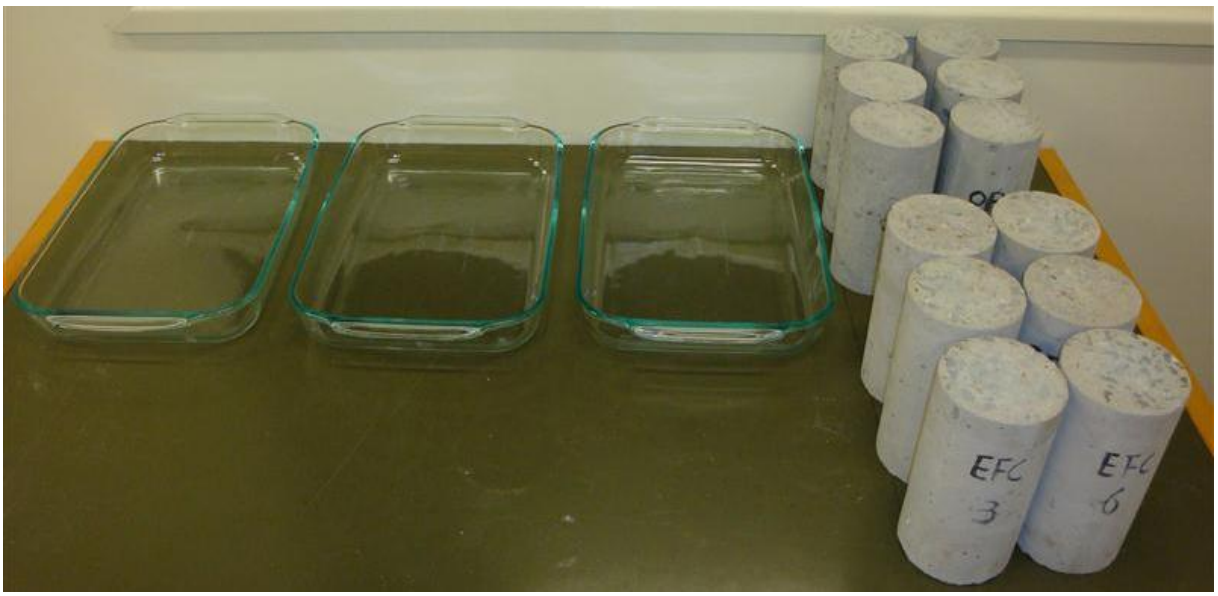

Figure 6: Pyrex Dishes used for Chemical Testing

Other things required for this project were the chemicals, chemical gloves, a thermometer, a pH tester, safety goggles, a gas mask, beakers, water jugs, a 6000g digital scale, a chemical face wash basin, cleaning rags and a water cleansing bottle.

3.3 High Temperature Testing

The testing laboratory in P2 contained an Australian made SEM oven of sufficient capacity to contain the necessary samples at the required temperature of 90^{O}C. Over a period of 56 days, the pH level of each solution was monitored for consistency every fortnight and the solution would be replaced where necessary. Evaporation at high temperature conditions was difficult to overcome even with a heat resistant thermoplastic cover. Without a covering, one litre would evaporate within 3 hours. The only solution was to monitor the solution as often as possible and top up the solution as required. Maintaining the original water level after any evaporation ensured the original pH was not diluted.

It becomes difficult to compare test results when chemical testing is performed at two vastly different temperatures. As indicated by Lynch (2011), the relative chemical age of the samples tested at high temperature involves collision theory. Confirmed by Volland (2005), this theory states that an increase in 10 degrees Kelvin roughly doubles the chemical reaction rate. This theory is an approximation, and the number of variables in this particular experiment is significantly greater than a typical reaction. This consequently decreases the accuracy of approximation. Consequently a 7 day test specimen at 90^{O}C compared to the same specimen at 20^{O}C has a relative chemical age of 2.5±1 year. Similarly, a 14 day test specimen in the same situation has a relative age of 5±2 years. A 28 day specimen will have a relative age of 10±5 years and a 56 day test specimen will have a relative age of 20±10 years. Some of the variables that create the need for such large tolerances include the fact that concrete is a composite material which already exhibits complex chemical reactions, concrete naturally absorbs carbon dioxide but it will release carbon dioxide in the presence of strong chemicals and water from the diluted chemical solutions is constantly evaporating.

3.4 Grinding of Samples

With the assistance of Wagners, concrete samples were made flush with the use of a custom made grinding machine. This machine grinds three samples simultaneously with a variable tipped circular blade. As the grinder is activated, water is pumped internally via a hose to keep frictional temperatures on the blade low during operation. Risk of injury with this machine is minimal to none as all movable parts are enclosed and tightened before the grinding process begins. The concrete surface on the lid side of the mould was grinded as that is the only side that isn't flush. This was the same side which was placed in chemical solution for testing.

3.5 Measure Mass

Before chemical testing of the concretes began, the individual mass of each sample was measured. This was done to quantify absorption properties from the changes in mass that were documented after testing was complete.

Table 9: Inital Mass of OPC and FAGC Samples

	OPC (g)	FAGC (g)
1	3663.7	3810.0
2	3668.0	3783.2
3	3672.7	3792.0
4	3666.7	3778.7
5	3672.8	3789.0
6	3684.4	3779.9
7	3660.7	3794.5
8	3642.2	3810.6
9	3686.4	3781.4
10	3647.7	3809.0
11	3704.7	3750.6
12	3679.1	3836.5
13	3670.6	3848.5
14	3708.5	3755.7
15	3680.8	3787.5
16	3680.0	3789.2
17	3671.4	3812.6
18	3696.9	3790.9
19	3678.5	3816.6

3.6 Chemical Testing

3.6.1 Practical

The surface area of concrete in contact with chemical solutions is calculated below.

Total Surface Area:

$= \pi . D . H + 2(\pi . r^2)$

$= \pi.100.200 + 2(\pi.50^2)$

$= 78{,}539.81mm^2$ *eq 1*

Submerged Surface Area:

$= \pi.D.h + \pi.r^2$

$= \pi.100.40 + \pi.50^2$

$= 20{,}420.35mm^2$ *eq 2*

S.A. under Chemical Attack:

$= \frac{eq\ 2}{eq\ 1} \times 100 = 26\%$

Therefore the surface area of concrete under chemical attack is approximately 26%. OPC and FAGC samples were placed approximately 40mm deep in chemical solution on Friday 12 August. On this same day the RMGC mix design was prepared. On Monday 15 August the RMGC was cast in a Haldwell Bennet mixer in Z1.101. In casting the RMGC, the recommended practice for geopolymer concrete was followed (CIA 2011). Following this recommended process meant dense graded aggregate was placed in the mixer first, followed by sand, binder, design water, activator and additives (see Section 6.1).

3.6.2 Measured Chemical Conditions

Chemical operating conditions were designed for the attacking solutions to contain 1M of sulphuric acid (H^+) and 1M of sodium hydroxide (OH^-). The chemical to water ratios were 1:19 and 1:18.2, and the average measured pH level was measured as 1.5 and 11.8 respectively (see Section 3.6.3).

3.6.3 Calibrated pH Testing

After concrete samples had endured a fortnight of chemical attack, it was typical for each chemical solution to have a high percentage suspended solids (from leaching and deterioration) at which point the solution was entirely replaced. In between these fortnightly replacements, the pH level was tested several times to ensure consistency and reliability in the final results.

Table 10: Calibrated pH Testing

Testing Condition	Concrete Type	Initial 4 Weeks			Final 4 Weeks		
20^OC H_2SO_4	OPC	1.5	1.4	1.4	1.7	1.5	1.4
	FAGC	1.6	1.8	1.9	2.0	1.7	1.6
90^OC H_2SO_4	OPC + FAGC	1.2	1.4	1.3	1.1	1.2	1.4
20^OC NaOH	OPC	12.3	11.9	11.8	11.6	11.7	12.0
	FAGC	11.5	11.4	11.4	11.2	11.6	11.4
90^OC NaOH	OPC + FAGC	12.2	11.9	11.9	11.8	12.1	11.9

As shown by these measurements, the pH level was consistently maintained and only varied slightly.

3.7 Mass Gain/Loss

The mass of each sample was measured after testing to determine the change in mass and quantify the absorption properties. These results are specified and discussed further in Chapters 4 and 5.

Table 11: Mass After Testing

Testing Condition	OPC (kg)		FAGC (kg)	
20^{O}C H_2SO_4	3676.4	+0.347%	3819.1	+0.239%
	3663.5	-0.123%	3863.5	+1.431%
	3667.3	-0.147%	3795.6	+0.095%
	3664.1	-0.071%	3783.1	+0.116%
	3661.7	-0.302%	3797.0	+0.211%
90^{O}C H_2SO_4	3610.6	-2.003%	3737.8	-1.910%
	3587.7	-2.468%	3690.4	-3.205%
	3561.0	-2.724%	3653.1	-3.355%
	3524.7	-3.226%	3713.5	-2.135%
20^{O}C NaOH	3706.8	+0.553%	3825.2	+1.158%
	3665.2	+0.480%	3796.8	+0.359%
	3726.9	+0.599%	3810.2	+1.589%
	3698.7	+0.533%	3897.3	+1.585%
	3720.8	+1.109%	3916.4	+1.764%
90^{O}C NaOH	3606.0	-2.032%	3752.4	-0.971%
	3604.5	-2.499%	3709.3	-2.153%
	3590.8	-2.174%	3786.3	+0.815%
	3666.5	-1.133%	3839.7	+1.378%

3.8 Sulphur Capping & Compression Testing

After chemical testing was complete and the samples were measured for their change in mass, the samples would be taken to the Z1.101 lab and sulphur capped in preparation for compression testing (see Figure 7). Care was always taken to ensure the caps were flush, but this was not always possible. This was undesirable as it has inevitably affected the validity of test results. Leaving the sulphur caps to cure for a minimum of 24 hours, the compressive strength was determined and compared to the average characteristic strength (see Section 7.1 and 7.3). All compressive strengths were obtained at the University of Southern Queensland using the Avery Compression Testing machine located in Z108. Characteristic strength was obtained for the OPC and FAGC samples at the approximate age of 28 and 56 days. Due to time constraints, characteristic strength of the RMGC samples was only obtained at an age of 16 and 32 days.

Figure 7: Sulphur Capped Samples

3.9 Macro & Micro Analysis

3.9.1 Macro Analysis

The area of concrete under attack has been photographed in order to understand and discuss any potentially damaging physical manifestations. These photographs focus on the depth and severity of chemical attack on the relevant end of the sample. An example of the images used for this analysis is shown by Figure 8.

(a) OPC - H_2SO_4 - 14d - 90^{O}C (b) FAGC - H_2SO_4 - 28d - 20^{O}C (c) RMGC - Unaffected

Figure 8: OPC exposed to H_2SO_4 at 90^{O}C

Due to the extent of images used please refer to APPENDIX F for the entire macro analysis. These images have been studied and the findings are shown on the following page.

Table 12: Macro Analysis Results

Testing Conditions	Sample ID		Results
20^{O}C H_2SO_4	7d	OPC-1	At 7 days, the sample began corroding. A yellow colouration indicated oxidation of hydrogen sulphide. This has been produced by the deposition or penetration of elemental sulphur into the concrete surface. White spots are also evident which indicate calcium carbonate ($CaCO_3$) has decomposed into gypsum ($CaSO_4$) (Shook & Bell 1998).
	14d	OPC-2	After 14 days in sulphuric acid, more aggregate has become visible which indicates prolonged attack and some loss of mass.
	28d	OPC-3 OPC-4	More aggregate became visible in the 28 day samples which indicated the concrete paste was being attacked. The yellow colouration of hydrogen sulphide was again noted, this time at the water level where the most oxidation occurs. As indicated by a very soft outer layer, the cement paste had began weakening.
	56d	OPC-5	Observations for this sample are similar to OPC-7
	7d	FAGC-1	Inconsistent spots of discolouration were noticed up to 40mm above the attack line. No spalling had occurred. Very minor attack was noticed on coarse sand particles and finer aggregate.
	14d	FAGC-10	No damage has occurred yet the colour of the entire specimen (except the top 40mm) is a patchy dark grey colour.
	28d	FAGC-3 FAGC-4	FAGC-3: No attack has occurred on the submerged 40mm cylindrical section. However corrosion was noticed on the underside of the sample. FAGC-4: Observed behaviour was identical to FAGC3. In addition, 1-5mm circumferential cracking was noted.
	56d	FAGC-5	At this stage, there had been minimal attack evident on the side of the sample. Circumferential cracking had developed up to 3mm thick around the entire sample. Minor to medium corrosion had begun to progress on the bottom surface. Some white patchiness had developed in the centre of the base.
90^{O}C H_2SO_4	7d	OPC-6	At 7 days, corrosion was well advanced and the yellow colouration of hydrogen sulphide formation is

			present.
	14d	OPC-19	The 14 day sample displayed a greater quantity of hydrogen sulphide and a number of cracks began developing up to 3mm from the circumference
	28d	OPC-7	Significant attack is evident on this 28 day sample. White spots and streaks indicate decomposition of $CaCO_3$ to $CaSO_4$ (gypsum). At the water level, differential oxygen levels have promoted the growth of hydrogen sulphide. This is also evident on OPC-5.
	56d	OPC-8	A large quantity of hydrogen sulphide formed on this sample also with white streaks indicating decomposition of $CaCO_3$ to $CaSO_4$. Substantial corrosion of the concrete surface caused cracking several millimetres deep throughout both the cement and the aggregate.
	7d	FAGC-8	Concrete surface only just begun to corrode. No spalling was evident at this stage. Yellow colouration has developed on the bottom surface. Dark grey colour exists at the line of chemical attack.
	14d	FAGC-17	With more severe corrosion 3mm circumferential cracking and attack of aggregates became evident. No change in colouration was noticed.
	28d	FAGC-6	Chemical attack had begun to interfere with the interface between the binder paste and aggregate causing cracking. Minor spalling (up to 1mm thick) was evident from the penetration of acid solution into the concrete. The effect was uniform across the submerged section.
	56d	FAGC-7	By this stage a large amount of corrosion had occurred which caused 3-5mm circumferential cracking around the entire sample and revealing more aggregate. A uniform yellow colouration had also developed on the attacked surface.
	7d	RMGC-7	At an age of 7 days, this RMGC sample had a limited yellow colouration on the bottom surface coupled with a white formation where the water level was.
	14d	RMGC-9	A white formation at the water level was again noted. At this stage no corrosion had occurred. A concentration of very small reflective minerals was noticed at the water level. The cause of this could be oxidation of minerals.
	28d	RMGC-8	As with the 7 and 14 day sample, a yellow and white

			formation formed at the water level. After 28 days no spalling was evident and minimal corrosion had occurred. The attacked surface decomposed slightly, turning the binder paste into a greyish colour. The decomposed and grey coloured surface appeared to resist further chemical attack.
20^{O}C NaOH	7d	OPC-9	Minor efflorescence was noted with no damage.
	14d	OPC-10	At 14 days a 70mm thick dark grey colouration developed above the level of chemical attack. There was no damage and still only minor efflorescence at this stage.
	28d	OPC-11 & OPC-12	For both of these samples the same dark colouration as with OPC-10 developed (70mm thick) with a greater degree of efflorescence on these samples.
	56d	OPC-16	Efflorescence was its most severe at 56 days. Where these salts redeposited on the concrete surface very minor damage was caused. No damage was noted on the bottom of the specimen.
	7d	FAGC-9	No damage was visible. Minor efflorescence on one side was noted.
	14d	FAGC-2	No damage had developed. A dark grey coloured ring was observed 40mm thick immediately above the line of chemical attack. White colouration was evident on the submerged end from hydroxide salts.
	28d	FAGC-11 & FAGC-12	FAGC-11: Efflorescence had encompassed 60% (by height) of the sample. Some minor spalling was noted around the attacked area (<1mm thick). Dissolving the efflorescence revealed spalling which made aggregate visible. This was caused by external alkali induced ASR (refer Figure 19). FAGC-12: Observed behaviour was identical to sample 11. However, the efflorescence was more widespread on this sample. (Note: The rough state of the 'attacked' surface on this sample was from the grinding process. This appearance is found on other samples too)
	56d	FAGC-13	Severe efflorescence had developed across 70% of the sample (by height)
90^{O}C NaOH	7d	OPC-15	At 7 days of age, no damage or spalling was visible. There was a minimal build up of hydroxide salts on the bottom of the sample.
	14d	OPC-18	After 14 days, there was again no visible damage.

			The build up of hydroxide salts was larger.
	28d	OPC-13	White spots which appeared to be calcium hydroxide $Ca(OH)_2$ developed on the attacked end of the specimen. NaOH salts were deposited on the surface leaving a white colour and no damage was observed.
	56d	OPC-14	This sample exhibited a 40mm thick dark discolouration above the area of attack. The sample end under attack was white from NaOH salts. At this age, there was again no damage or spalling.
	7d	FAGC-16	No spalling or damage was noticed. The remnant colour of the attacked area was not only white from the hydroxide salts, but a dark grey colour. A darker version of this colour had concentrated at the line of chemical attack.
	14d	FAGC-18	Hydroxide salts remained on the attacked end of the sample. Minor spalling was noted around 1/6 of the circumference.
	28d	FAGC-14	The surface under chemical attack was stained a light brown colour and a grey coloured ring had developed at the line of chemical attack. Hydroxide attack appeared to focus on coarse sand particles.
	56d	FAGC-15	No attack occurred on this sample. The flush surface obtained from grinding was still there. A quantity of hydroxide staining was evident with a consistent patch of light brown spread across the attacked area.
	7d	RMGC-4	There was minimal, if not zero indication of chemical attack at this age.
	14d	RMGC-5	After 14 days, RMGC-5 exhibited micro cracks. However, these cracks may have been pre-existing. The typical white colour of sodium hydroxide remained and no damage was noted.
	28d	RMGC-6	Apart from potentially pre-existing micro cracks, the white colour of NaOH salts still remained and nil damage was observed.

3.9.2 Micro Analysis

For this section, 28 day samples at 90^{O}C have been cut to an approximate 50mm thickness, sanded flat and analysed at 20x magnification. Half of these images were taken from the unaffected end of each specimen. The remaining images focus on areas of chemical attack in order to compare and discuss any irregularities.

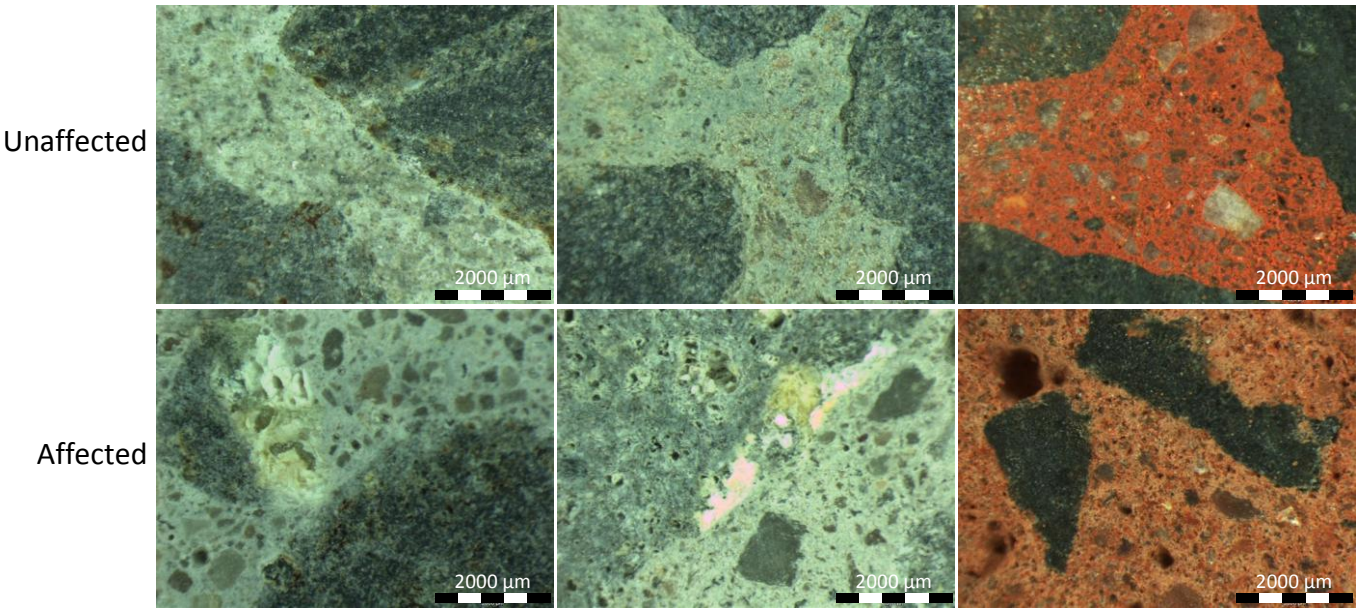

(a) OPC (b) FAGC (c) RMGC

Figure 9: Samples in H_2SO_4 at 90^{O}C for 28d

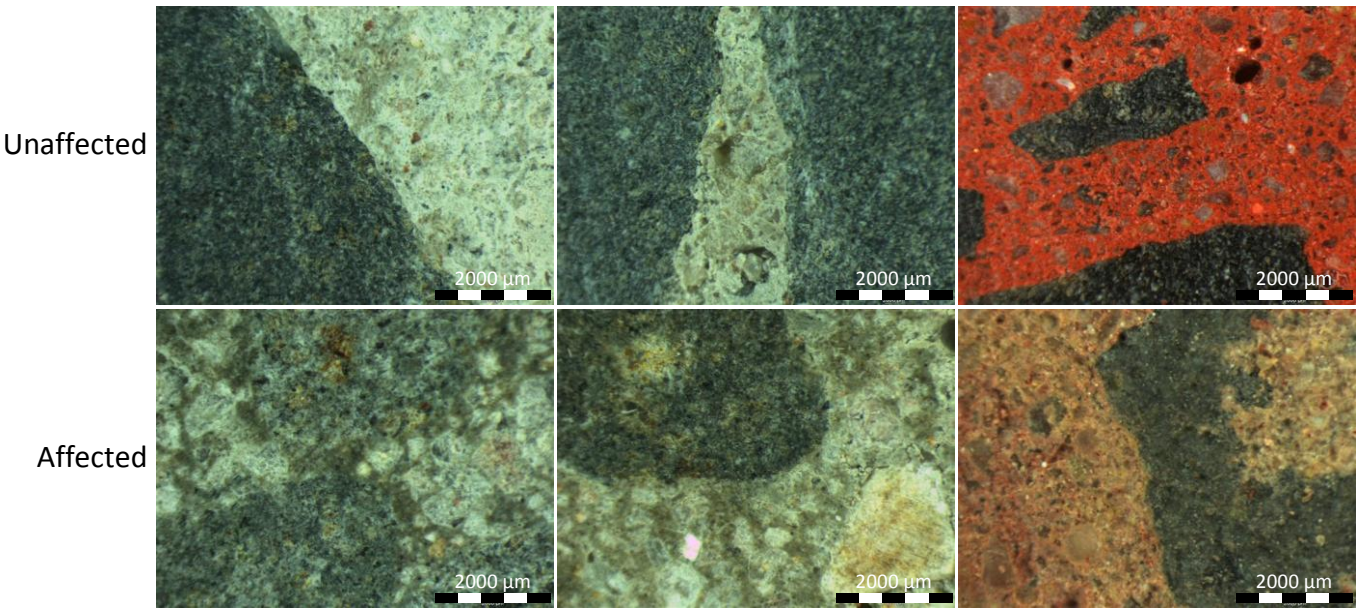

(a) OPC (b) FAGC (c) RMGC

Figure 10: Samples in NaOH at 90^{O}C for 28d

A discussion of this analysis can be found on the following page. To view all of the images taken during micro-analysis see APPENDIX G.

Table 13: 28 Day Micro Analysis Results

Testing Conditions	Sample ID	Results
90^{O}C H_2SO_4	28d OPC	More aggregate is visible per unit area on the attacked version of this sample. The white formation in Figure 9(a) appears to gypsum formed from decomposed $CaCO_3$ (Shook & Bell 1998).
	28d FAGC	Some mineral deposits can be seen on the aggregate, potentially from the acid. Some white and yellow spots of colouration are visible at the binder-aggregate interface (gypsum and hydrogen sulphide).
	28d RMGC	Instead of corroding, the affected material shows some deposit or transfer of material onto the aggregate. It is potentially sulphur remnants from a reaction with H_2SO_4 and the concrete surface.
90^{O}C NaOH	28d OPC	Comparing the effects in this condition, the cement paste (not aggregate) has been clearly affected as indicated by a darkened grey colour. The paste-aggregate interface has been compromised in some sections.
	28d FAGC	Deposition of hydroxide salts has occurred. Minor cracking has developed in some sections at the binder-aggregate interface.
	28d RMGC	Similar to RMGC in the acid environment, it appears that a combination of the binder paste and hydroxide salts has coated the surface. This conclusion was made because the unaffected sample did not have such an appearance.

CHAPTER 4 Ordinary Portland Cement Concrete

4.1 Mix Design

The OPC samples for this project contained 56.25%, 18.75% and 25% Portland cement, B.F.S. and F.A. respectively. Whilst the term OPC has been used – implying no addition of pozzolans – the mix design was blended. Over the past several decades standards have been redefined and papers have been published that promote the use of F.A., B.F.S. and other pozzolans in ordinary concrete mixes to reduce material cost by using less Portland cement whilst improving specific properties. This practice means that in today's construction industry, 100% Portland cement is rarely used. The use of pozzolans and additives is now considered ordinary practice and while some would refer to this as multi-blended cement, this dissertation has referred to all of these samples as OPC.

4.2 Casting Process

Mixing and casting of the OPC samples was well controlled as it was done in the laboratory at Wagners on 21 June 2011. The slump of this batch was measured as 200mm from a specified slump of 160mm. After mixing the batch in a Haldwell Bennett mixer, the samples were poured in two layers into standard 200x100mm cylindrical moulds and placed on a vibrating table to reach standard compaction. Out of the 22 samples, 2 were not compacted sufficiently by the table and consequently were not used for testing purposes. These samples were placed in low pH curing baths for 3 days to allow sufficient curing before being collected and transferred to the lab in P2 at USQ.

(a) Casting (b) Finished Samples

Figure 11: OPC Sample Preparation

4.3 Results

4.3.1 Absorptivity

These samples were placed approximately 40mm deep in chemical solution for testing purposes, which equates to 26% of the samples' total surface area. Of all the samples, one was submerged in the same level of water to observe its absorptivity. Measurements were taken several times and the change is expressed as a percentage relative to the initial mass.

Table 14: Absorptivity of OPC-17 in Water

Absorption Time (days)	M_i	M_f	ΔMass (%)
14	3671.4	3690.0	0.507
24	3671.4	3687.1	0.428
28	3671.4	3687.1	0.428
42	3671.4	3684.1	0.346
56	3671.4	3683.9	0.340

M_i = inital mass

M_f = final mass

The results in Table 14 indicate that constant exposure to water allows the concrete to continuously hydrate. This causes further expansion of the cement paste gel. As the paste expands, the void ratio decreases which causes permeability and absorptivity to decrease. The change in mass (wt.%) for the chemically tested samples is shown in Table 15.

Table 15: OPC Absorptivity in Chemicals

Testing Condition	Absorption Time (days)	M_i	M_f	ΔMass (%)
20^OC H_2SO_4	7	3663.7	3676.4	+0.347%
	14	3668.0	3663.5	-0.123%
	28	3672.7	3667.3	-0.147%
	28	3666.7	3664.1	-0.071%
	56	3672.8	3661.7	-0.302%
90^OC H_2SO_4	7	3684.4	3610.6	-2.003%
	14	3678.5	3587.7	-2.468%
	28	3660.7	3561.0	-2.724%
	56	3642.2	3524.7	-3.226%
20^OC NaOH	7	3686.4	3706.8	+0.553%
	14	3647.7	3665.2	+0.480%
	28	3704.7	3726.9	+0.599%
	28	3679.1	3698.7	+0.533%
	56	3680.0	3720.8	+1.109%
90^OC NaOH	7	3680.8	3606.0	-2.032%
	14	3696.9	3604.5	-2.499%
	28	3670.6	3590.8	-2.174%
	56	3708.5	3666.5	-1.133%

The first five samples were those in 20^{O}C H_2SO_4 starting at 7 days submersion time. At this stage, the acid solution had not been in contact with the sample long enough to cause corrosion of the material. The solution is actually absorbed by the concrete increasing its mass by 0.35%. As time progressed, it was seen that the 56 day sample experienced a progressively decreasing percentage change in mass until reaching -0.3%. The change in mass for those samples in sulphuric acid at high temperature was much higher starting with a -2% reduction in mass. This was attributed to all free water within the concrete being evaporated. Over the total 8 week testing period, the remaining change in mass was attributed to corrosion of the material which resulted in the mass linearly dropping from -2% to -3.2%.

Those samples submerged in sodium hydroxide at room temperature exhibited no progressive change in mass with time. The majority of samples exhibited very similar gains in mass (around +0.5 to +0.6%). As the solution is absorbed by the concrete and the hydroxide salts are redeposited on the surface of the concrete, the mass of those salts is added to the mass of the sample. Samples tested in sodium hydroxide at 90^{O}C exhibited similar losses to those samples in acid. This was because the percentage change in mass was typically -2% in both situations which is again attributed to evaporation of free water within the samples. Efflorescence was not an issue in the oven-based testing due to the fact that the concrete samples were completely dry. Thus the only evaporation that could occur was directly from the pyrex dishes.

4.3.2 Characteristic Strength

OPC samples were placed in solution for chemical testing on 12 August at 52 day strength along with the FAGC samples. At the milestone testing day, samples were removed from the solution for sulphur capping and subsequent compression testing. This next table summarises the characteristic and failure strengths of each sample.

Table 16: OPC Characteristic Strength

Sample Age	Sample ID	F'_C (MPa)
28	OPC-20	41.9
28	OPC-21*	24.9
56	OPC-22	47.0
N/A	AVG (20, 22)	44.5

The compression testing result from sample OPC-21* was excessively low compared to the other tests. Inspection of this sample during testing revealed non-flush sulphur capping. For this reason, that result was excluded from the average. Shown next are the stress strain plots which were used to determine the characteristic strength of OPC. Images of OPC-20 and OPC-22 have been paired with the plots to provide an indication of the casting quality. For an indication of the characteristic strength of OPC at 28 and 56 days, see Figure 12. A typical failure mechanism is exhibited by the 28 day sample which experiences a 45^{O} shear failure at approximately 42 MPa.

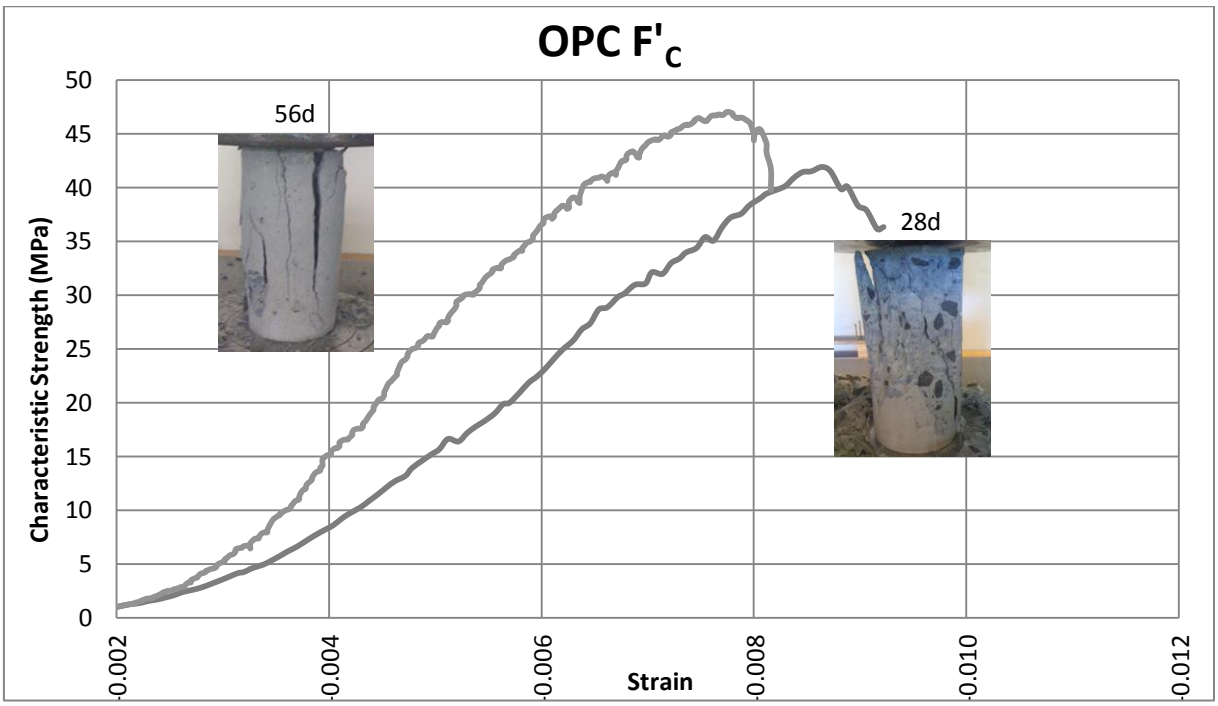

Figure 12: Characteristic Strength of OPC

4.3.3 Strength after Acid and Alkaline Attack

Strength after acid attack over the testing period is shown by Table 17 and Figure 13. Those at 20^{O}C for 7 days and 90^{O}C for 14 days were classed as outliers and excluded from the plot.

Table 17: Failure Strength of OPC in H_2SO_4 (MPa)

Age	H_2SO_4 20^{O}C	H_2SO_4 90^{O}C
0	44.5	44.5
7	26.9	39.5
14	41.3	23.7
28	41.9	39.7
56	33.1	33.4

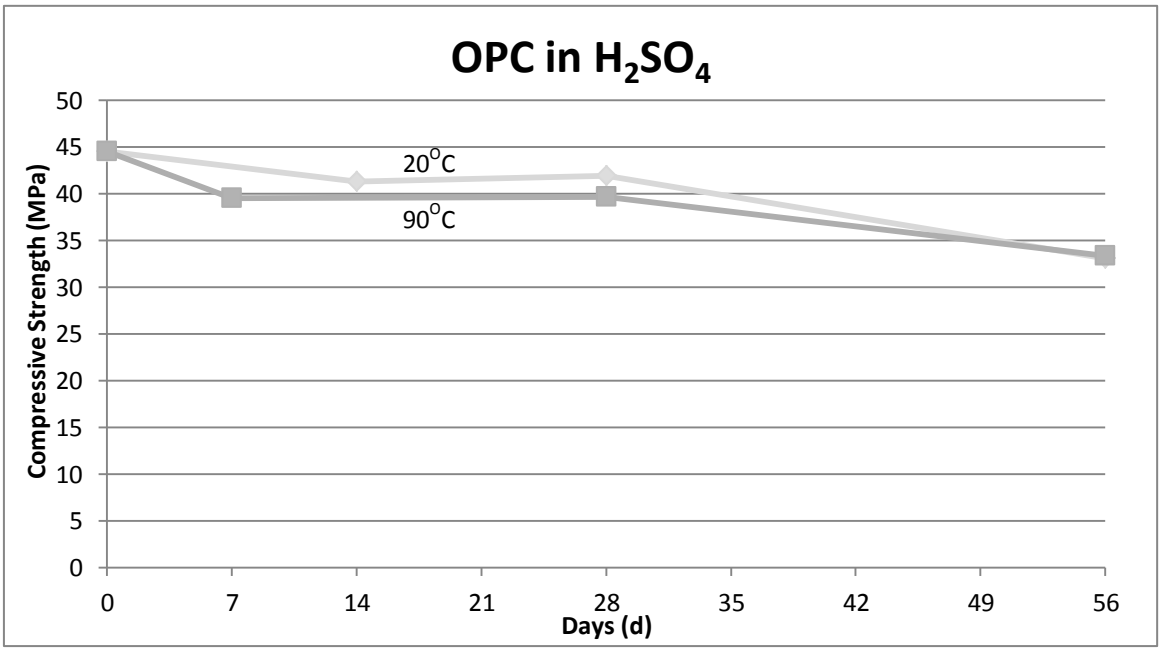

Figure 13: Failure Strength of OPC in H_2SO_4

The reliable results indicate that OPC experiences some strength deterioration in sulphuric acid. In both conditions, OPC fails at approximately 33 MPa which is 11 MPa less than its original strength.

Investigating Table 18 reveals samples at 20^{O}C for 7 days and 90^{O}C for 14 days are unreliable. These values have been considered outliers and are excluded from the plot.

Table 18: Failure Strength of OPC in NaOH (MPa)

Age	NaOH 20^{O}C	NaOH 90^{O}C
0	44.5	44.5
7	44.4	30.3
14	37.1	44.4
28	29.5	27.1
56	43.5	38.6

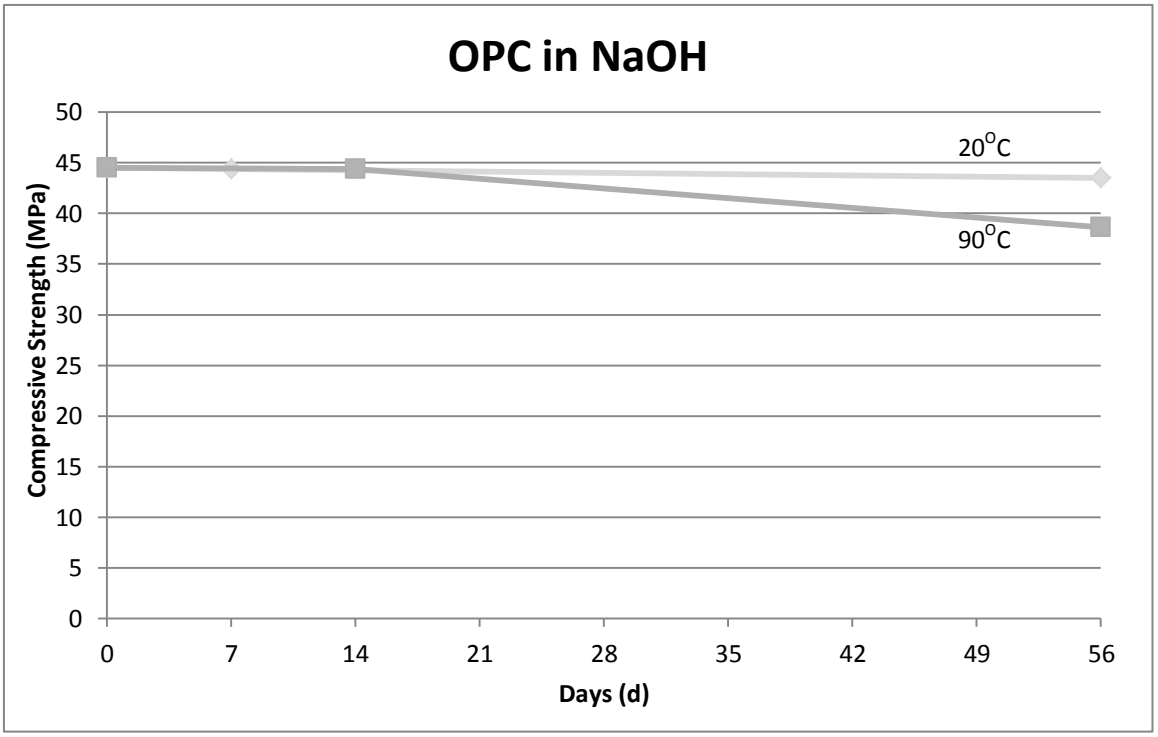

Figure 14: Failure Strength of OPC in H_2SO_4

Whilst the general trend of OPC in sodium hydroxide is a decrease in strength, the 56 day test samples at both temperatures have performed rather well compared to the preceding results. After plotting the relevant data, OPC exhibits negligible strength deterioration in sodium hydroxide at room temperature (<1 MPa). High temperature results indicate strength deterioration to 38.6 MPa which is 86% of its original strength. To view all of the stress strain plots that relate to these figures see APPENDIX C.

CHAPTER 5 Fly Ash Geopolymer Concrete

5.1 Casting Process

The FAGC samples were cast on 19 April 2011. The specified slump was 160mm and the actual slump was 200mm. After standard pouring and compaction with two layers and tamping 25 times per layer in standard 200x100mm moulds, these samples were trowelled, covered and left to cure on site over a period of 24 hours. After this time they were transferred to the lab in P2 at USQ.

(a) Casting (b) Finished Samples

Figure 15: Preparation of FAGC Samples

5.2 Results

5.2.1 Absorptivity

The FAGC samples were also placed approximately 40mm deep in chemical solution for testing purposes (26% by the samples' total surface area). Of all the samples cast, one was placed in the same level of water to quantify absorption properties over time. The following table indicates the change in mass of this sample (FAGC-19). Measurements were taken several times and the change is expressed as a percentage of the initial mass.

Table 19: FAGC Absorptivity in Water (Sample FAGC-19)

Absorption Time (days)	M_i	M_f	ΔMass (%)
14	3816.6	3863.1	1.218
24	3816.6	3860.0	1.136
28	3816.6	3856.0	1.032
42	3816.6	3849.4	0.859
56	3816.6	3862.1	1.191

While these results may first indicate that FAGC absorbs more than twice the amount of water that OPC absorbs – relative to the original mass – this is more likely due to the quality of compaction performed during casting resulting in a higher void ratio. Since water and hydration is not the hardening mechanism for geopolymer concrete, the relative rate of

absorption in water over this testing period is almost constant. The small variance between results can be attributed to evaporation.

Table 20: FAGC Absorptivity in Chemicals

Testing Condition	Absorption Time (days)	M_i	M_f	ΔMass (%)
20^OC H_2SO_4	7	3810.0	3819.1	+0.239%
	14	3809.0	3863.5	+1.431%
	28	3792.0	3795.6	+0.095%
	28	3778.7	3783.1	+0.116%
	56	3789.0	3797.0	+0.211%
90^OC H_2SO_4	7	3810.6	3737.8	-1.910%
	14	3812.6	3690.4	-3.205%
	28	3779.9	3653.1	-3.355%
	56	3794.5	3713.5	-2.135%
20^OC NaOH	7	3781.4	3825.2	+1.158%
	14	3783.2	3796.8	+0.359%
	28	3750.6	3810.2	+1.589%
	28	3836.5	3897.3	+1.585%
	56	3848.5	3916.4	+1.764%
90^OC NaOH	7	3789.2	3752.4	-0.971%
	14	3790.9	3709.3	-2.153%
	28	3755.7	3786.3	+0.815%
	56	3787.5	3839.7	+1.378%

The fly-ash geopolymer concrete samples in room temperature acid solution experienced no decrease in mass. Referring to the respective images (Appendix F.2), it is evident that only minor corrosion occurred by the end of the testing period. High temperature testing in acid shows free water in the FAGC samples has evaporated, but the changes in mass were not progressive. This is most likely due to evaporation of water from the diluted chemical solution which has caused the concrete samples to absorb different quantities of solution over the 56 days. At an age of 7 days – unlike its OPC counterpart – FAGC had not begun corroding. According to the images in Appendices F.2.1 and F.2.2, corrosion was not evident until the FAGC had been in solution for 14 days. This explains the sudden change in mass at 7 days from -1.9% to -3.2% at 14 days.

Room temperature testing of sodium hydroxide exhibited a consistent increase in mass of 1.2 to 1.7% which can be attributed to deposition of hydroxide salts through efflorescence. The changes in FAGC mass at high temperature were also erratic. This may be from prolonged exposure to the alkaline solution causing greater deposition of hydroxide salts.

5.2.2 Characteristic Strength

Chemical tests for the FAGC samples ensued when the samples were at a subsequent age of 115 days on 12 August. The information below summarises the characteristic and failure strengths of the FAGC specimens.

Table 21: FAGC Characteristic Strength

Sample Age	Sample ID	F'_c (MPa)
29	FAGC-20	28.0
29	FAGC-21	29.9
64	FAGC-22	26.7
174	FAGC-19	31.0
N/A	AVG(19-22)	28.9

All compression tests for these samples were consistent with a variability of only 3 MPa across the four samples. The stress and strain plot that illustrates FAGC characteristic strength is shown by Figure 16.

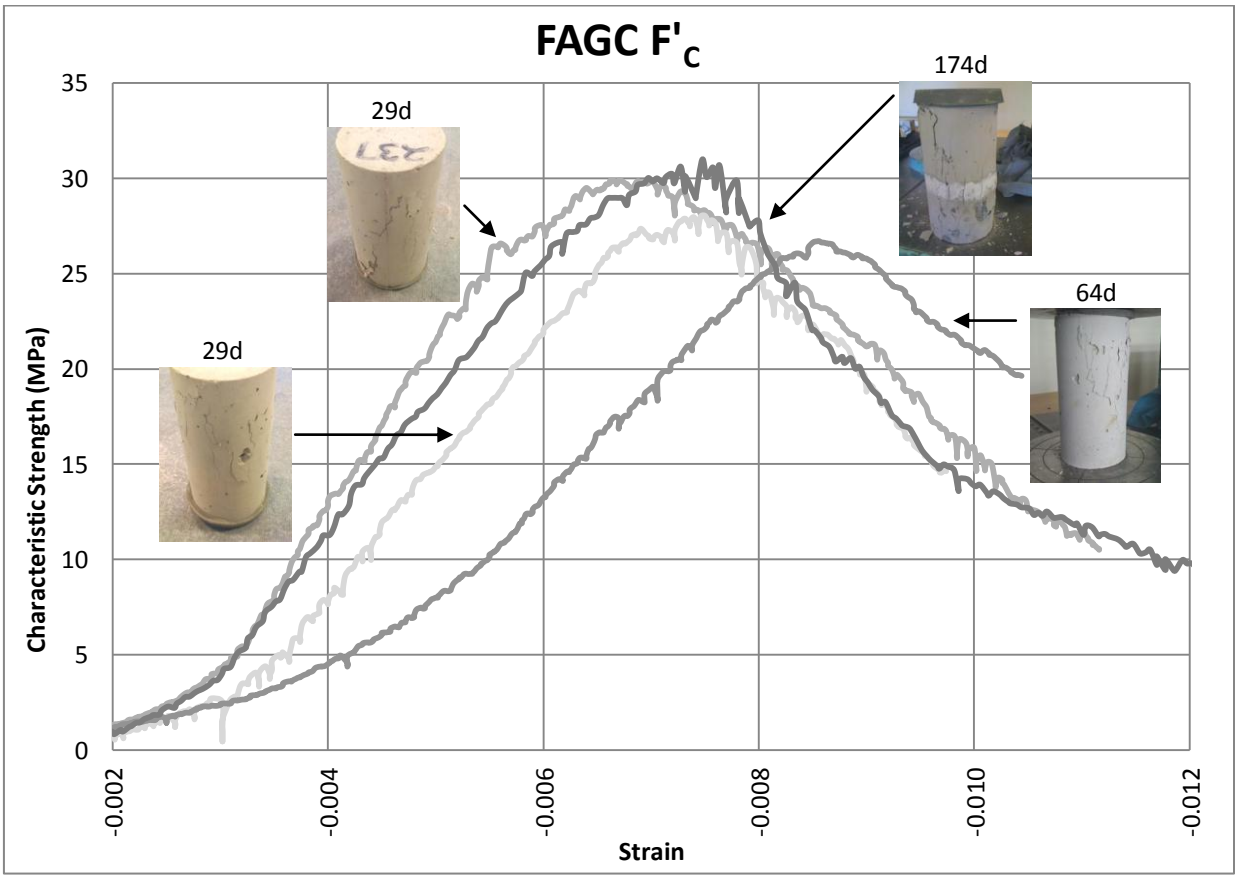

Figure 16: Characteristic Strength of FAGC

The 174 day strength reading was taken from the same sample that quantified FAGC absorptivity. Even after 174 days, the characteristic strength did not vary much from its 28 day characteristic strength. This is a good indicator that water has no hardening or weakening effect on geopolymer concrete.

As indicated by these stress strain plots (and those from APPENDIX D), all the geopolymer concrete samples that were compression tested exhibit an almost symmetric bell curve. This suggests that geopolymer concrete undergoes a ductile failure mechanism (unlike OPC) which is advantageous as it better satisfies serviceability criteria. Conversely, almost every OPC sample failed unpredictably within seconds of reaching ultimate compressive strength.

5.2.3 Strength after Acid and Alkaline Attack

With the average characteristic strength calculated, the failure strength at 7, 14, 28 and 56 days is now shown and discussed. In room temperature acid, this concrete experienced a slight increase in strength. At 90^{O}C, strength steadily declined to 24 MPa. As indicated by Table 22 and Figure 17, FAGC exhibits both strength enhancement and strength deterioration in sulphuric acid.

Table 22: Failure Strength of FAGC in H_2SO_4 (MPa)

Age	H_2SO_4 20^{O}C	H_2SO_4 90^{O}C
0	28.9	28.9
7	30.3	28.0
14	34.3	29.9
28	33.2	23.6
56	30.0	23.9

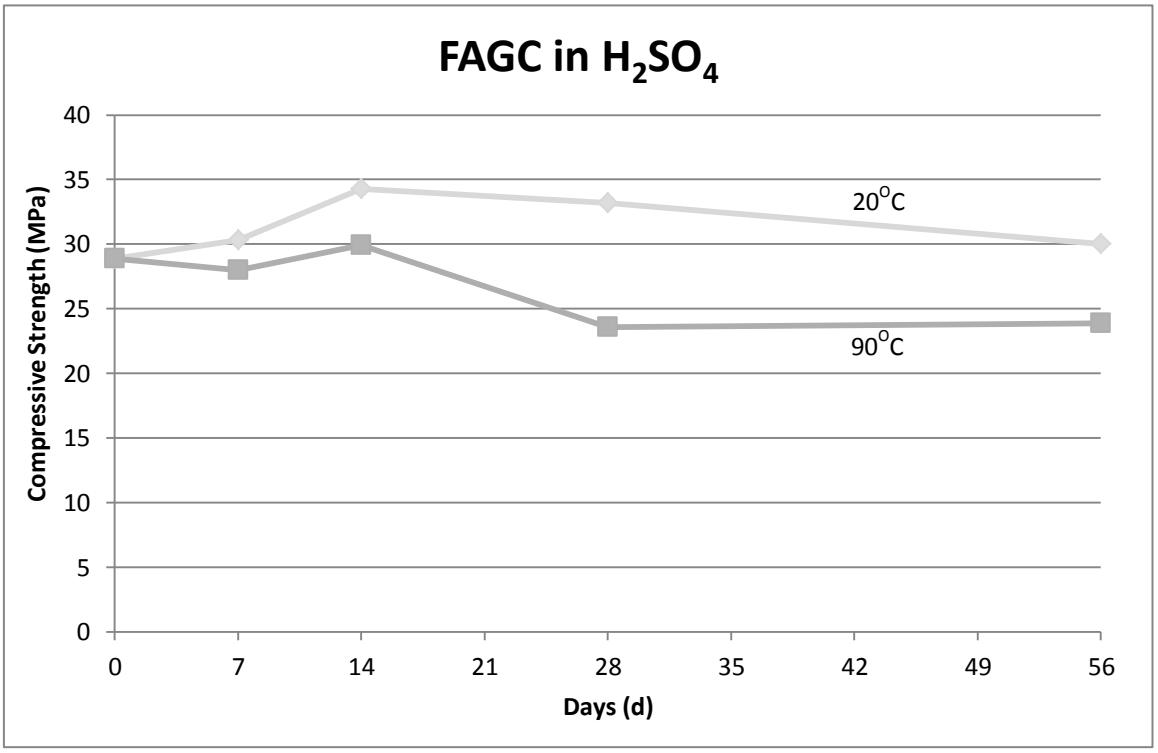

Figure 17: Failure Strength of FAGC in H_2SO_4

Performance of FAGC in sodium hydroxide is now discussed (see Table 23 and Figure 18). The 20^{O}C results indicate FAGC experiences strength enhancement of 8 MPa. The result from 14 days in NaOH at 90^{O}C is considered an outlier and has therefore been disregarded. The reliable data in this condition indicate FAGC undergoes strength enhancement of 16 MPa.

Table 23: Failure Strength of FAGC in NaOH (MPa)

Age	NaOH 20^{O}C	NaOH 90^{O}C
0	28.9	28.9
7	31.4	32.0
14	31.0	25.3
28	32.5	38.0
56	37.3	45.0

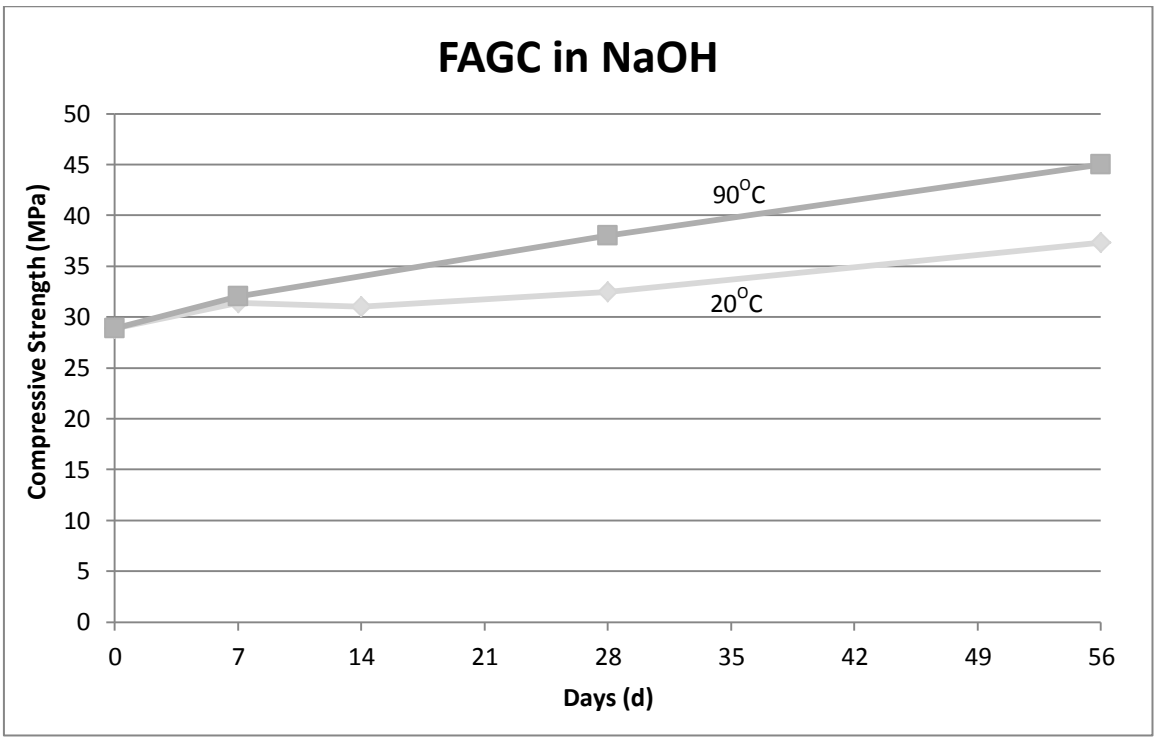

Figure 18: Failure Strength of FAGC in NaOH

The 174 day sample was the sample that was submerged in water to obtain results on absorption in Section 5.2.1. Comparing this information to the failure strength after being tested in 20^{O}C NaOH for any of the test periods (1-8 weeks) reveals that water has no impact on the compressive strength of geopolymer concrete. It also reveals that in the presence of a highly alkaline solution (even after curing), the compressive strength of geopolymer concrete will increase.

5.3 Efflorescence & ASR

By testing in a strong alkaline solution, there is potential for the alkali silica reaction (ASR) to be induced (see Section 2.8) at an earlier than usual concrete age (Bensted and Barnes 2002). At 28 days submersion, FAGC samples tested in NaOH at 20^{O}C began spalling in the same localised areas as severe efflorescence which appeared to be the result of external alkali induced ASR. Figure 19 shows this effect on both FAGC and OPC to provide a comparison.

(a) FAGC (b) FAGC (c) OPC (d) OPC

Figure 19: 28d Efflorescence & Induced ASR

Figure 19 illustrates the efflorescence salts being dissolved in the presence of water. These images also indicate that efflorescence is much less active on the OPC samples. The same phenomenon at 56 days is now shown by Figure 20.

(a) FAGC (b) FAGC (c) OPC (d) OPC

Figure 20: 56d Efflorescence & Induced ASR

These images reinforce that the OPC samples in sodium hydroxide experienced significantly less efflorescence than FAGC and no external alkali induced ASR. It appears the partial submersion testing condition in combination with the ASR phenomenon promotes the damage to FAGC as shown by Figure 21. This figure illustrates the underlying surface damage of the specimen shown in Figure 20(b) after the efflorescence salts have been dissolved. Despite the spalling which occurred, there was no noticeable damage to structural performance (see Table 23). Furthermore, OPC in the same condition experienced a decline in compressive strength even though it did not spall. To eliminate or minimise any damage from efflorescence and external alkali induced ASR it is recommended – where possible – to keep any unsubmerged sections of concrete wet.

Figure 21: Dissoled Efflorescence Revealing ASR and Spalling

CHAPTER 6 Red Mud Geopolymer Concrete

6.1 Casting Process

The RMGC samples were prepared in a Haldwell Bennett mixer and cast in standard 200x100mm cylindrical moulds. These samples were cast on 15 August 2011 in the Z1.101 laboratory at USQ under the supervision of a technical officer. Two layers were poured for each mould and given 25 tamps per layer with a standard tamping rod. Following the recommended practice for geopolymer concrete (CIA 2011); the mixing process was performed in the following steps (see Table 25 for the mix design):

1. Dense Graded 20mm Aggregate (DG20) was added
2. Dense Graded 10mm Aggregate (DG10) was added
3. Sand was added
4. Haldwell Bennet Mixer was turned on to mix the aggregate
5. The Binder Mix was added (40% Calcined R.M., 30% F.A. and 30% B.F.S.)
6. Haldwell Bennet Mixer was turned on to mix the aggregate with the binder
7. Half the design water was added to the mix while the Bennet mixer was active
8. Na_2SiO_3 & NaOH activator at a ratio of 2:1 was slowly added after the design water
9. Superplasticiser was used to increase workability after performing a slump test

Mixing the ingredients after step six revealed a very wet mix which resulted in the first slump test failing (at over 250mm). A geopolymer mix should become less fluid with increased mixing time (CIA 2011, p. 13). Upon performing a second slump test 2 minutes later this theory proved correct with the slump only falling to 140mm with the mix quickly becoming less workable. After placing back in the mixer, superplasticiser was added and the mixer was turned on for approximately 90 seconds. The RMGC was then poured into the moulds in two layers, tamping each layer to standard compaction.

(a) Casting Process (b) Slump Testing

Figure 22: Casting of RMGC Samples

These samples were then left to cure at ambient temperatures in the Z1.101 lab before being transferred to P2 for storage. Of the 11 samples that were cast, 2 were not used due to insufficient compaction. The remaining samples were used to measure characteristic strength at 16 and 32 days and chemical resistance in 90^{O}C solutions of H_2SO_4 and NaOH. Chemical testing of RMGC was only performed for 28 days at 90^{O}C (refer Table 26 for these results).

(a) Casting Moulds (b) Finished Samples

Figure 23: Appearance of RMGC Samples

6.2 Material Ratio's and Mix Design

Referring to Table 24, the RMGC mix ratios for water, binder, aggregate and activator components (NaOH and $Na_2Si\ O_3$) have been summarised.

Table 24: RMGC Mix Ratios

Material	Ratio
Water:Binder:Aggregate	1 : 4.3 : 19.5
Binder:Aggregate	1 : 4.5
Water:Activator	1 : 1.5
NaOH:Na_2SiO_3	1 : 2

In the creation of this mix design, recommended practice for geopolymer concrete and other typical mix designs were consulted (CIA 2011). The blend of aluminosilicates used in the binder represents 16% of the final concrete by mass. This binder was designed to comprise 40% R.M., 30% F.A. and 30% B.F.S. Including dense graded 20mm aggregate (DG20), DG10 and sand; the aggregate was approximately 74% of the concrete by mass. The remaining materials comprised 6% activator (8M OH^- concentration), 4% design water and 0.25% superplasticiser. The activator for this mix consisted of 3.7% sodium silicate (Na_2SiO_3) and 1.85% sodium hydroxide (NaOH) at a concentration of 8M and a respective ratio of 2:1. The following table shows the mix design used to make the RMGC samples that were used for this project (see Table 25).

Table 25: RMGC Mix Design

Component	Percentage	Density (kg/m^3)	3 kg Batch Size
Red Mud	6.30%	163.2	2.996
Fly Ash	4.72%	122.4	2.247
Slag	4.72%	122.4	2.247
DG20	32.52%	842.5	15.466
DG10	14.18%	367.5	6.747
Sand	24.62%	638.0	11.712
Admix	0.23%	6.0	0.110
Water*	7.14%	185.0	3.396
NaOH Activator	1.85%	48.0	0.881
Na_2SiO_3 Activator	3.71%	96.0	1.762
TOTAL	100.00%	2591.0	47.57

*Based on the first slump test, only half the design water was used.

Chemical concentrations were calculated and used as follows: Concentration of Sulphuric Acid:

$$pH3 \rightarrow 1M\ H_2SO_4$$

$$H^+\ 1M = 50g/1000g$$

Concentration of Sodium Hydroxide:

$$pH13 \rightarrow 1M\ NaOH$$

$$OH^-\ 1M = 48g/1048g$$

6.3 Results

6.3.1 Characteristic Strength

Chemical tests for the RMGC samples ensued when the samples were at an age of 49 days on 5 September. As done for OPC and FAGC chemical testing, 26% sample surface area was submerged in chemical solution. The information below summarises the characteristic and failure strength of the RMGC specimens.

Table 26: RMGC Characteristic Strength

Sample Age	Sample ID	F'$_C$ (MPa)
16	RMGC-1	28.52
16	RMGC-2*	16.04
32	RMGC-3	25.72

Due to poor quality compaction, the compression testing result from sample RMGC-2* was comparatively low to all other tests. For this reason, this result was excluded from the average. The stress strain plots which indicate 16 and 32 day characteristic strength of RMGC is shown on the following page (see Figure 24). Images have been paired with the plots to provide an indication of casting quality.

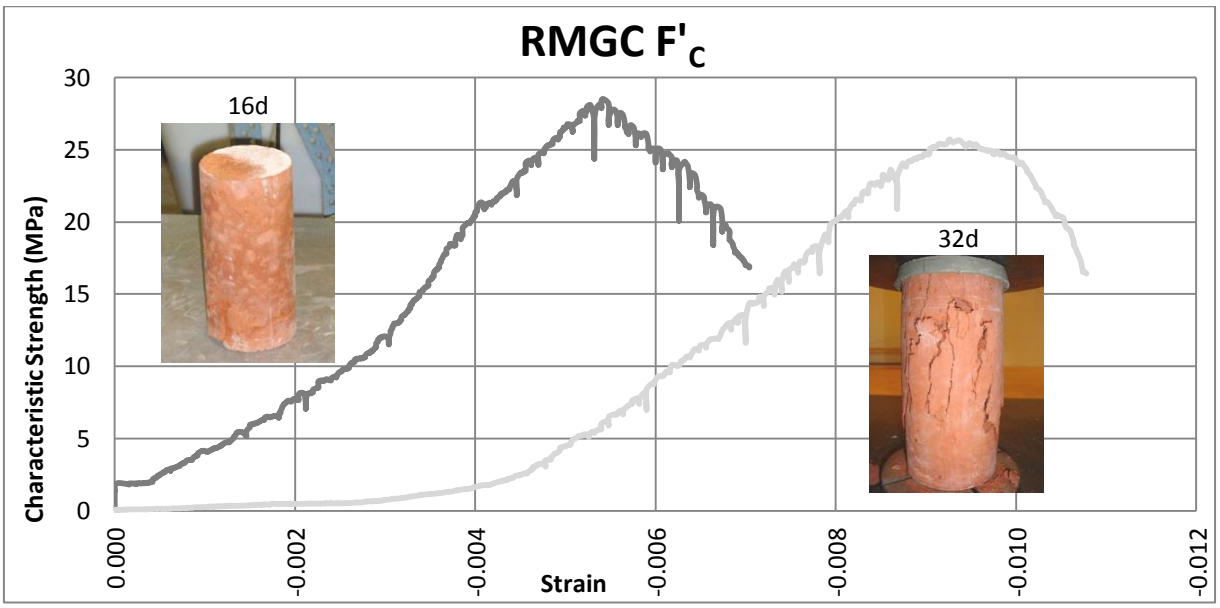

Figure 24: Characteristic Strength of RMGC

Being geopolymer concrete, it is again noticed (see APPENDIX E) that the stress strain plots result in near symmetric bell curves. This observation supports the argument made on FAGC testing at the end of Section 5.2 which suggests this concrete undergoes a ductile failure mechanism, better satisfying serviceability criteria.

6.3.2 Strength after Acid and Alkaline Attack

The failure strength of RMGC in both chemicals at 90^{O}C for the 28 day testing period is summarised by Table 27. The result obtained from 14 days in sulphuric acid at 90^{O}C has been deemed an outlier and excluded from the plot (refer Figure 25).

Table 27: Failure Strength of RMGC (MPa)

Age	H_2SO_4 90^{O}C	NaOH 90^{O}C
0	27.1	27.1
7	39.4	43.1
14	31.0	44.0
28	41.3	40.8

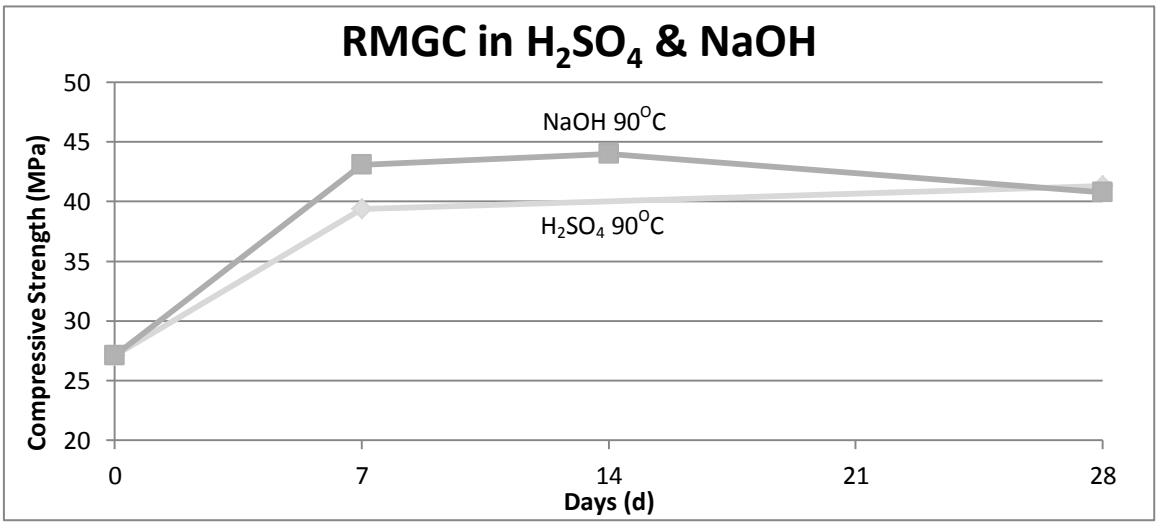

Figure 25: Failure Strength of RMGC in H_2SO_4 and NaOH

The results for this material show great potential, as the relative increase in strength exceeds that of OPC and FAGC. With a characteristic strength of only 27 MPa and then exceeding 40 MPa within 28 days of chemical testing warrants further research of this material. More importantly, industry should start to utilise red-mud in geopolymer concrete as a construction material.

6.4 Composition Analysis of RMGC Binder

Conducted by Cement Australia, x-ray fluorescence (XRF) and particle size distribution (PSD) was performed on the various binders used to create the RMGC samples. This analysis provides an understanding of the major elements present in each Al-Si source and the respective particle sizes. To observe the results of the PSD refer to Figure 26.

Major elements in the R.M. as determined by XRF were iron oxide, silicon dioxide and aluminium oxide. The primary oxides present in Millmerran fly-ash were found to be silicon dioxide and aluminium oxide. Blast furnace slag used in this project was sourced from steel mills in South East Asia and XRF determined the primary oxides were calcium oxide, silicon dioxide and aluminium oxide. Table 28 shows the oxide composition of these materials.

Table 28: Oxide Composition in RMGC Binder Materials (wt.%)

Oxides	Fly Ash	Slag	Red Mud	Calcined R.M.
Fe_2O_3	3.1	0.7	28.0	31.8
SiO_2	53.3	33.4	19.3	20.6
Al_2O_3	32.5	14.4	18.8	21.1
Na_2O	0.27	0.23	7.18	7.68
TiO_2	1.6	0.6	5.8	6.4
CaO	6.9	43.2	5.2	5.2
MgO	0.9	6.1	0.6	0.6
SO_3	0.3	0.6	0.4	0.5
K_2O	0.59	0.34	0.19	0.2
P_2O_5	0.1	0.0	0.1	0.19
Mn_2O_3	0.1	0.4	0.1	0.1
SrO	0.1	0.1	0.0	0.0
LOI	0.5	-0.5	15.5	5.4
Total	100.2	99.4	101.0	99.6

The recommended maximum loss on ignition (LOI) without causing adverse effects on engineering properties is 5% (Czernin 1980). Raw R.M. has an unacceptably high LOI (15.5%) which is why it requires calcination to drive off excess water and burn organic matter. After calcination, LOI of the R.M. is still high at 5.4%. Whilst this LOI may raise concern, testing suggested structural performance was not affected.

6.5 Particle Size Distribution

Shown below is a particle size distribution (PSD) which was conducted by Cement Australia. The analysis reveals that the median particle size of R.M. prior to calcination is smaller then

fly-ash and blast furnace slag. PSD of calcined R.M. reveals that it has the highest median particle size. The information provided by Cement Australia is now plotted.

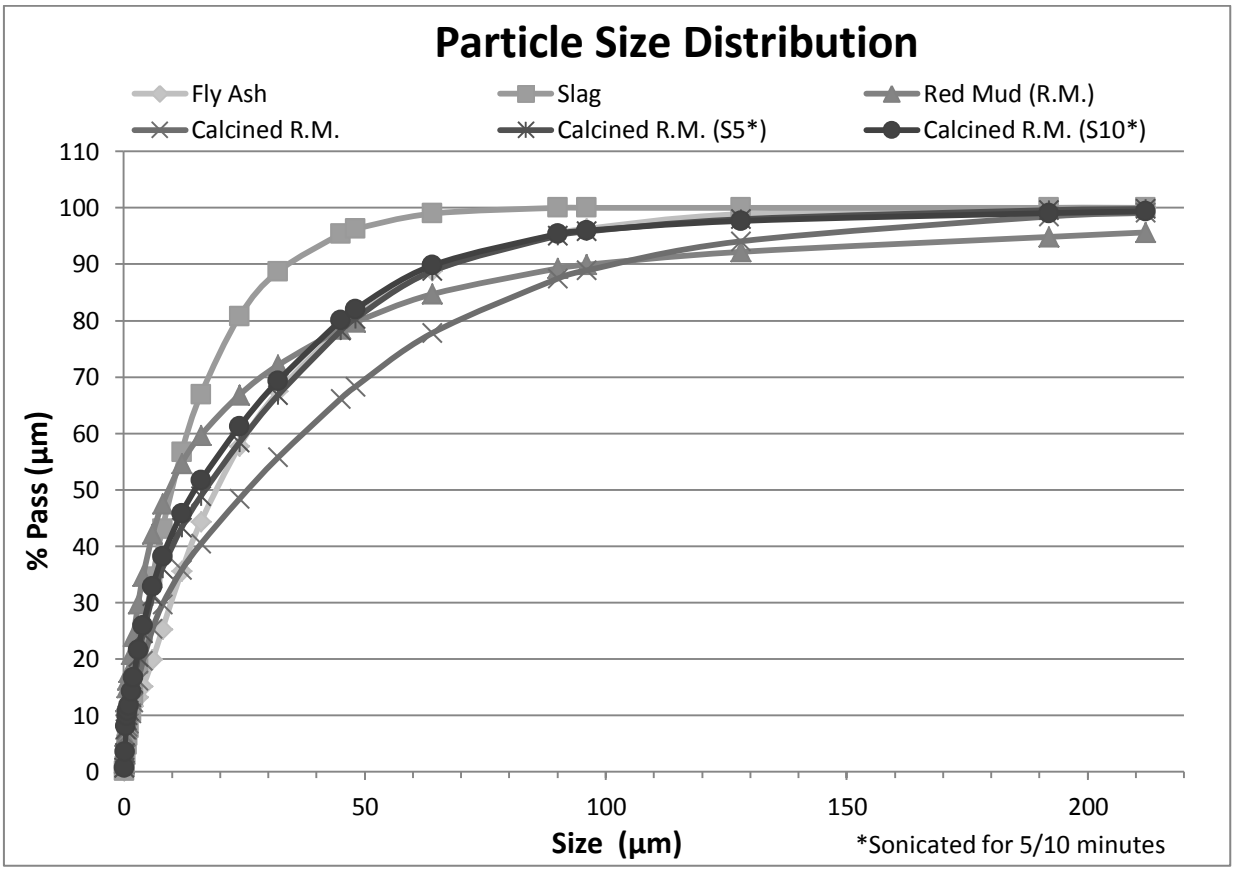

Figure 26: PSD of Binder Materials

6.6 Investigation of High R.M. Content RMGC

To further the investigation of R.M. and its impact on geopolymer concrete another three mixes were designed to incorporate varying contents of R.M. and F.A. as the binder. The first mix was designed with a binder content of 70% R.M. and 30% F.A., cast in 100x50mm moulds and left to cure at 45^{o}C for 2 days. Upon removing the samples from the oven and demoulding, the samples had successfully cured. However, the surface could be scratched and the edges flaked off with minimal effort. Based on these observations, increased R.M. binder content decreased the strength of the geopolymer concrete.

The second mix was designed with a binder content of 50% R.M. and 50% F.A., cast in the same size moulds and left to cure at room temperature for 2 days. At this age, curing was not successful and required oven curing. The third mix was designed with a binder content of 20% R.M. and 80% F.A., cast in the same size moulds and left to cure at room temperature for 2 days. Curing once again required placement in the oven. Observations at 2 days curing revealed the samples were still partially wet. To accelerate the curing process, the samples were placed in an oven at 50^{O}C. Upon demoulding the samples, each sample failed and separated into two pieces. Visual inspection revealed bonding of the three alternate samples was poor in comparison to the original RMGC mix. This confirms that only using sodium hydroxide as the activating solution results in weaker bonding between the aggregate and

binding paste. These mix designs can be seen below along with images of the finished samples.

Table 29: RMGC with 70% R.M. 30% F.A.

Component	Percentage	Density (g/kg)
Red Mud	10.50%	105.0
Fly Ash	4.50%	45.0
Coarse Sand	70.00%	700.0
Water	5.00%	50.0
NaOH Activator	10.00%	100.0
TOTAL	100.00%	1000.0

Figure 27: 70% R.M. 30% F.A.

Table 30: RMGC with 50% R.M. 50% F.A.

Component	Percentage	Density (g/kg)
Red Mud	7.50%	75.0
Fly Ash	7.50%	75.0
Coarse Sand	70.00%	700.0
Water	5.00%	50.0
NaOH Activator	10.00%	100.0
TOTAL	100.00%	1000.0

Figure 28: 50% R.M. 50% F.A.

Table 31: RMGC with 20% R.M. 80% F.A.

Component	Percentage	Density (g/kg)
Red Mud	3.00%	30.0
Fly Ash	12.00%	120.0
Coarse Sand	70.00%	700.0
Water	5.00%	50.0
NaOH Activator	10.00%	100.0
TOTAL	100.00%	1000.0

Figure 29: 20% R.M. 80% F.A.

Based on these results, it's suggested that future samples should use varying proportions of slag in the binder to increase strength. Sodium silicate should also be used with sodium hydroxide when activating to increase the bonding strength between binder and aggregate. Alternative activators such as sodium aluminate could also be tested.

CHAPTER 7 Comparative Analysis & Discussion

7.1 Comparison of Deterioration OPC, FAGC & RMGC

Show below is the absolute and relative performance of each concrete over the course of testing. As indicated by the results, the RMGC samples have shown significantly higher resistance than all other samples. Two factors to be aware of – which may or may not have had an effect on chemical resistance – is grinding of the samples and the age hardening each concrete has undergone. As was done for OPC and FAGC; RMGC samples were not processed in the grinding machine. The age of each concrete (OPC, FAGC and RMGC) before commencement of chemical testing was 49, 115 and 37 days respectively.

Table 32: Strength after Acid and Alkaline Attack (MPa)

Solution	Type of Concrete	Compressive Strength (% Strength Retention) 0	7	14	28	56
$20^{O}C$ H_2SO_4	OPC	44.5 (100)	26.9 (60.4)$^{-}$	41.3 (92.8)	42.0 (94.4)	33.1 (74.4)
	FAGC	28.9 (100)	30.3 (104.8)	34.4 (119.0)	33.2 (114.9)	30.0 (103.8)
$90^{O}C$ H_2SO_4	OPC	44.5 (100)	39.5 (88.8)	23.7 (53.3)$^{-}$	39.7 (89.2)	33.4 (75.1)
	FAGC	28.9 (100)	28.0 (96.9)	29.9 (103.5)	23.6 (81.7)	23.8 (82.4)
	RMGC	27.1 (100)	39.4 (145.4)	31.0 (114.4)$^{-}$	41.3 (152.4)	
$20^{O}C$ NaOH	OPC	44.5 (100)	44.4 (99.8)	37.1 (83.4)$^{-}$	29.5 (66.3)$^{-}$	43.5 (97.8)
	FAGC	28.9 (100)	31.4 (108.7)	31.0 (107.3)	32.5 (112.5)	37.3 (129.1)
$90^{O}C$ NaOH	OPC	44.5 (100)	30.2 (67.9)$^{-}$	44.3 (99.6)	27.1 (60.9)$^{-}$	38.6 (86.7)
	FAGC	28.9 (100)	32.0 (110.7)	25.3 (87.5)$^{-}$	38.0 (131.5)	45.0 (155.7)
	RMGC	27.1 (100)	43.1 (159.0)	44.0 (162.4)	40.8 (150.5)	

$^{-}$Indicates those results considered outliers which will not be plotted

Table 33: Relative Change in Strength over Testing Period (%)

Solution	OPC	FAGC	RMGC
$20^{O}C$ H_2SO_4	-25.6	+3.8	
$90^{O}C$ H_2SO_4	-24.9	-17.6	+52.4
$20^{O}C$ NaOH	-2.2	+29.1	
$90^{O}C$ NaOH	-13.3	+55.7	+50.5

The relative changes in strength from Table 32 and Table 33 has been used for conclusive purposes.

7.2 Comparison of Deterioration

To better illustrate the results from Section 7.1, the three concretes tested by Elena and Ivan (refer Table 6) will be investigated. The absolute and relative compressive strength of OPC and FAGC in H_2SO_4 at 20^OC has been used to compare these results.

Table 34: Failure Strength Comparison of Results and Literature (MPa)

Type of material	Strength Compressive (% Strength Retention)	
	Water	HCl
OPC*	46.0 (100)	38.6 (83.9)
BFSPC*	34.5 (100)	28.0 (81.2)
SAB*	37.3 (100)	28.6 (76.8)
	Water	H_2SO_4
OPC^+	44.5 (100)	33.1 (74.4)
$FAGC^+$	28.9 (100)	30.0 (103.8)

* Testing from literature at 90 days in HCl, see Section 2.7.2 (Elena & Ivan 2003, p. 146).

+ Testing from results at 56 days in H_2SO_4, see Table 17.

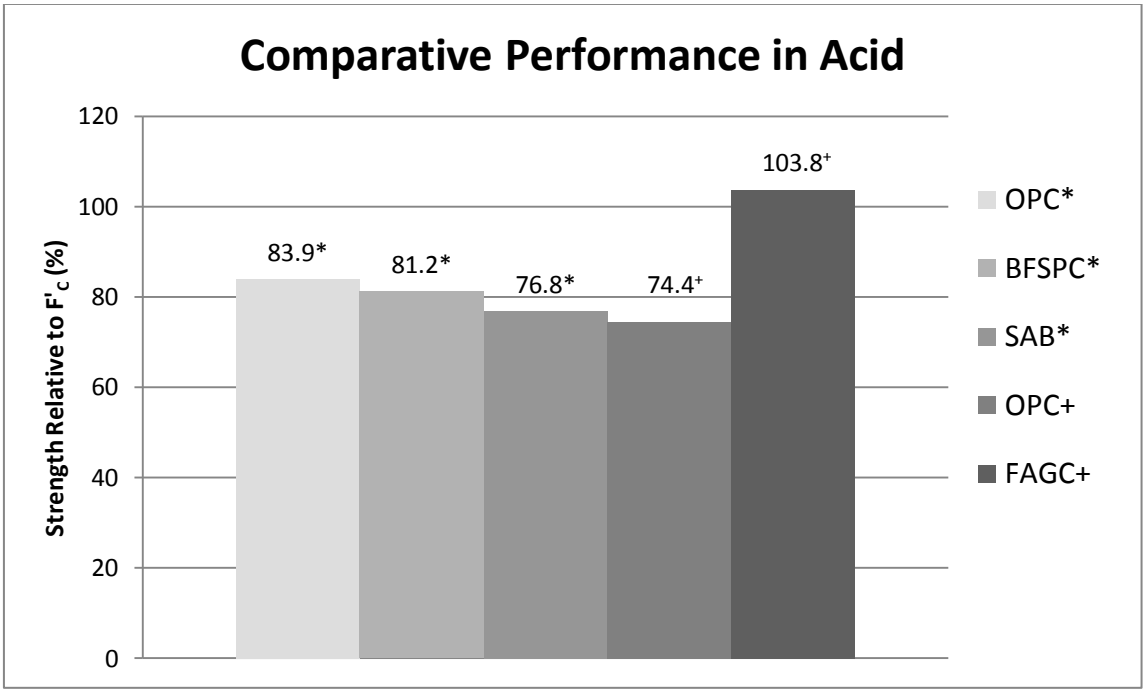

Figure 30: Relative Comparison (%) of Results and Literature

Sulphuric acid is considered more aggressive than hydrochloric acid. This fact is confirmed by greater relative damage to the OPC in this project when compared to the OPC investigated by Elena and Ivan (2003). The comparison of these two experiments also indicates FAGC exhibits the best performance when compared to all the materials that have been considered (this does not account for the high performance of RMGC).

7.3 Chemical Resistance

For an overview of the data used to create these plots and an indication of what data has been considered outliers, see Table 32.

7.3.1 H_2SO_4 20°C

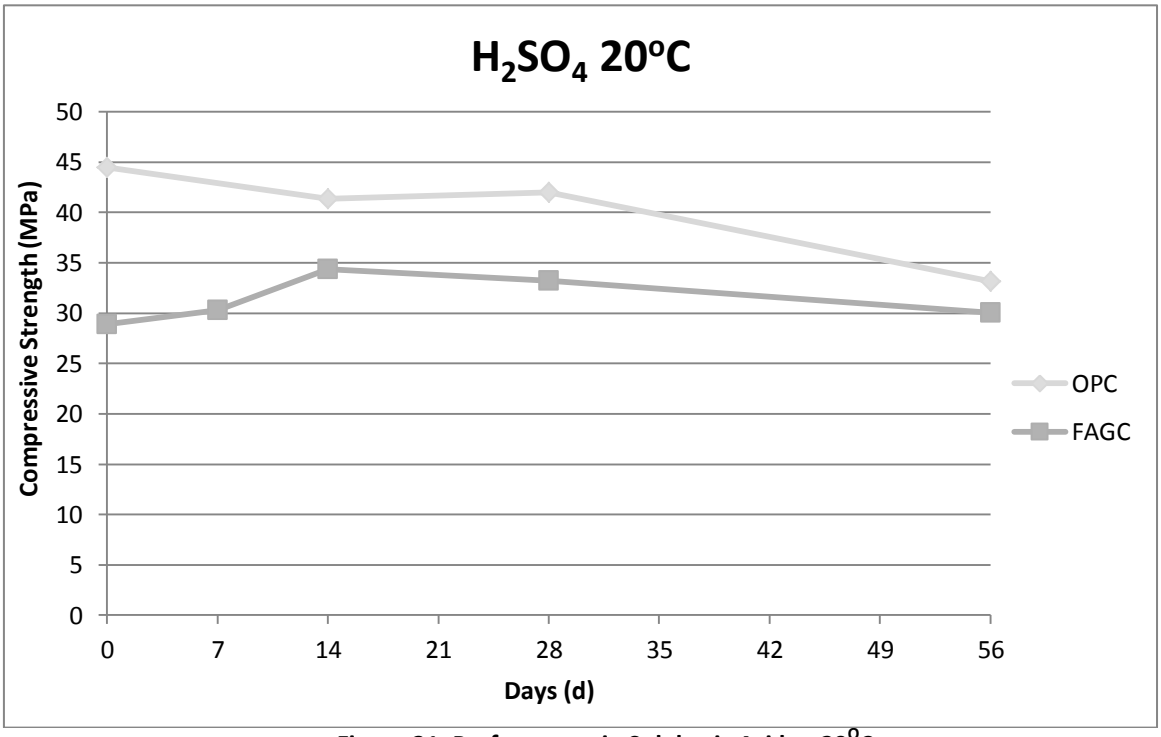

Figure 31: Performance in Sulphuric Acid at 20°C

For OPC, the initial strength is 44.5 MPa (refer Figure 31). After being submerged in 20°C H_2SO_4, its strength has slowly diminished. After 56 days its strength had fallen to 33.1 MPa, meaning OPC has retained 74.4% of its original strength.

For FAGC, the initial strength is 28.9 MPa. After being submerged in 20°C H_2SO_4, it has performed considerably better than OPC with results indicating a marginal strength increase to 30.0 MPa. After the 56 day testing period, FAGC has become 3.8% stronger than its original strength.

7.3.2 H_2SO_4 90°C

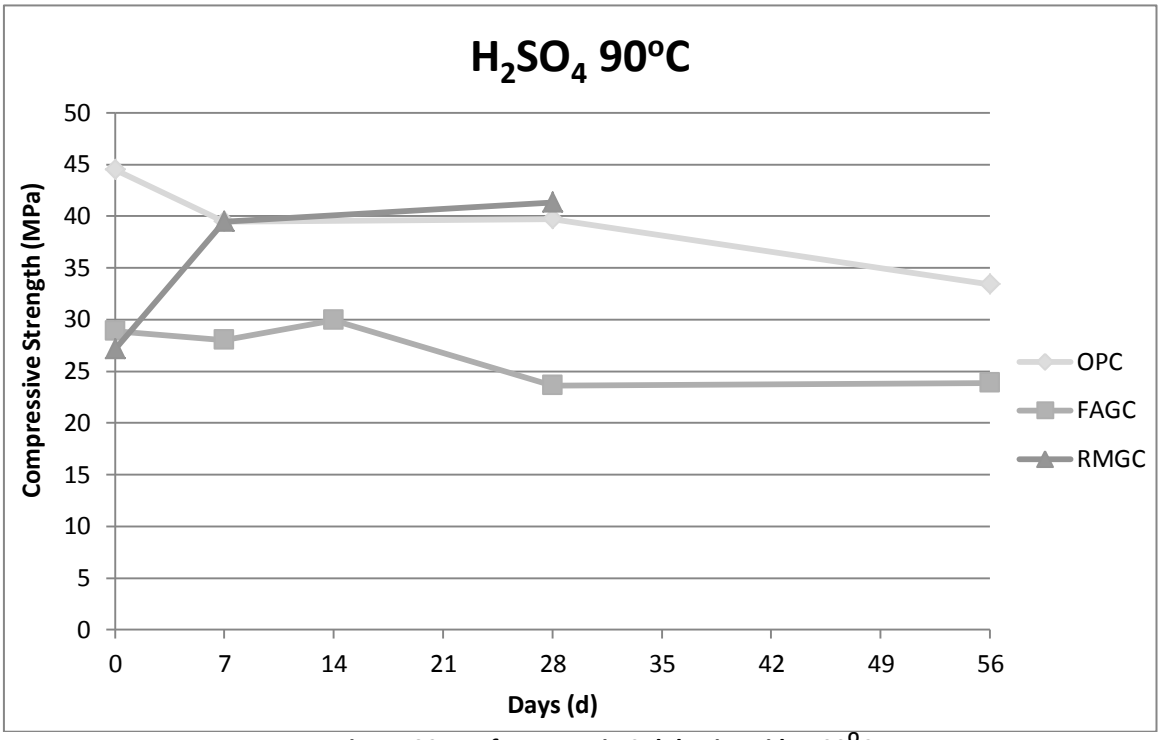

Figure 32: Performance in Sulphuric Acid at 90°C

For OPC, the initial strength was 44.5 MPa. As the material was submerged in 90°C H_2SO_4 the strength gradually decreased. After 56 days of chemical attack, the strength reduced to 33.4 MPa which is equivalent to 75% of its original strength.

For FAGC, the strength reduction by acid attack after 56 days is relatively mild. After this time the material has weakened from 28.9 MPa to 23.9 MPa, which signifies the concrete has retained 82% of its original strength.

For RMGC, its initial is 27.1 MPa and it's interesting to find that the material strength increases in an acid environment. After the 28 day testing period, the final strength is 14 MPa stronger than the initial result. Specifically, the strength has enhanced to 41.3 MPa which represents a strength increase of 52%.

7.3.3 NaOH 20^{O}C

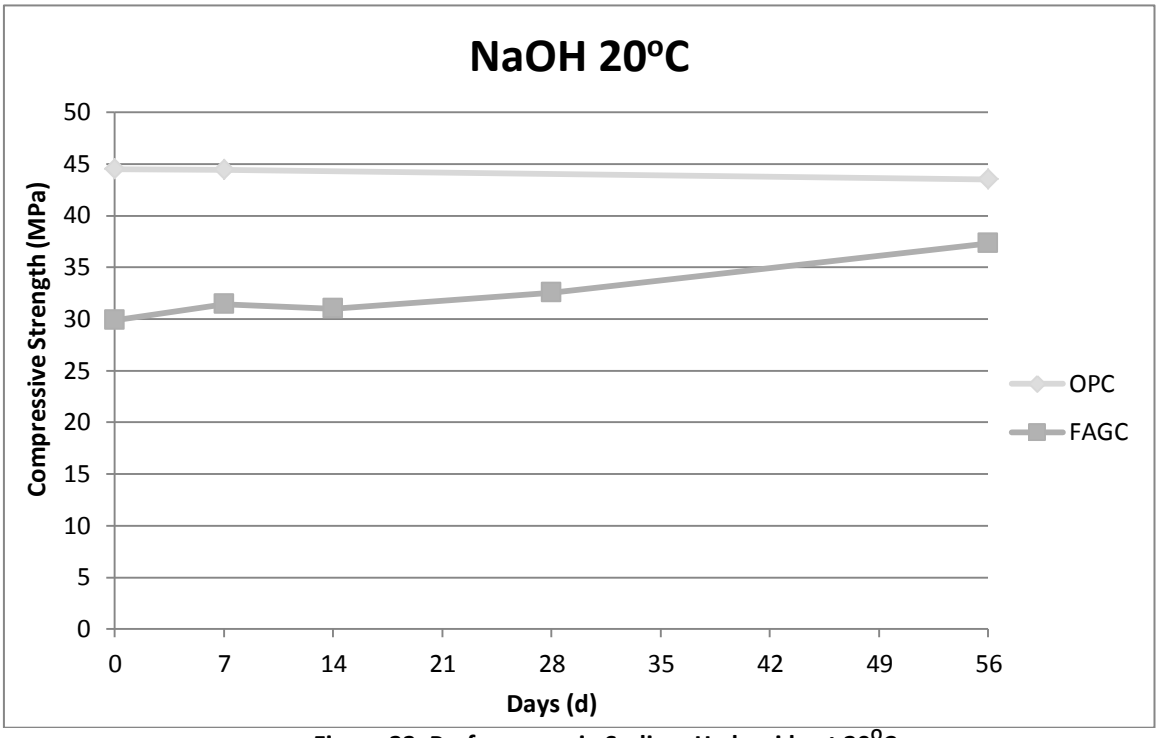

Figure 33: Performance in Sodium Hydroxide at 20^{O}C

After being submerged in 20^{O}C NaOH, OPC strength has only marginally decreased to 43.5 MPa over the 56 days. These results indicate that OPC exhibits 98% strength retention.

In this alkaline environment, the strength of FAGC has increased over the 56 day testing period. After this time the material has increased to 37 MPa, which indicates a 29% enhancement in strength. This performance suggests that FAGC would be suitable as a replacement for the existing bunding slab at QAL.

7.3.4 NaOH 90^{o}C

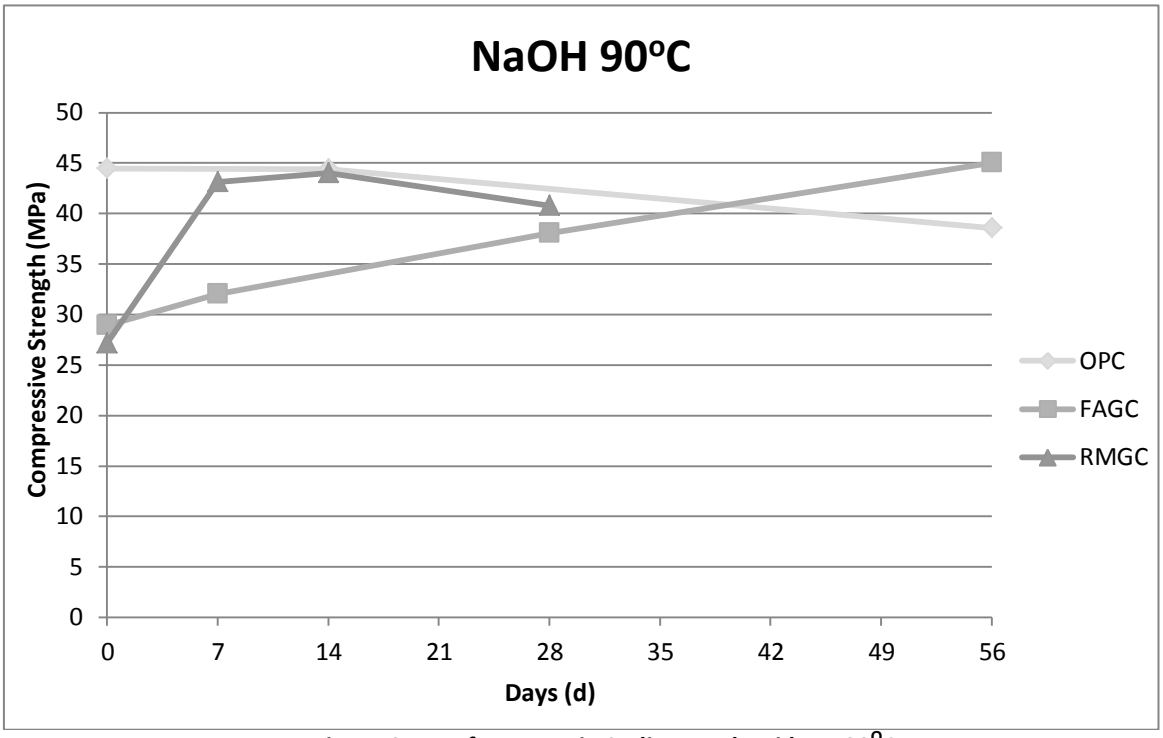

Figure 34: Performance in Sodium Hydroxide at 90^{O}C

The performance of OPC in 90^{O}C NaOH exhibits a decrease to 38.5 MPa. Thus over the 56 days of testing, the sample has retained 86.5% of its original strength.

In this condition, FAGC has performed significantly better than OPC. Over the 56 days of testing, it has increased to 45 MPa strength. This indicates the sample a 55% increase in strength.

For RMGC, its performance is similar to FAGC. Its initial strength was measured to be 27 MPa. After being submerged in 90^{O}C NaOH for 28 days, RMGC strength has increased by 50%.

Performance of FAGC and RMGC in this condition indicates they are both suitable replacements for the existing bunding slab at QAL.

CHAPTER 8 Conclusions and Future Work

Waste disposal methods and low carbon emissions are the primary advantages of geopolymer concrete. The large volumes, associated storage and maintenance cost of mine tailings that Australia produces, creates a viable waste disposal mechanism for mining companies. Excellent chemical resistance and stability also makes geopolymer concrete an excellent candidate for backfilling obsolete mines which may otherwise deteriorate the surrounding materials which are not resistant to acid or alkaline attack. Fly-ash, red-mud and slag based geopolymer concretes can also reduce carbon emissions by 80%. This has the potential to reduce global emissions by approximately 2.1 billion tonnes a year which is equivalent to taking two thirds of global traffic off the roads each year. These advantages are evident by the test results that were obtained in this project.

Chemical and compression testing indicated OPC experienced some strength deterioration in both an acid environment (-24.9 to -25.6%) and an alkaline environment (-2.2 to -13.3%). FAGC was found to have better acid resistance (+3.8 to -17.6%) and even experienced strength enhancement in sodium hydroxide (+29.1 to +55.7%). Interestingly, RMGC exhibited a strength increase of 52.4% in sulphuric acid while displaying strength enhancement of +50.5% in sodium hydroxide. This performance suggests that FAGC and RMGC are both suitable replacements for the existing bunding slab at QAL.

There is significant potential for future work in this field via more thorough investigation of R.M. based geopolymer concrete. This could investigate a range of concrete mix designs that look at the change in engineering properties between a geopolymer concrete with 10% R.M., 90% of other pozzolans and varying the R.M. content by 10% intervals up to and including 90% R.M. and 10% of other pozzolans. This investigation should also attempt each mix design with different activators to see their respective effects on the mix. Another topic could investigate the feasibility of utilising different mine tailings in the production of geopolymer concrete.

CHAPTER 9 References

AAC Ltd 2010, Bauxite Residue in Australia, *Australian Aluminium Council Ltd*, viewed 26 September 2011, < www.aluminium.org.au/_literature_78131/Australian_Bauxite_Residue>.

Alasali, MM & Malhotra, VM 1991, 'Role of concrete incorporating high volumes of fly ash in controlling expansion due to alkali-aggregate-reaction', ACI *Mat. J*, pp.159-163.

Alcoa World Alumina Australia 2005, *Existing Wagerup Refinery: Alumina Refining Process*, Bayer Process Flow Diagram, viewed 26 September 2011, <http://www.alcoa.com/australia/en/pdf/WAG_Chapter_4_Existing_Wagerup_Refinery.pdf>.

Allen, D & Brent, G 2010, 'Sequestering CO2 by mineral carbonation', *Stability against acid rain exposure*, Environmental Science and Technology, vol. 44, no. 7, pp.2735-2739.

Banvolgyi, G & Huan, TM 2010, 'Dewatering, disposal and utilization of red mud: state of the art and emerging technologies', *University of Patras*, viewed 26 September 2011, <http://www.redmud.org/Files/banvolgyi040110.pdf>.

Basell Polyolefins 2010, *Low, Medium and High Density PE Chemcial Resistance*, viewed May 13 2011, <https://polymers.lyondellbasell.com>.

Bensted, J & Barnes, P 2002, *Structure and Performance of cements*, 2nd edn, Spon Press, London.

Blatt, H & Robert, JT 1995, *Petrology: Igneous, Sedimentary, and Metamorphic*, 2nd edn, W.H. Freeman, New York.

BOM 2011, *Daily Maximum Temperature: Toowoomba Airport*, Bureau of Meteorology, viewed 8 October 2011, <http://www.bom.gov.au/jsp/ncc/cdio/weatherData/av?p_nccObsCode=122&p_display_type=dailyDataFile&p_startYear=2011&p_c=-352204384&p_stn_num=041529>.

Borealis 1999, *Chemicals Resistance Table*, *Low Density and High Density Polyethylene*, viewed May 15 2011, <http://www.borealisgroup.com/pdf/chemical-resistance/chemical-resistance-hdpe-ld.pdf>.

BPN 2011, *Global cement production set to soar*, viewed August 19 2011, <http://www.bpn.com.au/article/Global-cement-production-set-to-soar/528909.aspx>.

Cablik, V 2007, *Characterisation and applications of red mud from bauxite processing,* Ph.D., University of Ostrava, Ostrava-Poruba, viewed 3rd June 2011, <http://www.min-pan.krakow.pl/Wydawnictwa/GSM234/cablik.pdf>.

Carse, A & Dux, PF 1988, *Alkali-Silica Reaction in Concrete Structures*, 1st edn, University of Queensland, Brisbane.

CDIAC 2010, *Global Fossil-Fuel CO_2 Emissions*, viewed 9 September 2011, <http://cdiac.ornl.gov/trends/emis/tre_glob.html>.

Cement & Concrete Association of Australia, 'HB64-2002: Guide to Concrete Construction', *Cement & Concrete Association of Australia*, Sydney, 2nd edn, pp.2.12-2.13.

Cement Industry Federation 2009, *Australian Cement Industry: Statistics*, viewed May 18 2011, <http://cement.org.au/australias-cement-industry/information-about-the-australian-cement-industry>.

CEMBUREAU 2011, *Key facts & figures*, *cement production*, viewed May 21 2011, <www.cembureau.be/about-cement/key-facts-figures>.

Christiansen, EH & Hamblin, WK 2007, *Fundamentals of Planetary Science*, *the silicon-oxygen tetrahedron*, viewed August 12 2011, <http://explanet.info/Chapter02.htm>.

ConstructionZ.com, 'Development of Sustainable Cementitious Materials', viewed May 10 2011, <http://constructionz.com/articles/development-of-sustainable-cementitious-materials.html>.

Czernin, W 1980, *Cement Chemistry and Physics for Civil Engineers*, 2nd edn, Bauverlag, Wiesbaden.

Data Blog 2011, *World carbon dioxide emissions data by country: China speeds ahead of the rest*, viewed 9 September 2011, <http://www.guardian.co.uk/news/datablog/2011/jan/31/world-carbon-dioxide-emissions-country-data-co2>.

Davidovits, J 2008, *Geopolymer Chemistry and Applications*: *A Practical and Scientific Approach to Sustainable Development*, 2nd edn, Institut Geopolymere, France.

Deevasan, K & Ranganath, R 2011, 'Construction Materials', *Proceedings of the Institution of Civil Engineers*, vol. 164, no. 1, pp.43-50.

Duxson, P, van Deventer, JSJ, Lukey, GC & Provis, JL 2006, 'Technological, environmental and commercial drivers for the use of Geopolymers in a sustainable materials industry', *Sohn International Symposium*, vol. 3, pp.241-252.

Elena, D & Ivan, J 2003, 'Chemical resistance of Portland cement, blast- furnace slag Portland cement and sulphoaluminate-belite cement in acid, chloride and sulphate solution', *Ceramics - Silikaty*, vol. 47, no. 4, pp. 141-148, viewed 4 October 2011, ISSN: 08625468.

Geology.com 2011, *Basalt: What is Basalt, How Does it Form and How Is It Used?*, viewed 2nd September, <http://geology.com/rocks/basalt.shtml>.

Glasby, T 2011, email, 4 May 2011, <tom.glasby@wagner.com.au>.

Grace W.R. & Co.-Conn. 2006, 'Ground Granulated Blast-Furnace Slag: Its Chemistry and Use with Chemical Admixtures', *Technical Bulletin TB-0102*, Cambridge, MA, viewed 2nd September 2011, <http://www.na.graceconstruction.com/custom/concrete/downloads/TB_0102.pdf>.

Hardjito, D, Sumajouw, D, Wallah, S and Rangan, B 2005, 'Fly ash-based Geopolymer Concrete', *Australian Journal of Structural Engineering*, vol. 6, no. 1, pp.77-85.

Hou, Y, Wang, D and Li, Q 2007, 'Effect of activator on compressive strength of fly-ash based geopolymers', *Journal of Building Materials*, vol. 10, no. 2, pp.214-218.

IMPCO 2010, How Sodium Silicate Sealants Take Their Set, *IMPCO*, <http://www.impco-inc.com/page212.html>.

Lottermoser, B 2010, *Mine Wastes: Characterization, Treatment and Environment*, 3rd edn, Springer, Heidelberg, Germany.

Lynch, MJ 2011, email, 30 September 2011, <mark.lynch@usq.edu.au>.

Malhotra, VM 2005, *Role of fly ash in reducing greenhouse gas emissions during the manufacturing of Portland cement clinker*, viewed 10 September 2011, <http://www.watancon.com/documentation/technical/Malhotra_-_Role_of_Fly_Ash_in_reducing_GGE.pdf>.

Materials World 2003, *Dealing with Red Mud: by-product of the Bayer process for refining aluminium*, viewed 17 August 2011, <http://www.azom.com/article.aspx?ArticleID=2071>.

Nave, CR 2002, Abundances of the Elements in the Earth's Crust, *Georgia State University*, <www.hyperphysics.phy-astr.gsu.edu/hbase/tables/elabund.html>.

Neville, AM 1998, *Properties of Concrete*, 4th edn, John Wiley & Sons Inc, New York.

Orchard, DF 1979, *Concrete Technology: Properties of Materials*, vol. 1, 4th edn, Applied Science Publishers Ltd, London.

Orchard, DF 1979, *Concrete Technology: Practice*, vol. 2, 4th edn, Applied Science Publishers Ltd, London.

Phair, J & Van Deventer, JSJ 2002, 'Characterization of Fly-Ash-Based Geopolymeric Binders Activated with Sodium Aluminate', *American Chemical Society*, vol. 41, no. 17, pp.4242-4251, viewed 13 April 2011, I&EC Research, IE0109370.

Rangan, BV 2008, Studies on fly-ash based geopolymer concrete, *Malaysian Construction Research Journal*, vol. 3, no. 2.

Rawlinsons 2011, Australian Construction Handbook, 29th edn, Rawlinsons Publishing, Perth.

Sindhunata, van Deventer, JSJ, Lukey, GC & Provis, JL 2008, 'Structural Evolution of Fly Ash Based Geopolymers in Alkaline Environments', *American Chemical Society*, vol. 47, no. 9, pp.2991-2999, viewed 13 April 2011, I&EC Research, IE0707671.

Sindhunata, van Deventer, JSJ, Lukey, GC & Xu, H 2006, 'Effect of Curing Temperature and Silicate Concentration on Fly-Ash-Based Geopolymerization', *American Chemical Society*, vol. 45, no. 10, pp.3559-3568, viewed 13 April 2011, I&EC Research, IE051251P.

Shook, WE & Bell, LW 1998, Corrosion Control in Concrete Pipes and Manholes, Con Shield Technologies, viewed 17 October 2011, <http://www.conshield.com/site/LinkClick.aspx?fileticket=7ZvAKdy9kY0%3D&tabid=56>.

Tavor, D, Wolfson, A, Shamaev, A & Shvarzman, A 2007, 'Recycling of Industrial Wastewater by Its Immobilization in Geopolymer Cement', *American Chemical Society*, vol. 46, no. 21, pp.6801-6805, viewed 13 April 2011, I&EC Research, IE0616996.

Trevor, JB 2007, 'Comparative assessment of medium-term properties and performance of fly ash and metakaolin geopolymer systems', *Journal of Australian Ceramic Society*, vol. 43, no. 2, pp.131-137, viewed 4 October 2011, ISSN: 0004-881X.

Volland, W 2005, *Effects of temperature, concentration, catalysts, inhibitors on reaction rates: Collision theory and temperature effect on rates*, viewed 30 September 2011, <http://www.800mainstreet.com/7/0007-005-rea-t-cat.html>.

Wagners 2011, 'EFC: Earth Friendly Concrete', *Product Summary*, vol. 1, no. 7, pp.1-5.

Williams, RP, Janine, L, van Riessen, A & Corder, GD 2011, 'Costs and carbon emissions for Geopolymer pastes in comparison to ordinary Portland Cement', *Journal of Cleaner Production*, vol. 19, no. 10, pp. 1080-1090.

World Resources Institute 2011, *CO_2 emissions from vehicles*, Viewed 9 September 2011, <http://www.wri.org/publication/content/8468>.

Young, JF, Mindess, S, Gray, RJ & Bentur, A 1998, *The Science and Technology of Civil Engineering Materials*, Prentice Hall, New Jersey.

Zhang, L, Ahmari, S & Zhang, J 2011, 'Synthesis and characterisation of fly ash modified mine tailings-based Geopolymers', *Construction and Building Materials*, vol. 25, no. 9, pp. 3773-3781.

APPENDIX A

Project Specification

University of Southern Queensland

FACULTY OF ENGINEERING AND SURVERYING

ENG4111/ENG4112 Research Project
PROJECT SPECIFICATION

FOR:	**BROCK TOMKINS**
TOPIC:	CHEMICAL RESISTANCE OF GEOPOLYMER CONCRETE AGAINST H_2SO_4 & NaOH
SUPERVISORS:	Dr. Hao Wang, USQ Lecturer, Manufacturing/Materials Engineering. Tom Glasby, EFC Project Manager, Wagners Pty Ltd.
ENROLME NT:	ENG4111 – S1, 2011 ENG4112 – S2, 2011
PROJECT AIM:	To develop innovative environmental green concretes and study the performance, particularly the chemical resistance. Concretes will include fly-ash based geopolymer concrete (FAGC) and red-mud based geopolymer concrete (RMGC). Chemical tests will involve Sodium Hydroxide (NaOH) and Sulphuric Acid (H_2SO_4) at various temperatures. Results will be compared to Ordinary Portland cement concrete (OPC).
SPONSORSHIP:	Wagners Pty Ltd.
CONFIDENTIALITY:	The mix design for EFC is part of the intellectual property owned by Wagners and is not made publicly available.
PROGRAMME:	**Issue C, 27th October 2011**

1. **Understand** what a geopolymer is through publicly and privately accessible literature.
   The history of geopolymers, where they were first used, who pioneered their use in concrete, their significance and the comparative advantage of geopolymer concretes to ordinary concretes.
2. **Investigate Chemical Resistance** properties of OPC, FAGC & RMGC.
   Cast 22 OPC, 22 FAGC and 11 off RMGC concrete samples. Each type of concrete will be tested at 7, 14, 28 and 56 days in the following conditions:
   - H_2SO_4 solution: 20^{O}C and 90^{O}C
   - NaOH solution: 20^{O}C and 90^{O}C

   In each condition, 4 to 5 samples will be tested.
3. **Compare** properties of Chemical Resistance.
   Through chemical testing, compression testing and microscopy analysis, a comparison and conclusion will be made.

AGREED:

_____ (Student) _____, _____ (Supervisors)

___/___/2011 ___/___/2011 ___/___/2011

APPENDIX B

Project Timeline

ID	Task Name	Duration	Start	Finish	Predecessors
1	**Research Project**	**166 days?**	**Wed 9/03/11**	**Thu 27/10/11**	
2	**Research**	**43 days**	**Mon 18/04/11**	**Wed 15/06/11**	
3	Initial Research on Geopolymers	6 days	Mon 18/04/11	Mon 25/04/11	
4	Perform Literature review	10 days	Tue 26/04/11	Mon 9/05/11	3
5	Draft Literature Review	9 days	Tue 10/05/11	Sun 22/05/11	4
6	Appreciation	1 day	Mon 23/05/11	Mon 23/05/11	11
7	Review of Appreciation	14 days	Fri 27/05/11	Wed 15/06/11	6FS+24 hrs
8	**Deliverables**	**166 days?**	**Wed 9/03/11**	**Thu 27/10/11**	
9	Writing & Submission - Project Proposal	5 days	Wed 9/03/11	Tue 15/03/11	
10	Writing Project Specification	5 days	Wed 30/03/11	Tue 5/04/11	
11	Writing Appreciation	20 days	Mon 25/04/11	Mon 23/05/11	10
12	Test Result Input	84 days?	Tue 21/06/11	Mon 17/10/11	
13	Draft Dissertation Submission	5 days	Wed 19/10/11	Tue 25/10/11	12
14	Final Submission	45 days	Thu 25/08/11	Thu 27/10/11	13
15	**Professional Practice 2**	**24 days**	**Wed 20/07/11**	**Mon 22/08/11**	
16	PP2 Duties - Writing Extended Abstract	5 days	Wed 20/07/11	Tue 26/07/11	
17	PP2 Duties - Powerpoint Presention	14 days	Wed 3/08/11	Mon 22/08/11	16
18	**Casting of Materials**	**105 days**	**Tue 19/04/11**	**Tue 13/09/11**	
19	Cast FAGC Samples	0 days	Tue 19/04/11	Tue 19/04/11	
20	28 Day Compression Test	20 days	Wed 20/04/11	Tue 17/05/11	19
21	56 Day Compression Test	40 days	Wed 18/05/11	Tue 12/07/11	20
22	Cast OPC Samples	0 days	Tue 21/06/11	Tue 21/06/11	
23	28 Day Compression Test	20 days	Wed 22/06/11	Tue 19/07/11	22
24	56 Day Compression Test	40 days	Wed 20/07/11	Tue 13/09/11	23
25	Cast RMGC Samples	0 days	Wed 27/07/11	Wed 27/07/11	
26	16 Day Compression Test	12 days	Thu 28/07/11	Fri 12/08/11	25
27	32 Day Compression Test	12 days	Mon 15/08/11	Tue 30/08/11	26
28	**Testing of FAGC**	**39 days**	**Thu 21/07/11**	**Wed 14/09/11**	
29	7 Day Sample	5 days	Thu 21/07/11	Wed 27/07/11	
30	14 Day Sample	5 days	Thu 28/07/11	Wed 3/08/11	29
31	28 Day Sample	10 days	Thu 4/08/11	Wed 17/08/11	30
32	56 Day Sample	20 days	Thu 18/08/11	Wed 14/09/11	31
33	**Testing of OPC**	**39 days**	**Thu 21/07/11**	**Wed 14/09/11**	
34	7 Day Sample	5 days	Thu 21/07/11	Wed 27/07/11	
35	14 Day Sample	5 days	Thu 28/07/11	Wed 3/08/11	34
36	28 Day Sample	10 days	Thu 4/08/11	Wed 17/08/11	35
37	56 Day Sample	20 days	Thu 18/08/11	Wed 14/09/11	36
38	**Testing of RMGC**	**20 days**	**Tue 16/08/11**	**Mon 12/09/11**	
39	7 Day Sample	5 days	Tue 16/08/11	Mon 22/08/11	
40	14 Day Sample	5 days	Tue 23/08/11	Mon 29/08/11	39
41	28 Day Sample	10 days	Tue 30/08/11	Mon 12/09/11	40
42	**Microscopy**	3 days	Tue 27/09/11	Thu 29/09/11	41,37,32

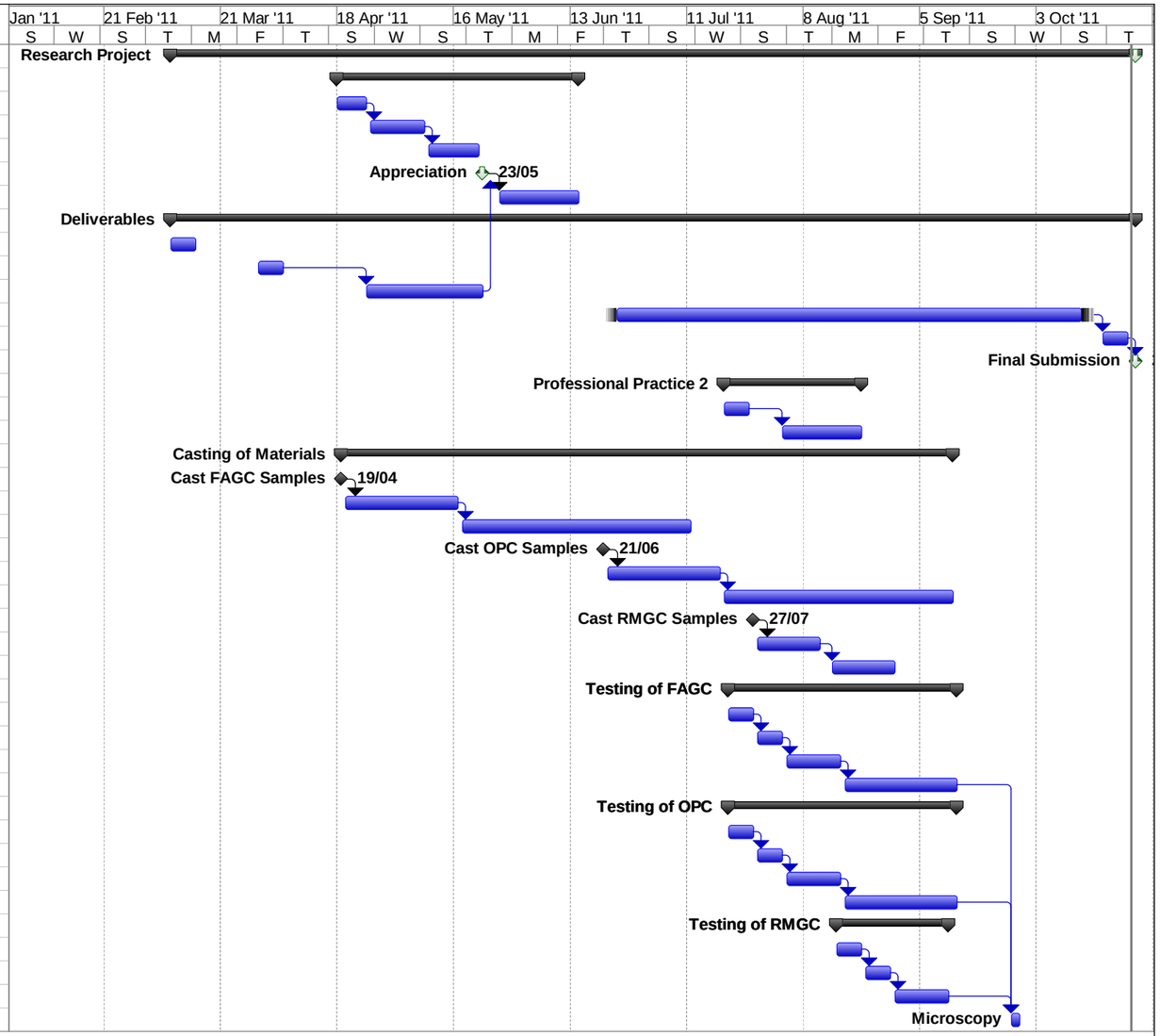

Project: Untitled
Date: Wed 26/10/11

Task	Project Summary	Inactive Milestone	Manual Summary Rollup	Progress
Split	External Tasks	Inactive Summary	Manual Summary	Deadline
Milestone	External Milestone	Manual Task	Start-only	
Summary	Inactive Task	Duration-only	Finish-only	

APPENDIX C

Compression Test Data:
Ordinary Portland Cement Concrete

C.1 H_2SO_4 20±2°C

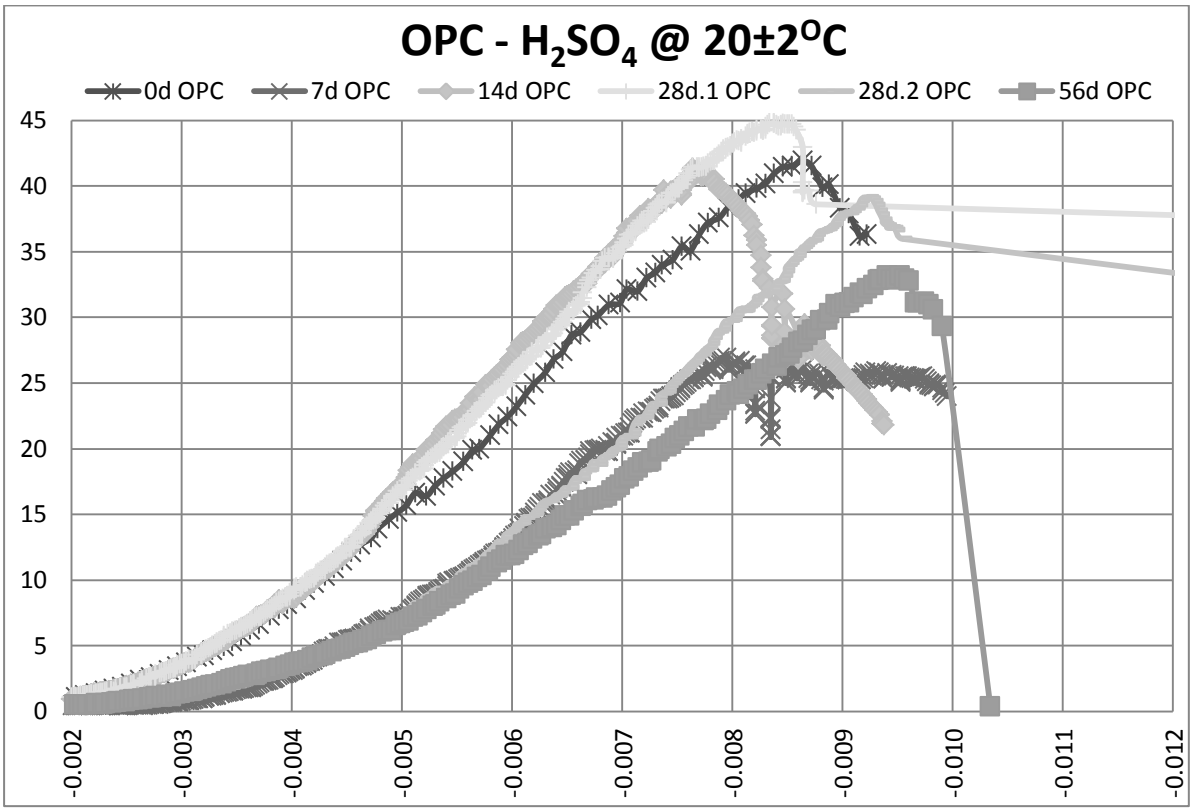

C.2 H_2SO_4 90°C

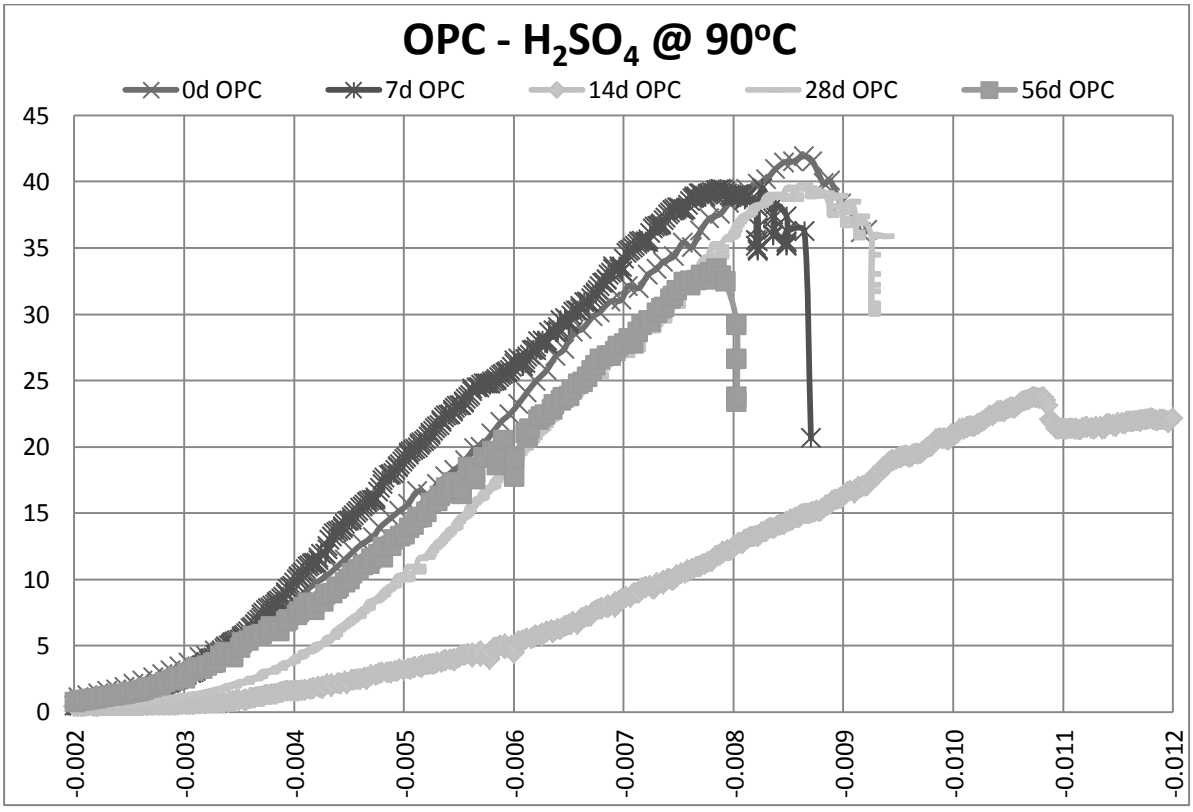

C.3 NaOH 20±2°C

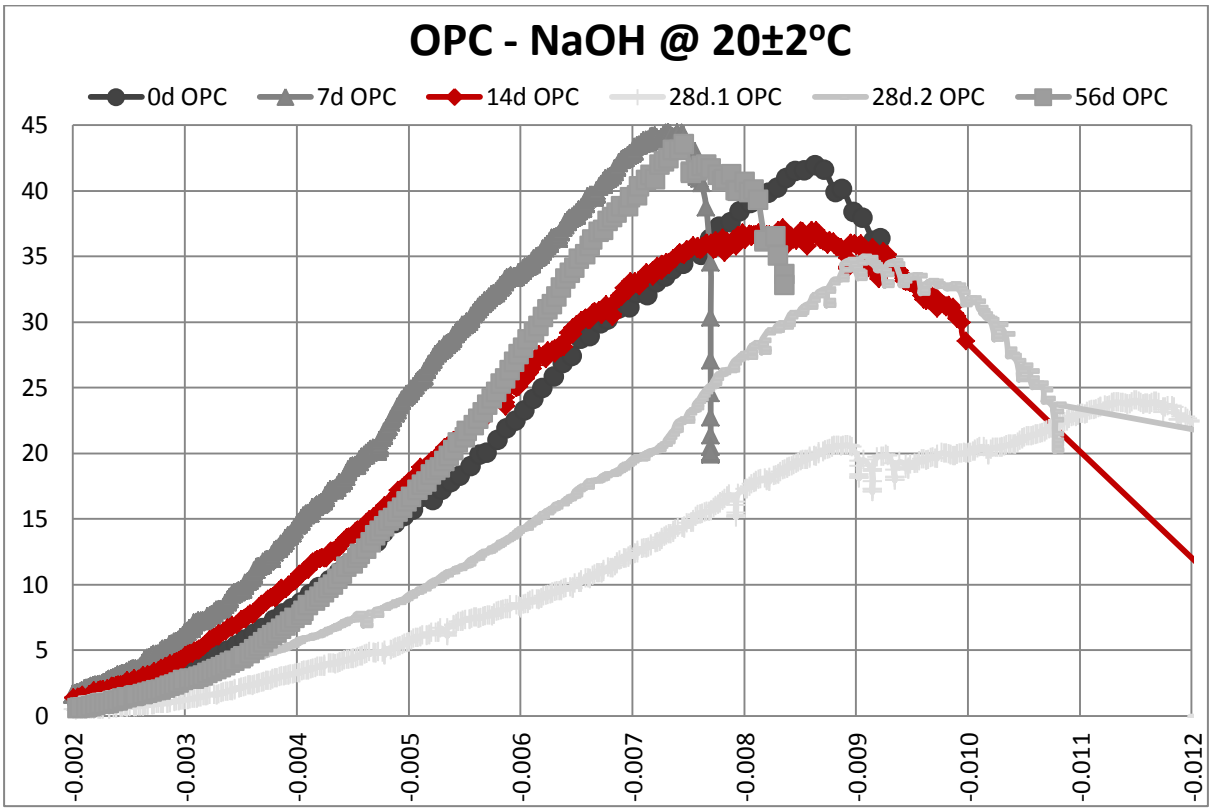

C.4 NaOH 90°C

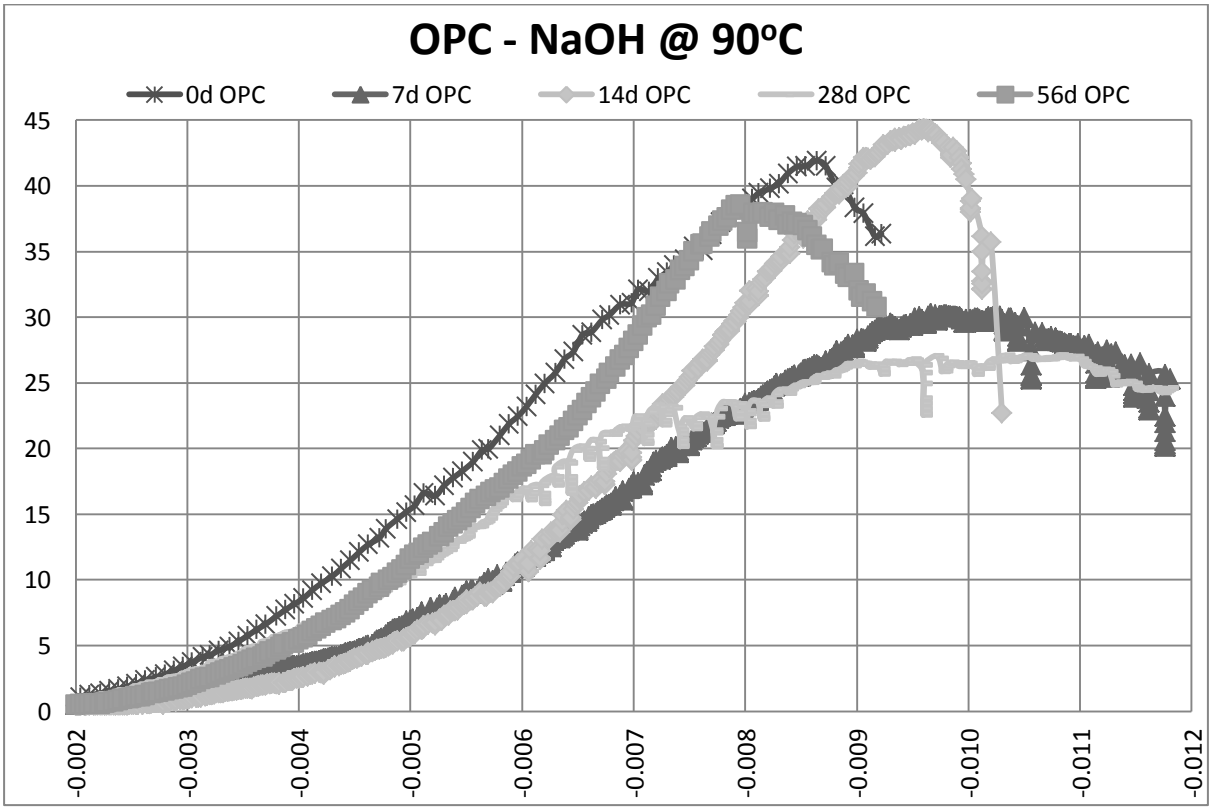

APPENDIX D

Compression Test Data:
Fly Ash Geopolymer Concrete

D.1 H_2SO_4 20±2°C

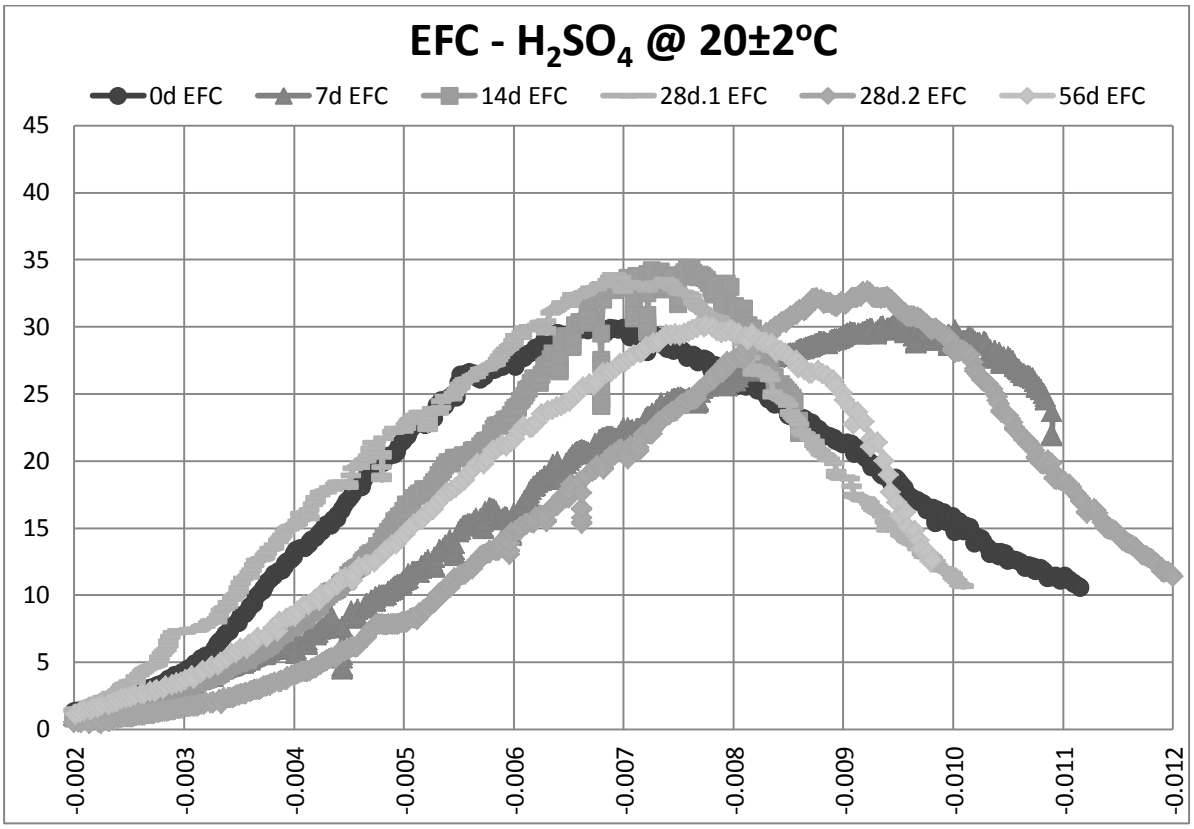

D.2 H2SO4 90°C

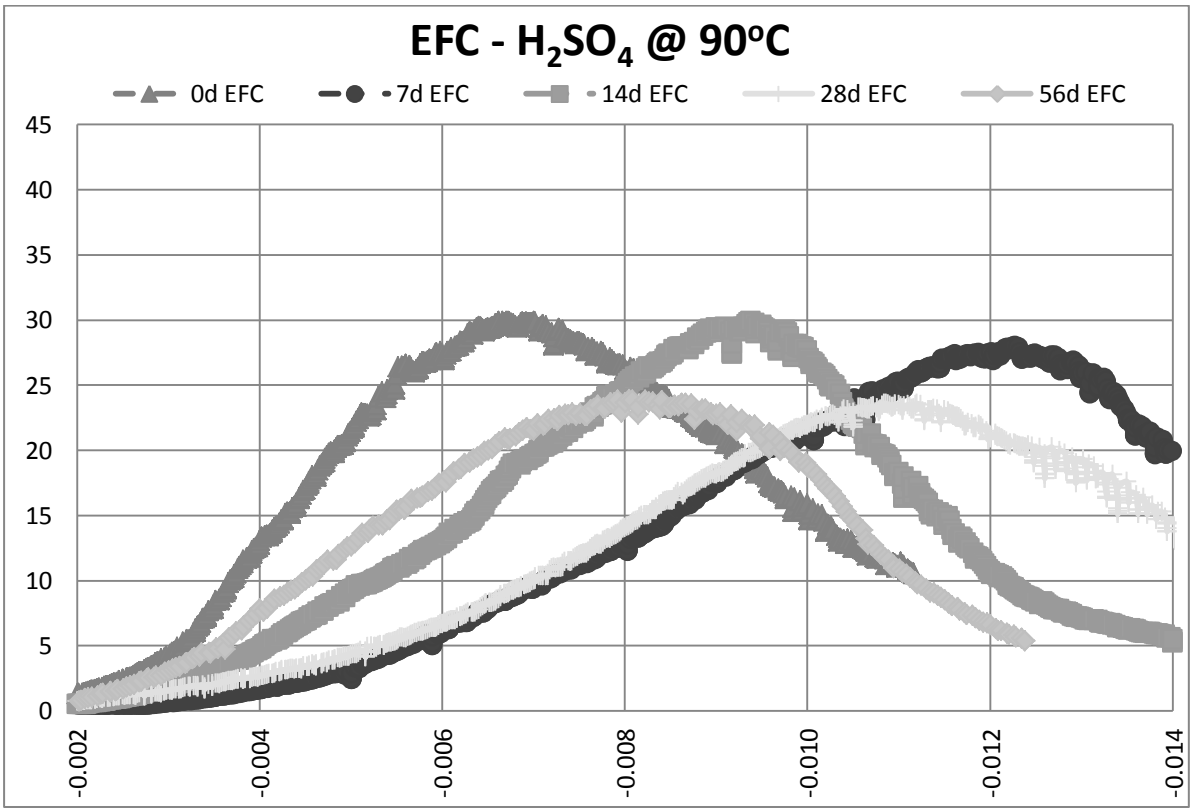

D.3 NaOH 20±2°C

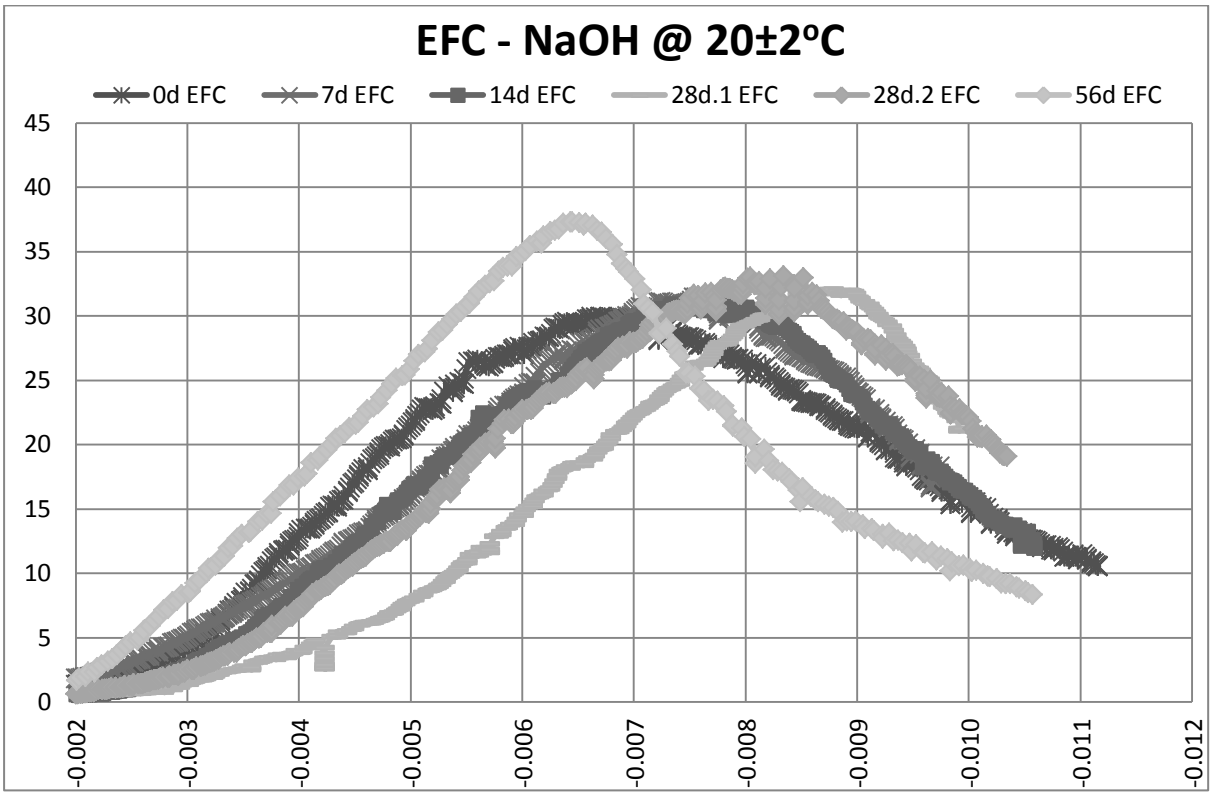

D.4 NaOH 90°C

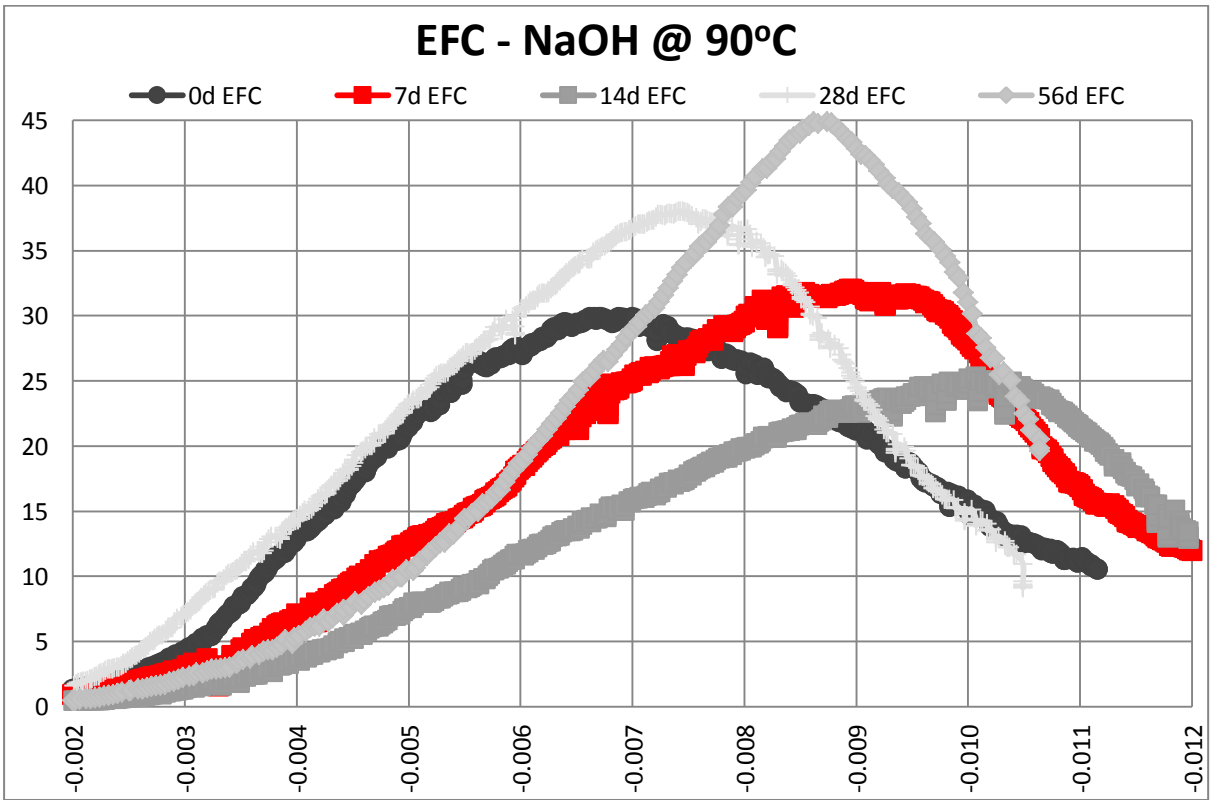

APPENDIX E

Compression Test Data:
Red Mud Geopolymer Concrete

E.1 H_2SO_4 90°C

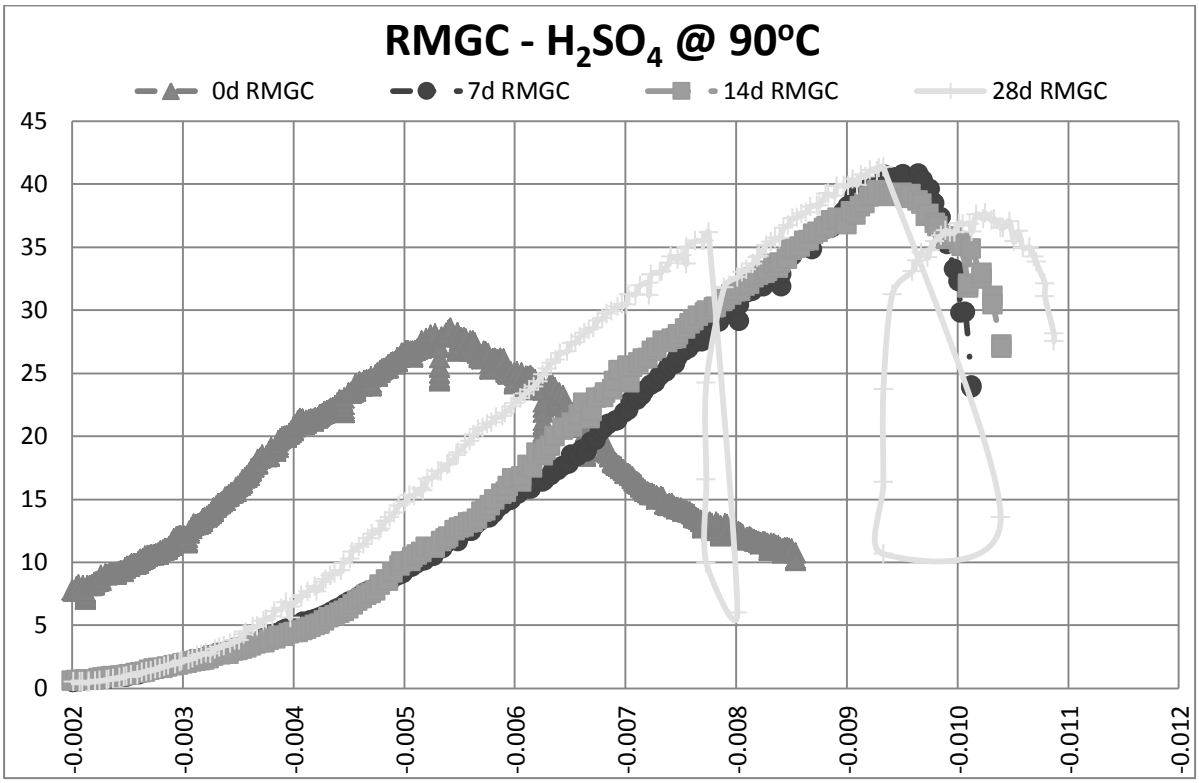

E.2 NaOH 90°C

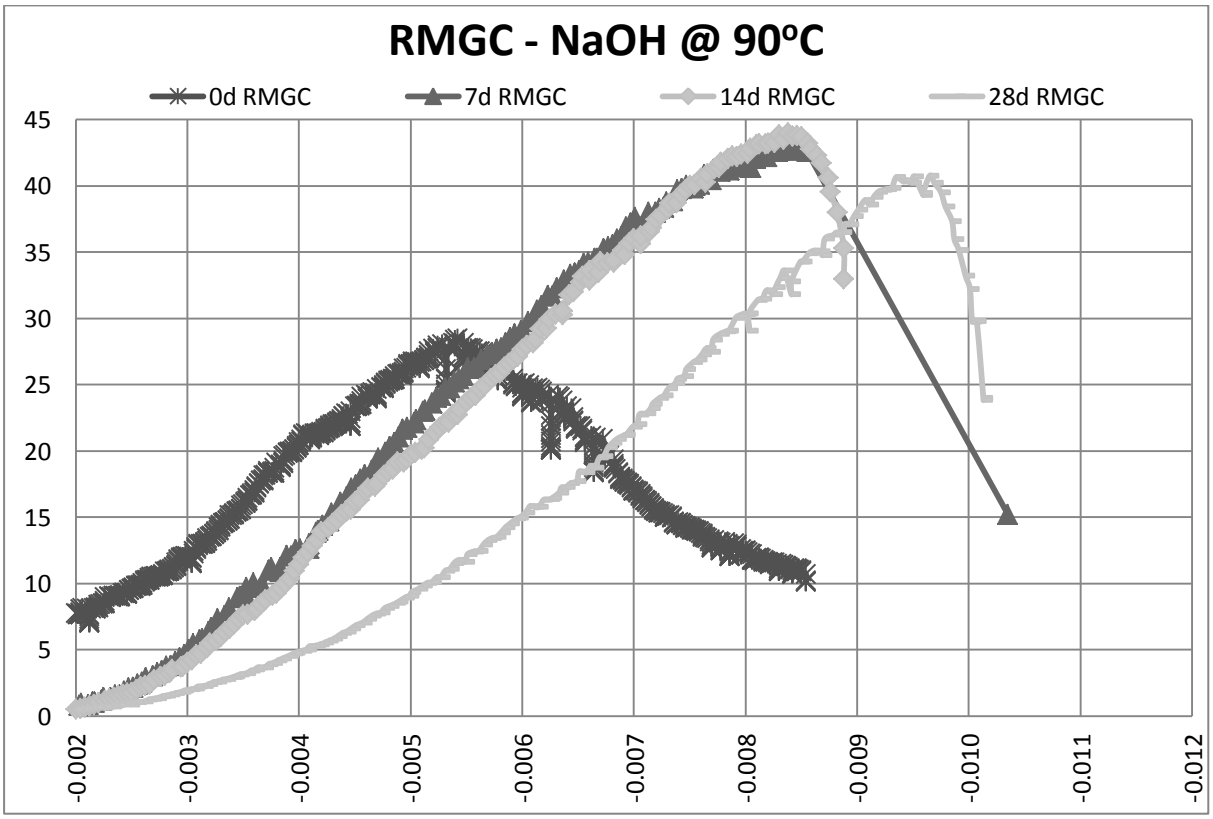

APPENDIX F

Macro Analysis

F.1 OPC Macro Analysis

F.1.1 7 Days


OPC
15
OPC
15
OPC
6
OPC
6

F.1.2 14 Days

F.1.3 28 Days


OPC
4
12
OPC
12


OPC


F.1.4 56 Days

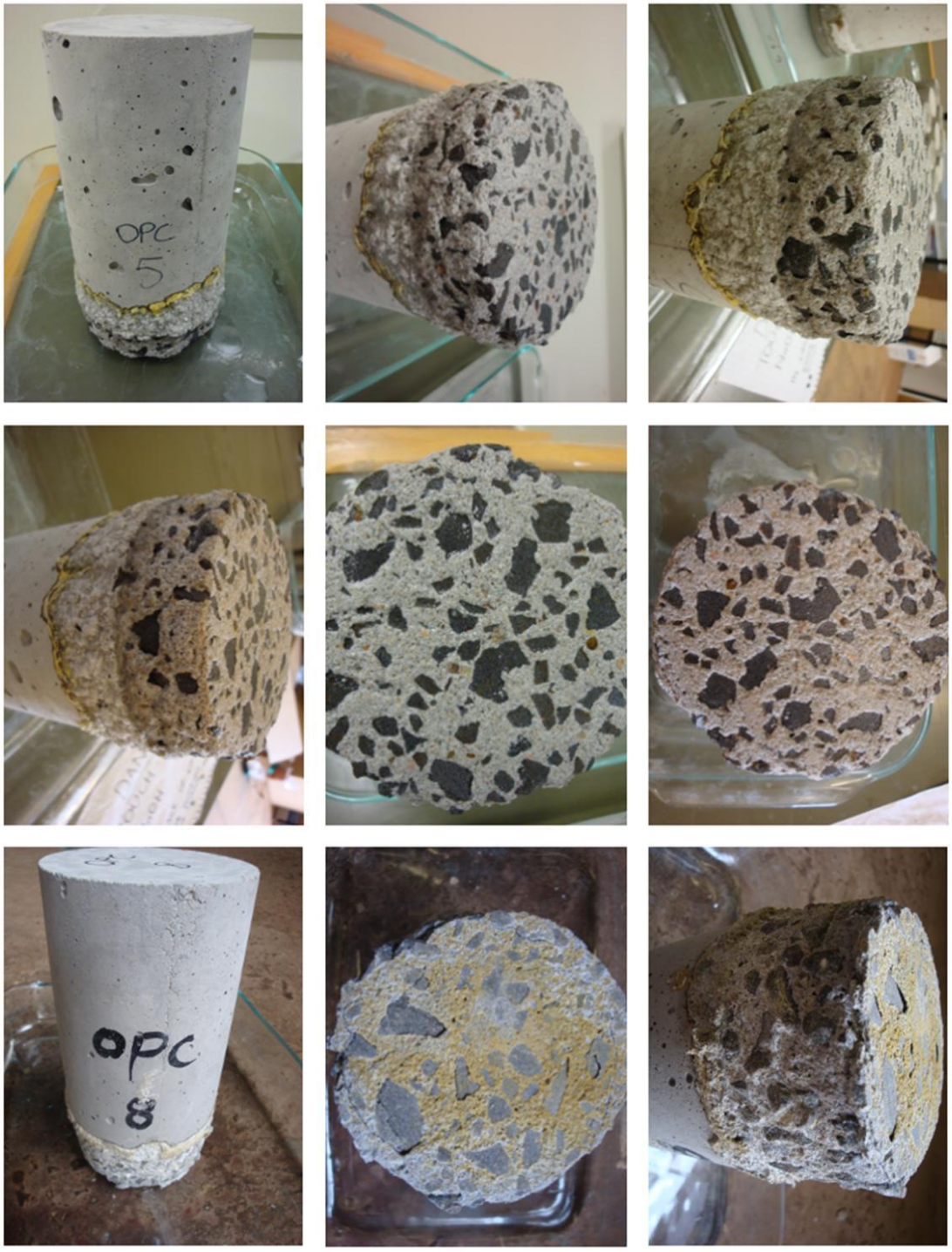


OPC
14
16
OPC




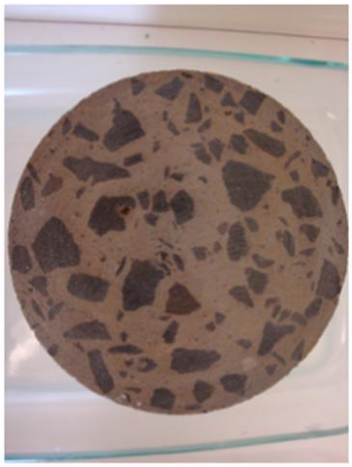


F.2 FAGC Macro Analysis

F.2.1 7 Days


EFC
EFC
8
EFC
8

F.2.2 14 Days



F.2.3 28 Days


EFC
4
12

F.2.4 56 Days

F.3 RMGC Macro Analysis

F.3.1 7 Days

F.3.2 14 Days

F.3.3 28 Days

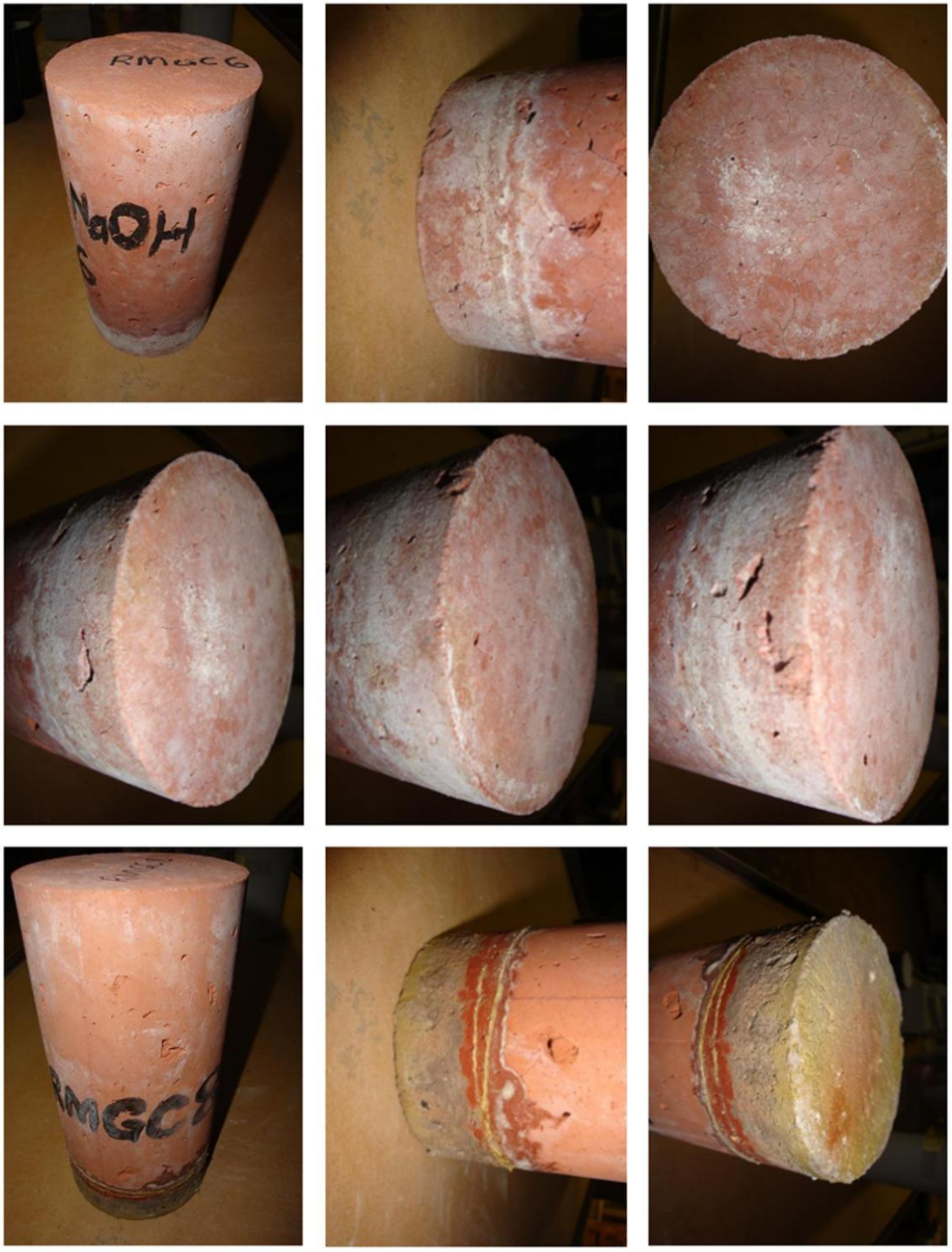





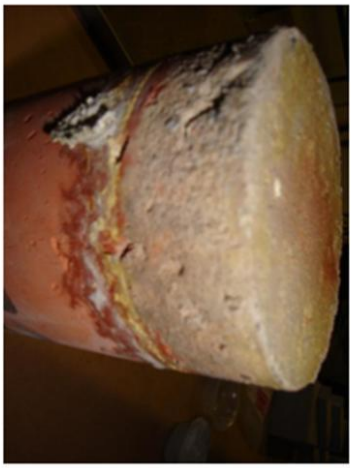

APPENDIX G

Micro Analysis - 28 days at 90^{O}C

This section shows images relevant to the micro analysis of all concretes under chemical attack for 28 days at 90^{O}C. To provide a comparison of the chemical changes between the paste and the aggregate, a saw cut was made. This cut exposes a flush section that has been unaffected in order to provide comparison to the area that was under chemical attack.

G.1 OPC Micro Analysis

This section shows images relevant to the micro analysis of the OPC samples. The analysis investigates samples OPC-7 and OPC-13.

G.1.1 Unaffected Surface of OPC-7 (H_2SO_4)

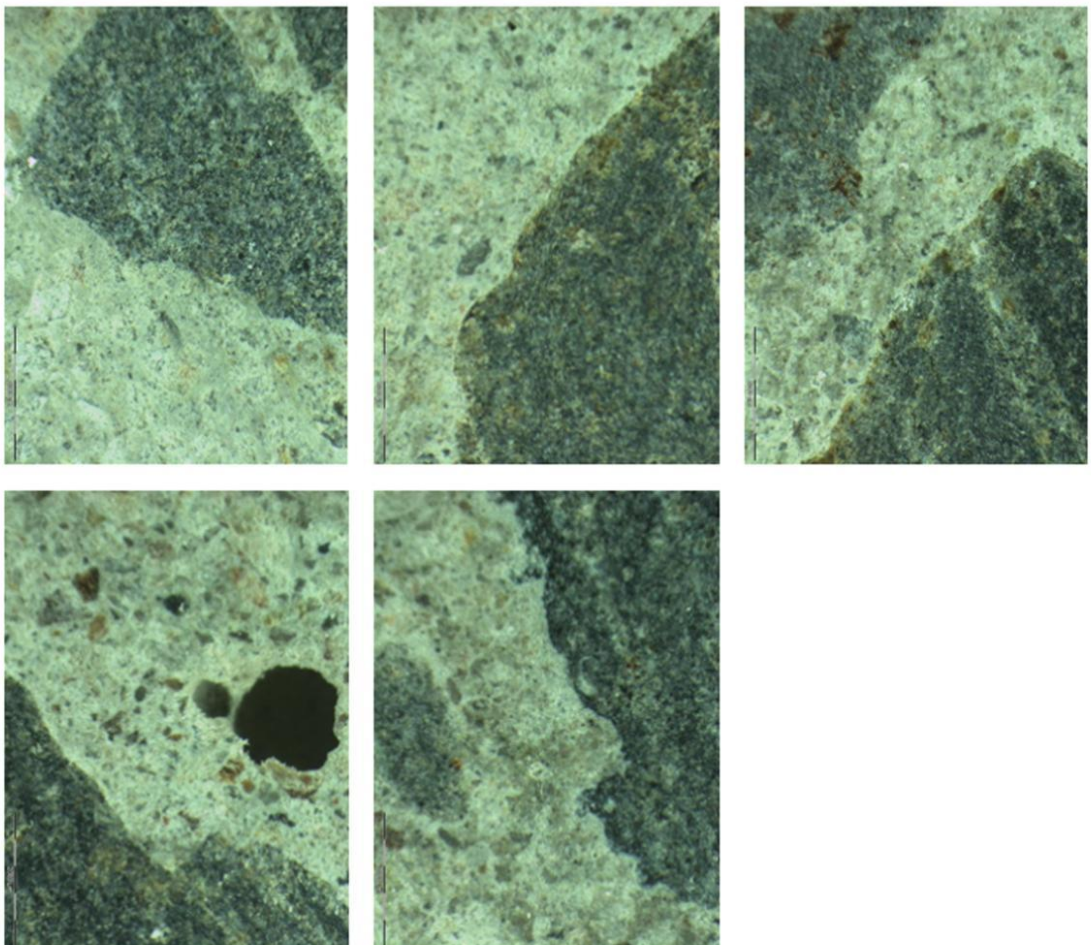

G.1.2 Affected Surface of OPC-7 (H_2SO_4)

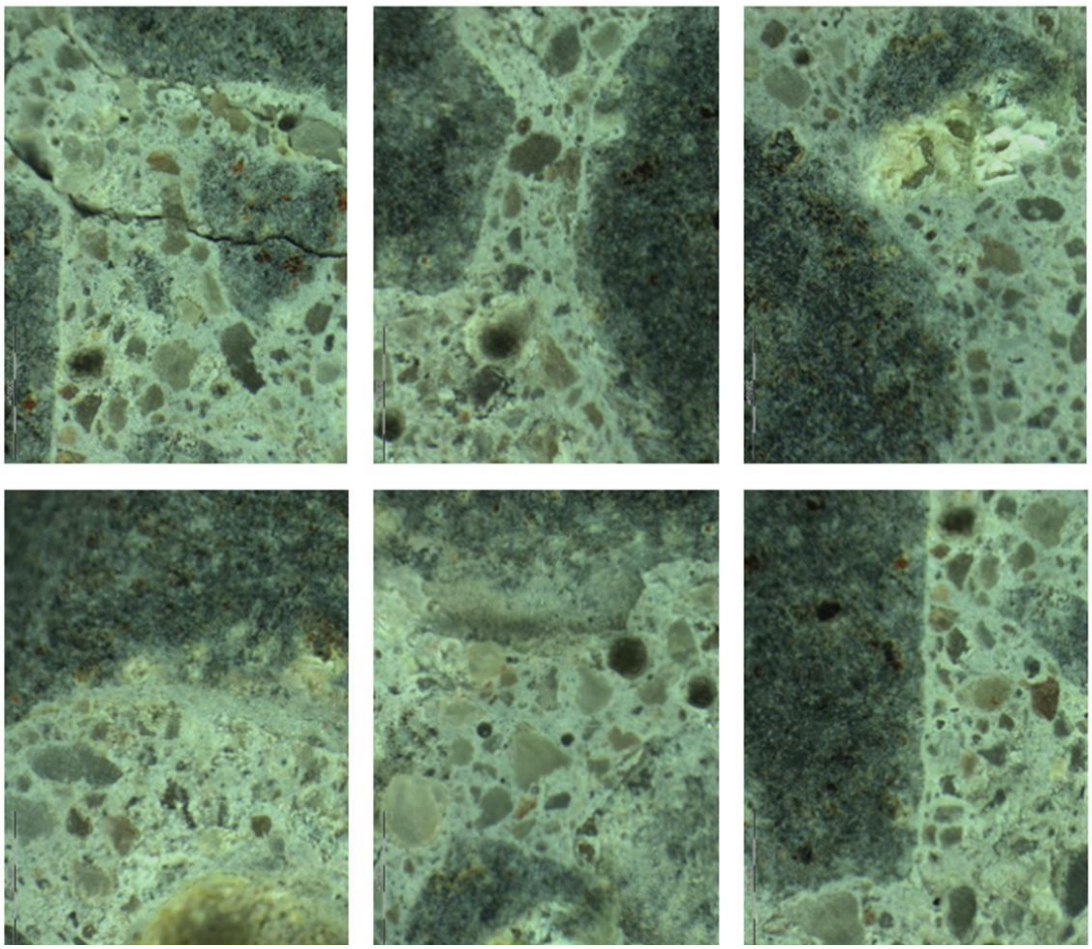

G.1.3 Unaffected Surface of OPC-13

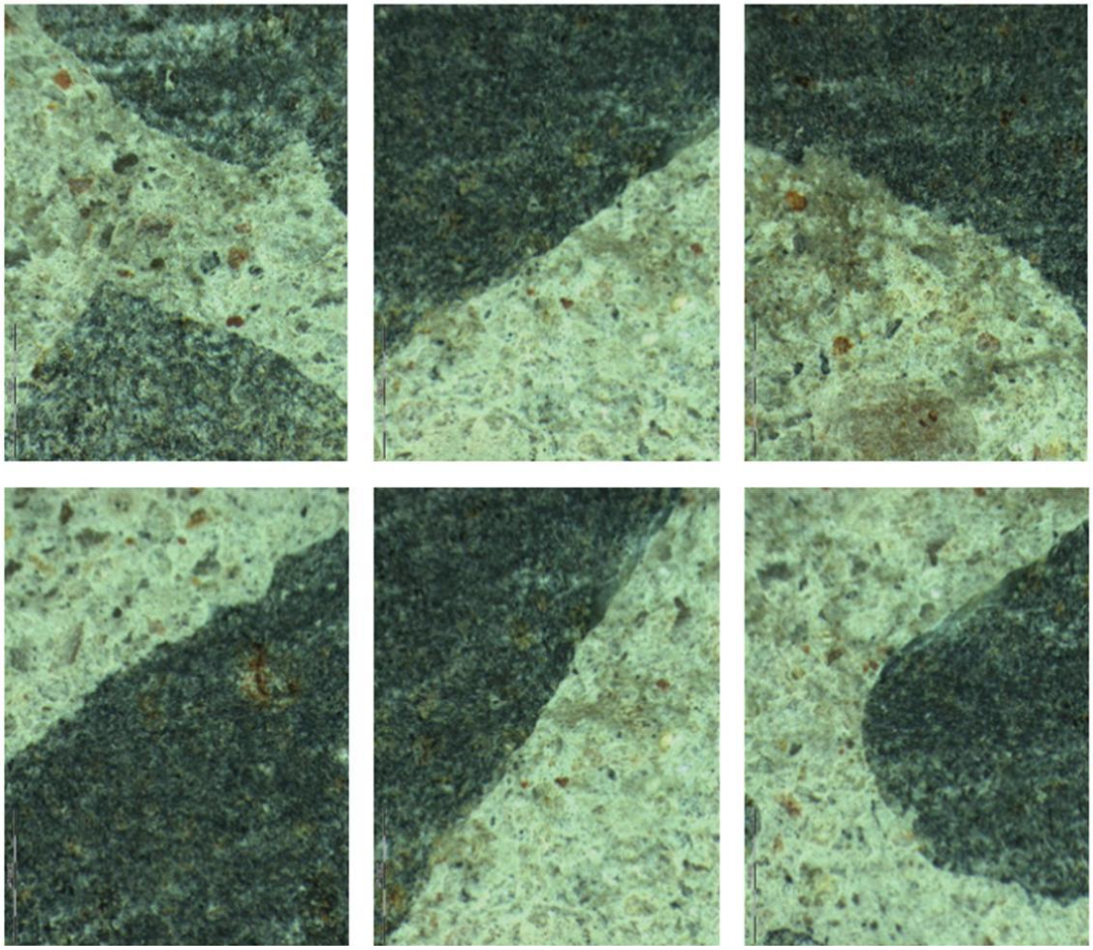

G.1.4 Affected Surface of OPC-13 (NaOH)

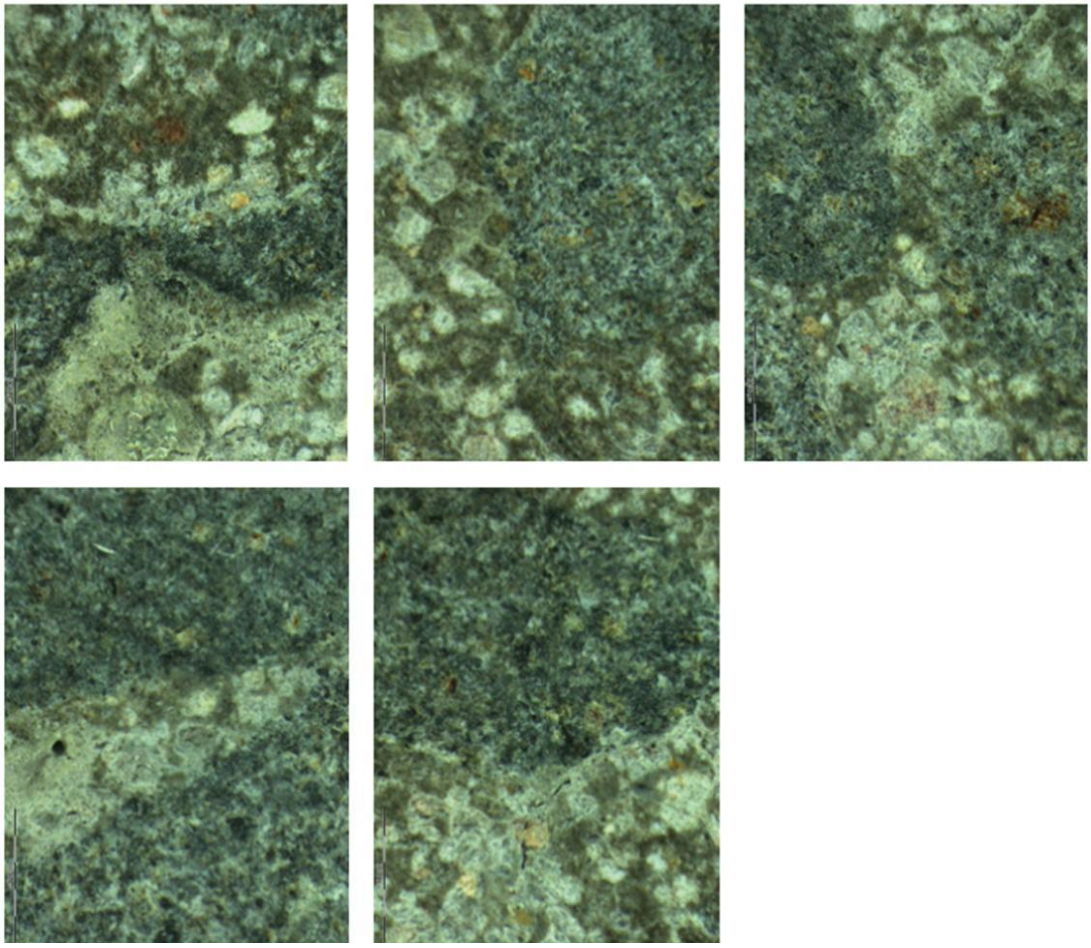

G.2 FAGC Micro Analysis

This section shows images relevant to the micro analysis of the FAGC samples. The analysis investigates samples FAGC-6 and FAGC-14.

G.2.1 Unaffected Surface of FAGC-6

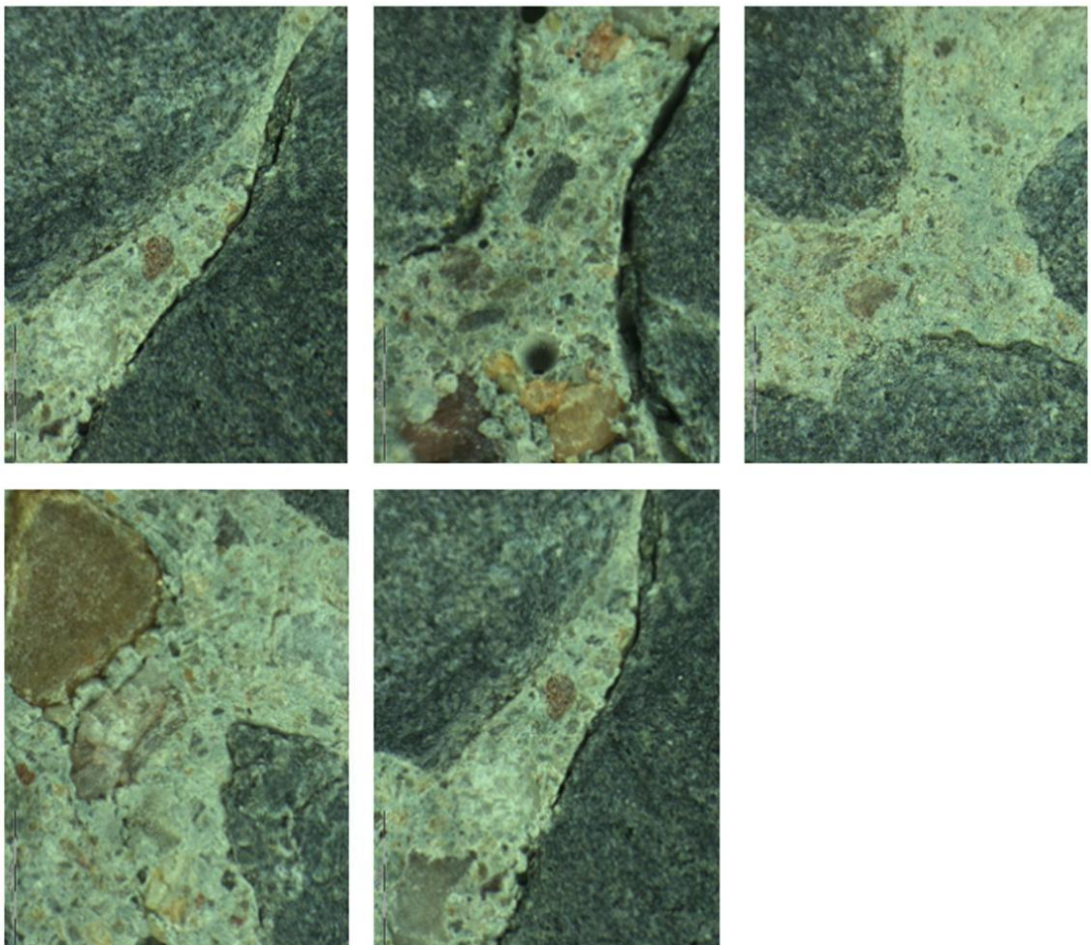

G.2.2 Affected Surface of FAGC-6 (H_2SO_4)

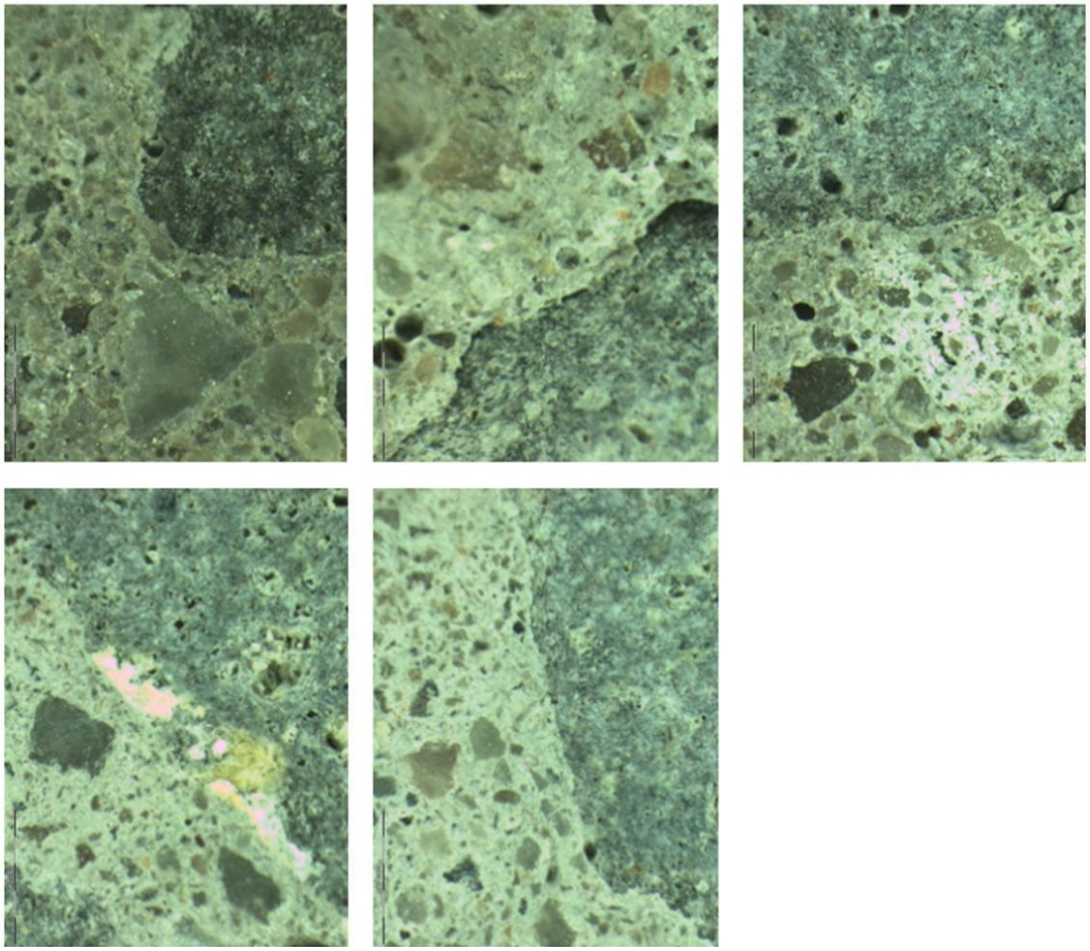

G.2.3 Unaffected Surface of FAGC-14

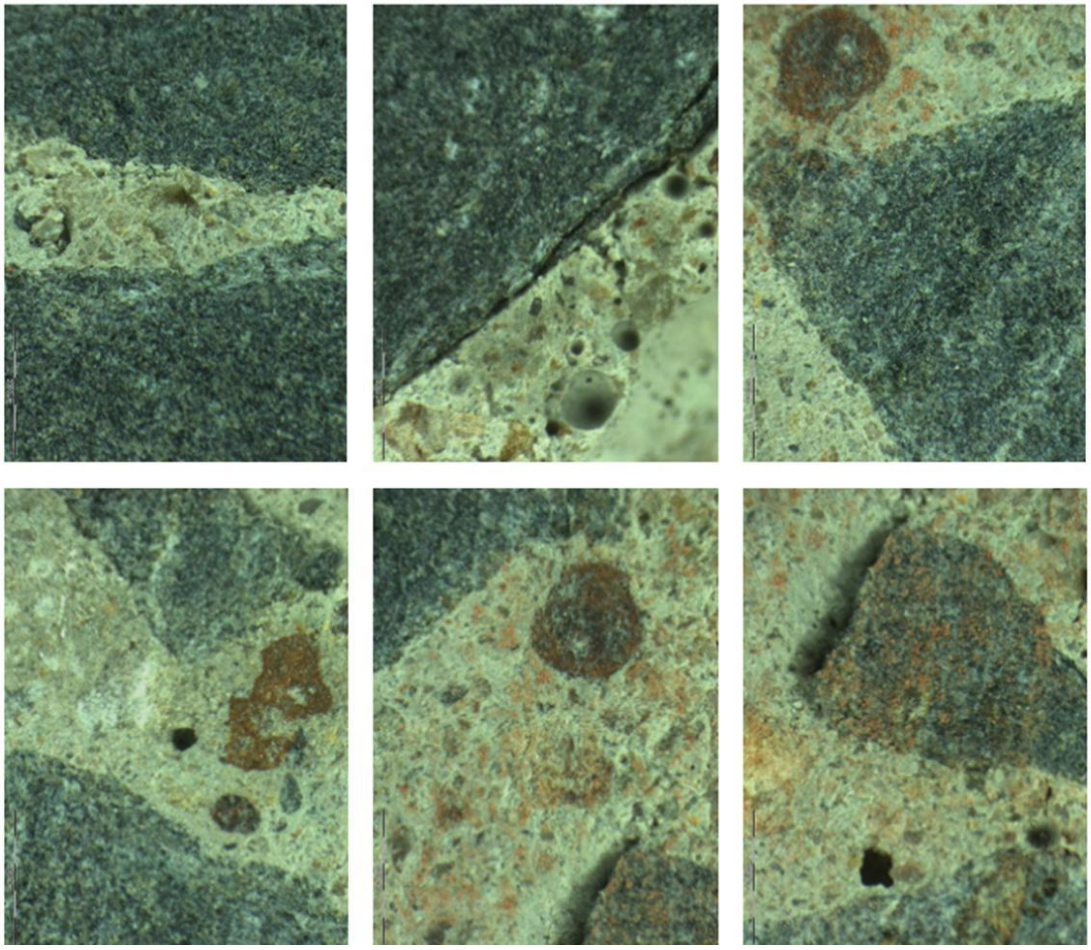

G.2.4 Affected Surface of FAGC-14 (NaOH)

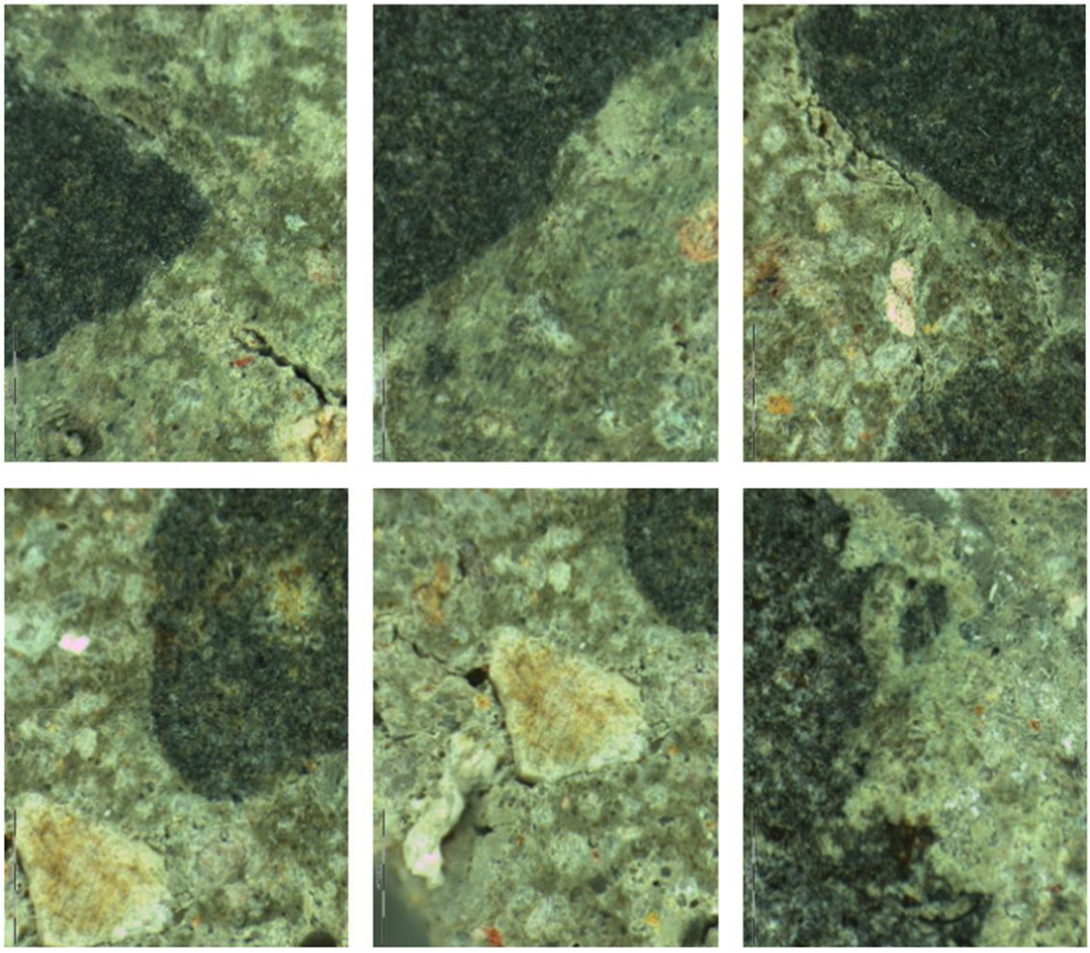

G.3 RMGC Micro Analysis

This section shows images relevant to the micro analysis of the OPC samples. The analysis investigates samples RMGC-6 and RMGC-9.

G.3.1 Unaffected Surface of RMGC-8

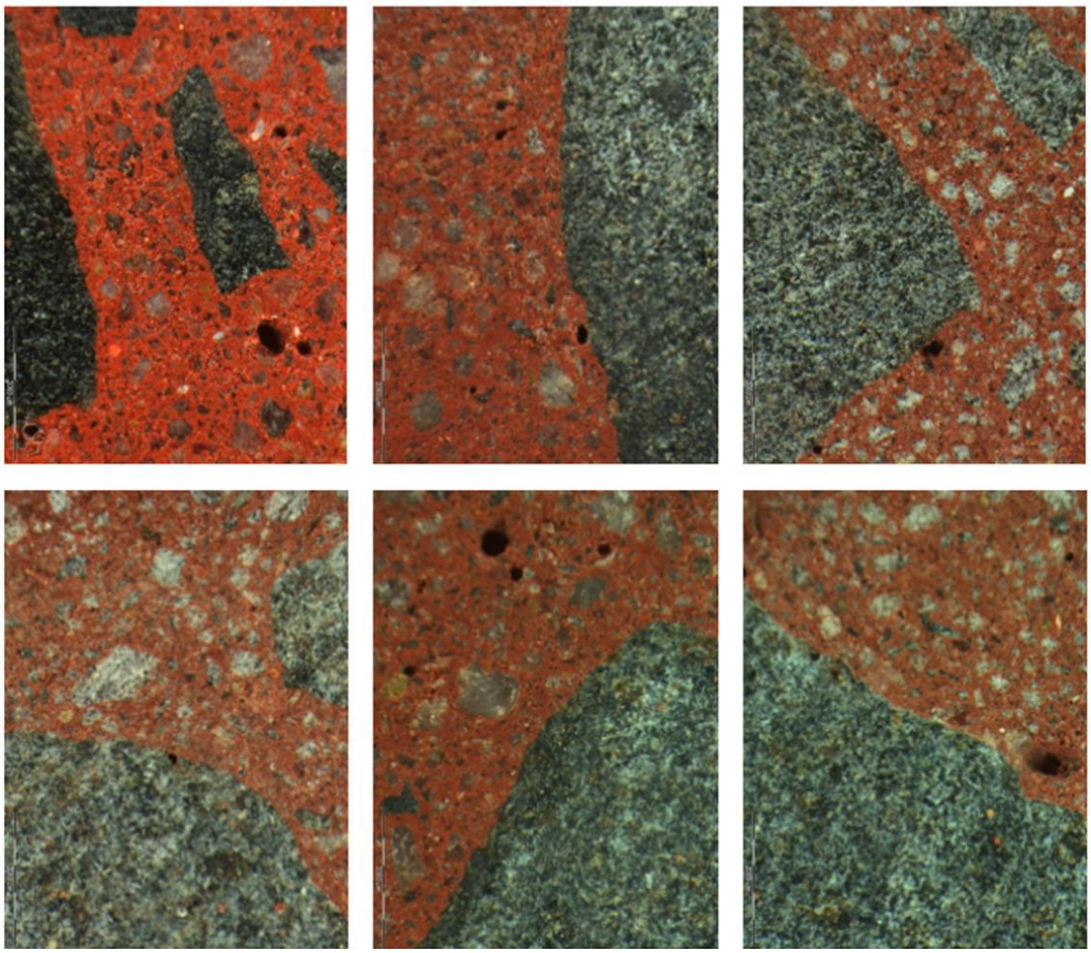

G.3.2 Affected Surface of RMGC-8 (H_2SO_4)

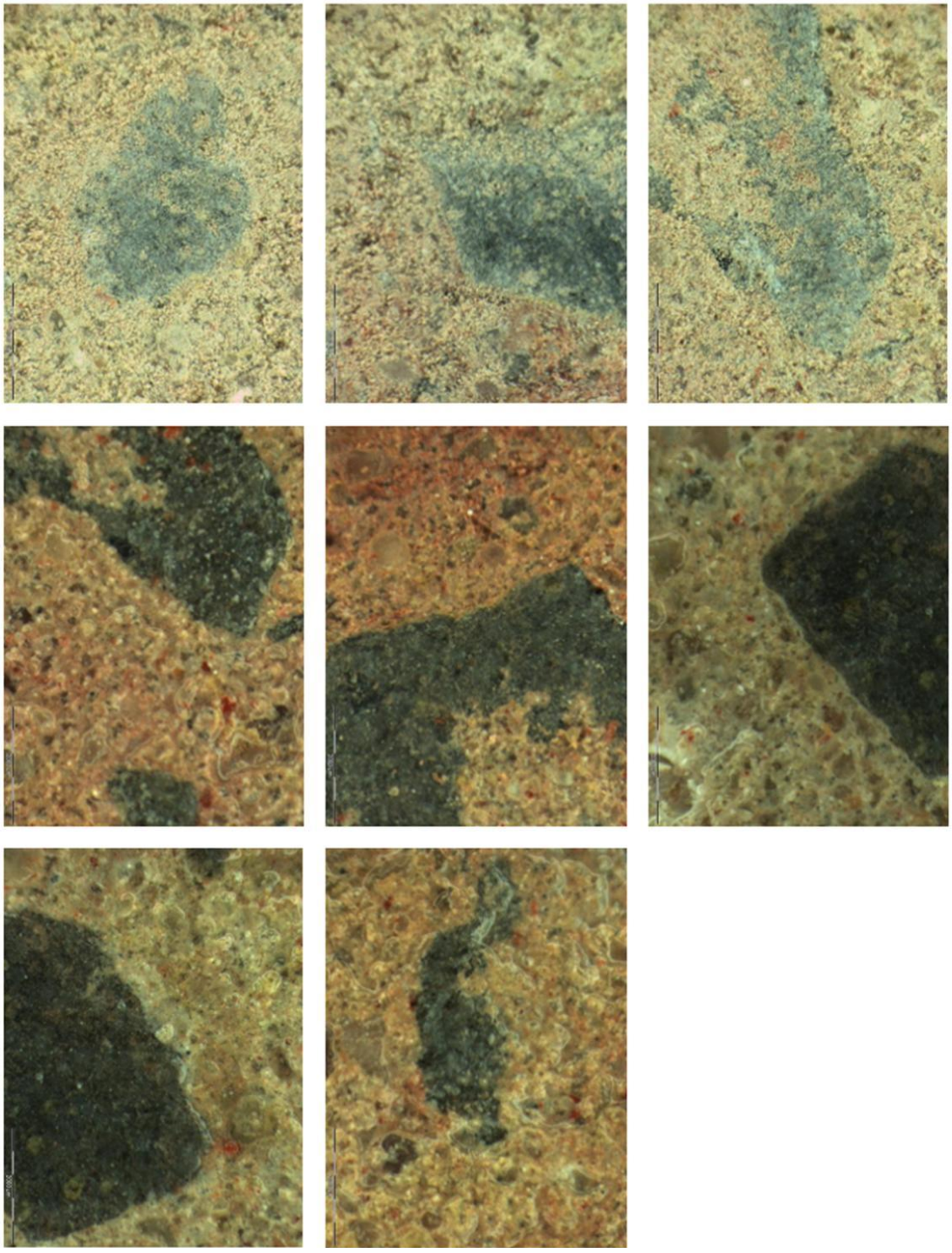

G.3.3 Unaffected Surface of RMGC-6

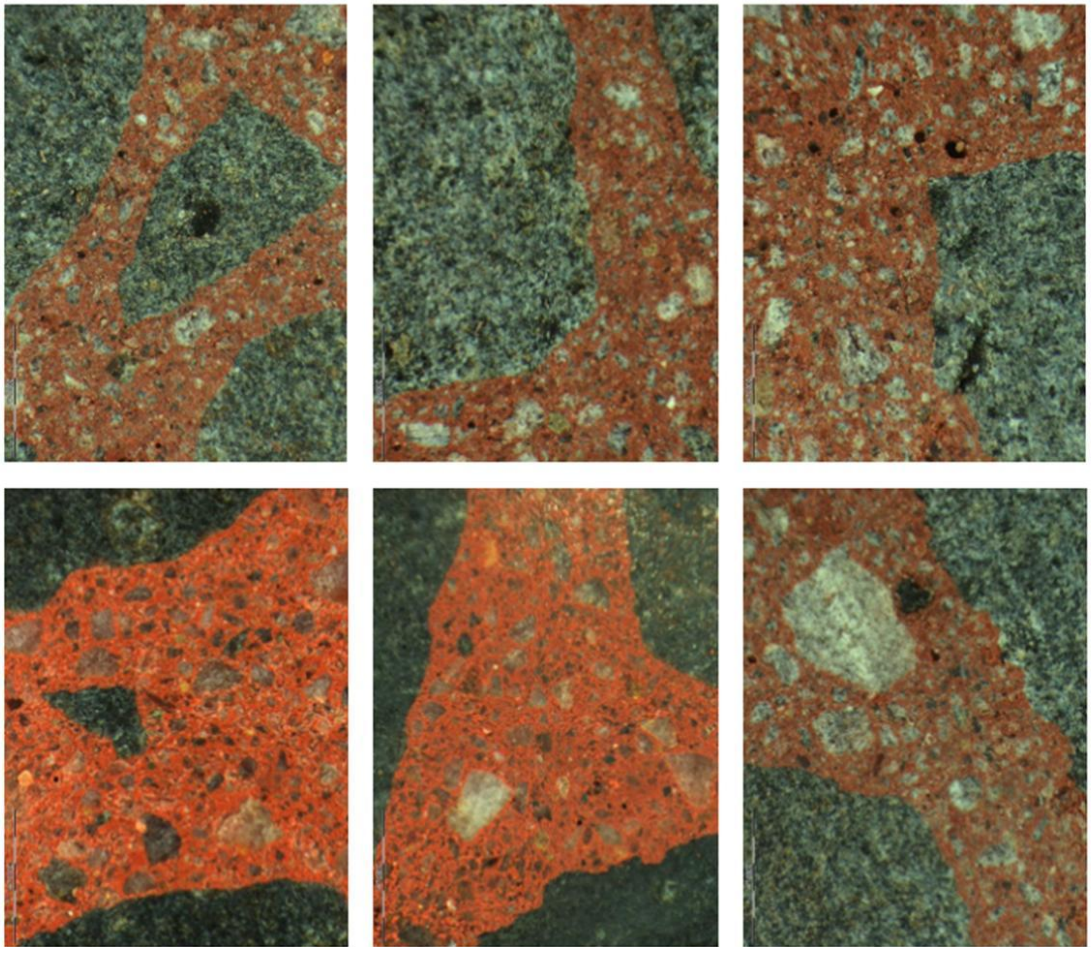

G.3.4 Affected Surface of RMGC-8 (NaOH)